

Characteristics of the Central Performance Drop

Cindy J. Potechin

A Thesis

in

The Department of Psychology

Presented in Partial Fulfillment of the Requirements
for the Degree of Doctorate in Philosophy at
Concordia University
Montreal, Quebec, Canada

November 2006

© Cindy J. Potechin, 2006



Library and
Archives Canada

Bibliothèque et
Archives Canada

Published Heritage
Branch

Direction du
Patrimoine de l'édition

395 Wellington Street
Ottawa ON K1A 0N4
Canada

395, rue Wellington
Ottawa ON K1A 0N4
Canada

Your file *Votre référence*
ISBN: 978-0-494-30124-1
Our file *Notre référence*
ISBN: 978-0-494-30124-1

NOTICE:

The author has granted a non-exclusive license allowing Library and Archives Canada to reproduce, publish, archive, preserve, conserve, communicate to the public by telecommunication or on the Internet, loan, distribute and sell theses worldwide, for commercial or non-commercial purposes, in microform, paper, electronic and/or any other formats.

The author retains copyright ownership and moral rights in this thesis. Neither the thesis nor substantial extracts from it may be printed or otherwise reproduced without the author's permission.

AVIS:

L'auteur a accordé une licence non exclusive permettant à la Bibliothèque et Archives Canada de reproduire, publier, archiver, sauvegarder, conserver, transmettre au public par télécommunication ou par l'Internet, prêter, distribuer et vendre des thèses partout dans le monde, à des fins commerciales ou autres, sur support microforme, papier, électronique et/ou autres formats.

L'auteur conserve la propriété du droit d'auteur et des droits moraux qui protègent cette thèse. Ni la thèse ni des extraits substantiels de celle-ci ne doivent être imprimés ou autrement reproduits sans son autorisation.

In compliance with the Canadian Privacy Act some supporting forms may have been removed from this thesis.

Conformément à la loi canadienne sur la protection de la vie privée, quelques formulaires secondaires ont été enlevés de cette thèse.

While these forms may be included in the document page count, their removal does not represent any loss of content from the thesis.

Bien que ces formulaires aient inclus dans la pagination, il n'y aura aucun contenu manquant.


Canada

ABSTRACT

Characteristics of the Central Performance Drop

Cindy Potechin, Ph.D.
Concordia University, 2006

The present experiments examine texture discrimination as a function of eccentricity. Before 1985, several studies showed that sensitivity to texture differences decreased with eccentricity. Kehrner (1987) found that the detection of a small patch of oblique lines oriented at ± 45 deg from vertical embedded in a background of orthogonal lines improved as the texture was moved away from the fovea. Kehrner (1989) attributed this so called "Central Performance Drop" (CPD) to a difference in processing speed of spatial-frequency selective filters across the visual field. Gurnsey et al. (1996) proposed a spatial account for the CPD, asserting that the CPD represents a mismatch between the texture scale and the spatial frequency selectivity of the texture detection mechanism.

It has been argued that a backward mask is critical to the emergence of a CPD. We show that the CPD can be elicited without a backward mask when performance is limited by manipulating the orientation variability within the foreground and background textures. (Potechin & Gurnsey, 2003).

Texture discrimination is often asymmetrical; i.e. Texture A embedded in Texture B may be easier to detect than vice versa. We examined texture discrimination as a function of eccentricity using four textures that were previously reported to elicit discrimination asymmetries. Three different patterns emerged in which the discrimination asymmetries were not necessarily constant across eccentricity and not all textures elicited a CPD. The results show that

“discriminability” of two textures depends upon the eccentricity of the target texture and on the arrangement of the two textures within the display (Potechin & Gurnsey, in press).

Both the spatial and temporal explanations for the CPD assume that lower spatial frequencies are not as efficiently processed in the fovea compared to higher spatial frequencies. It has been suggested that cross-frequency inhibition (CFI) or the preference given to high spatial frequency information at the fovea may underlie the CPD. We observed that high frequency attenuation of a stimulus by a Gaussian filter can improve discrimination performance at the fovea, suggesting that the CPD may be influenced by CFI.

ACKNOWLEDGEMENTS

Although this thesis bears only my name, I would not have been able to complete this work without the significant contribution of certain people who helped me along the way.

I would like to express my heartfelt thanks to Rick Gurnsey, under whose supervision this research was conducted. His guidance was indispensable and his door was always open when I had a question or an observation to discuss. I would also like to express my gratitude to my committee members, Dr. von Grünau and Dr. Segalowitz, for their careful reading of my thesis document and for the stimulating questions they posed during our meetings that pointed out the broader applications of my thesis project.

Special thanks to my lab mates Sandra Mancini, Sharon Sally and Francois Xavier Sezikeye. My many years researching this project would have been much harder without their input. I hope that we remain friends for many years to come.

The constant support of my family and friends who believed in me was invaluable. Two of these people who deserve special mention are my mother (who prepared the most delicious meals throughout my many years at Concordia) and Yvonne (who helped me with the formatting of the thesis).

Lastly, I am especially grateful to my subjects, who voluntarily give up (sometimes) long periods of their time and worked diligently on tasks that are not known for being easy. Their comments and their hard work helped me to

continue during the times when the answers were not apparent and the work was frustrating.

This study was supported in part by an FCAR grant to the author.

CONTRIBUTIONS OF THE AUTHORS

This thesis comprises the following three manuscripts:

Potechin, C., and Gurnsey, R. (2003). Masking is not required to elicit the central performance drop. *Spatial Vision*, 16, 393-406.

Potechin, C., and Gurnsey, R. (2006). Texture discrimination asymmetries across the visual field. *Spatial Vision*, 19, 389-412.

Potechin, C., and Gurnsey, R. (in preparation). Cross-frequency inhibition and the central performance drop.

All of the experiments were designed in collaboration with my supervisor, Dr. Rick Gurnsey. The internal thesis committee was composed of Dr. Michael von Grünau, Dr. Norman Segalowitz and Dr. Rick Gurnsey. The software used in the testing was created by Dr. Gurnsey and modified by Cindy Potechin, when necessary. The psychophysical testing and data analyses were conducted by Cindy Potechin. All manuscripts were written by Cindy Potechin and edited by Dr. Gurnsey.

TABLE OF CONTENTS

List of Figures	xii
Chapter 1	
Thesis Introduction:	
Texture Segmentation Across the Visual Field.....	1
What is visual texture?	1
Effortless Texture Segmentation	4
Similarity between texture segmentation and visual search.	6
Theories of Texture segmentation	7
Image Statistics	8
Image Features	9
Spatial Filtering	10
Filter-based Models of Texture Segmentation	12
Limitations on Visual Processing Across the Visual Field	17
The Central Performance Drop (CPD)	20
Explanations of the CPD	22
A Temporal Explanation	22
A Spatial Explanation	24
Texture Discrimination Asymmetries	26
Weber-type explanations	27
Signal Detection (Noise-based) Explanations	30
A Subjective Completion Explanation	30
Cross-Frequency Inhibition	32

Overview of the thesis	36
Chapter 2	
Backward Masking is not required to elicit the Central Performance Drop	38
Abstract.....	39
Introduction.....	40
Experiment 1	45
Method	46
Results and Discussion	48
Experiment 2	50
Method	50
Results and Discussion	51
Experiment 3	52
Method	53
Results and Discussion	55
General Discussion	56
Chapter 3	
Texture Discrimination Asymmetries across the Visual Field.	59
Abstract.....	60
Introduction.....	61
Experiment 1	68
Method	68
Results	74
Discussion	77
Experiment 2	78

Method	78
Results	80
Discussion	83
General Discussion	84
Chapter 4	
Cross-Frequency Inhibition and the Central Performance Drop	94
Abstract.....	95
Introduction.....	96
Experiment 1	104
Method	104
Results and Discussion	107
Experiment 2	109
Method	110
Results and Discussion	111
Experiment 3	114
Method	114
Results and Discussion	117
General Discussion	118
Chapter 5	
Summary and Conclusions	123
Eliminating temporal factors as an explanation for the CPD	123
Eccentricity dependence of texture discrimination asymmetries.....	124
The influence of CFI on the CPD.....	125
Refining the bandwidth procedure.....	127
Factors that may contribute to a difficulty obtaining a CPD across studies	128

Concluding remarks..... 128

References 130

LIST OF FIGURES

Chapter 1

Figure 1.1 Examples of characteristic textures in common objects1	2
Figure 1.2 Examples of texture gradient.....	2
Figure 1.3 Example of visual texture made up of oriented line elements	3
Figure 1.4 Examples of microelement pairs	5
Figure 1.5 Illustration of the Filter-Rectify-Filter Model.....	14
Figure 1.6 Example of visual texture asymmetry	27
Figure 1.7: Illustration of the effects of cross-frequency inhibition.	32

Chapter 2

Figure 2.1. Top. Stimulus set-up used in Experiment 1 and 2 and examples of different bandwidths	45
Figure 2.2. Example of orientation threshold bandwidth	49
Figure 2.3. Results of Experiment 1	49
Figure 2.4. Results of Experiment 2	52
Figure 2.5. Stimulus pattern used in Experiment 3	54
Figure 2.6. Results of Experiment 3	56

Chapter 3

Figure 3.1. Data replotted from Meinecke and Kehrner (1994)	67
Figure 3.2. Examples of the four stimulus continually used in the experiments..	69
Figure 3.3. Examples of LX textures of different bandwidth	70
Figure 3.4. L-type micropatterns embedded in X-type micropatterns	72
Figure 3.5. Summary of the results of Experiment 1	75

Figure 3.6. Summary of the results of Experiment 2	81
Figure 3.7. Averaged data from the orientation (a) and size (b) experiments and σ values that fit the orientation data (c) and size data (d)	86
Figure 3.8. Averaged data from the orientation (a) and size (b) experiments and s values that fit the orientation data (c) and size data (d)	89
Chapter 4	
Figure 4.1. Examples of the stimulus patterns used in Experiment 1.....	106
Figure 4.2. Results of Experiment 1	108
Figure 4.3. Examples of the stimulus patterns used in Experiment 2.....	112
Figure 4.4. Results of Experiment 2	113
Figure 4.5. Examples of the stimulus and mask patterns used in Experiment 3	116
Figure 4.6. Results of Experiment 3	117

CHAPTER 1

THESIS INTRODUCTION

Texture Segmentation Across the Visual Field

What is visual texture?

The visual system uses a number of elementary properties such as luminance, color, texture, depth, and motion to segregate a visual image into coherent, or uniform regions. Many of these properties have physical dimensions that can be specified. For example, colors can be described in terms of hue, saturation and brightness. Unlike, other segmentation cues, texture is difficult to define. There are no consistent physical properties that define all visual textures. Image properties that give rise to texture segmentation include variations in contrast, color, spatial frequency and orientation. Landy and Graham (2004) described texture as a statistical property that is not directly extracted by the visual system. However, the intuitive notion underlying texture is that of a local pattern or patterns that repeat across space

Naturally occurring objects exhibit a large variety of textured surfaces. The visual component of these textures can be useful in a number of ways. First, visual texture provides strong cues to the observer that may be used in the identification or classification of the objects and/or surface material. Many objects (such as those shown in Figure 1.1) exhibit characteristic texture patterns. When a texture pattern cannot be used directly to identify an object it may convey information about the material properties of a surface. For example, texture provides information about the “roughness” or “smoothness” of a surface.

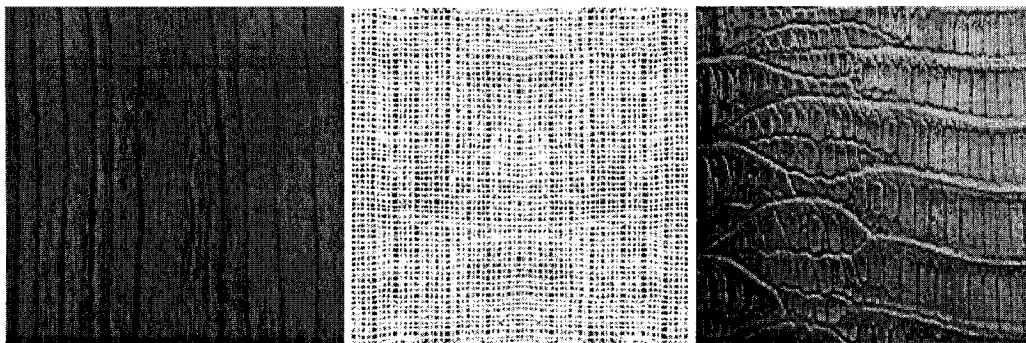


Figure 1.1 Examples of characteristic textures in common objects. The panel of the left represents wood grain. The middle panel is represents burlap. Snakeskin can be seen in the panel on the right. (Photos provided courtesy of Paul Bourke, Swinton Institute of Technology.)

Second, texture can aid in the recovery of three-dimensional surface structure. Texture gradients can convey information about the three dimensional shape of an object and the relative placement of objects within a three dimensional space. As a textured surface recedes from the observer the projection of the texture elements in the image becomes smaller and denser (Gibson, 1950) until the individual texture units become indistinguishable at large distances. Another example of depth cues in texture can be seen in Figure 1.2.a. In a similar fashion texture microelement variation or distortion across an

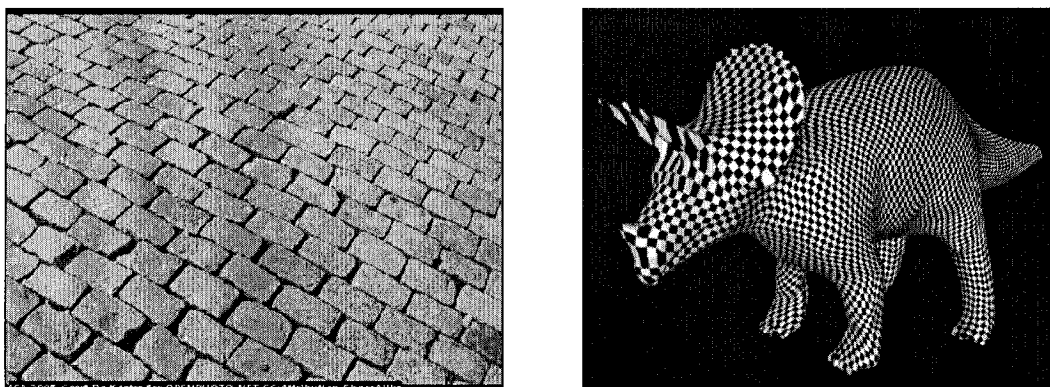


Figure 1.2 Examples of texture gradient. A) In the image of street pavement shown in the left panel, a perception of depth is created by the relative decrease in size of the cobblestones with increasing distance. (Photo by Geert de Kooter <http://openphoto.net>.) B) In the right panel, distortion of the checked microelements give the impression of distance and curvature.

object allows the observer to estimate the object's shape, as can be seen in Figure 1.2.b.

The present research concerns a third aspect of texture perception, the separation of texture images into figure and background. Wolfson and Landy (1998) made a distinction between the segregation and the discrimination of textures. Segregation implies that the observer uses edge detection-like processes to specify the boundary between two distinct textures, while discrimination implies that the observer distinguishes regions based on texture properties that differ between the abutting regions without a boundary being formed. In natural scenes, abrupt changes in texture often occur when two different objects are placed next to each other. Alterations of mean orientation along a subjective plane have consistently led to strong segmentation of textures in different studies (e.g. Bergen & Landy, 1991, Gurnsey, Pearson, & Day, 1996; Nothdurft, 1985; Yeshurun & Carrasco, 1998). An example of an oriented line texture is presented in Figure 1.3.

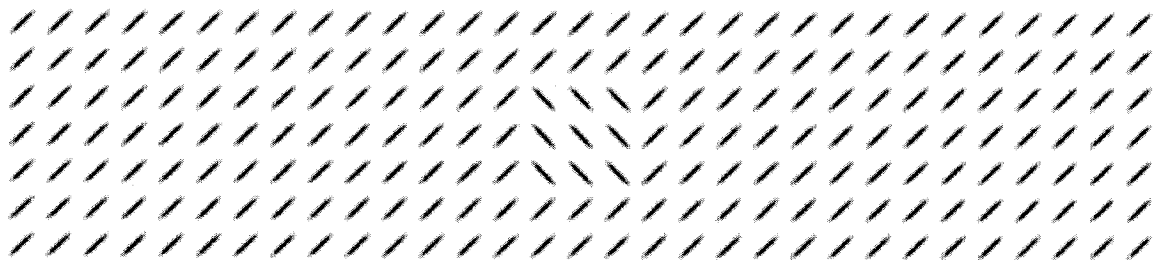


Figure 1.3 Example of visual texture made up of oriented line elements. A subjective boundary is seen where the line of one orientation are placed adjacent to line segments with an orientation difference of 90 degrees.

In the physical world, objects are rarely segmented on the basis of texture differences alone. To isolate the texture component of a visual display in the laboratory, synthetic textures--such as shown in Figure 1.3--are often used. In this

type of display, a foreground region made up of a number of identical elements or micropatterns is presented within a much larger background region containing contrasting micropatterns. The micropatterns may be presented in a number of random orientations. In the absence of color or luminance variation across the texture boundary, a smooth continuous boundary is seen. In this case, the texture border occurs at the point where the lines change orientation. In a typical texture segmentation task, two texture patterns are placed adjacently or one texture is embedded inside another on half the trials. Only one texture is presented on the other half of the trials. The subject's task is to determine whether a particular texture (target) was present on that trial.

Effortless Texture Segmentation

The notion of effortless texture discrimination is well illustrated with a classic example taken from Julesz and Bergen (1983). As seen in Figure 1.4, without close inspection a rectangular area of "+" micropatterns is easily distinguished from the surrounding "L" micropatterns. Segmentation seems to be instantaneous. On more careful inspection of the display, one notices a second rectangular area of "T" micropatterns that is almost indistinguishable from the surrounding "L" micropatterns. Only by slow and effortful scrutiny of each element can this area be identified.

Not all textures that can be discriminated give rise to effortless texture discrimination. Differences in the time and amount of effort required to identify a target or segment a texture were initially used as proof of the existence of two separate visual processes. The attentive versus preattentive processing dichotomy was first proposed by Neisser (1967). Attentive or serial processing was taken to occur when the texture or target was found using a slow exhaustive

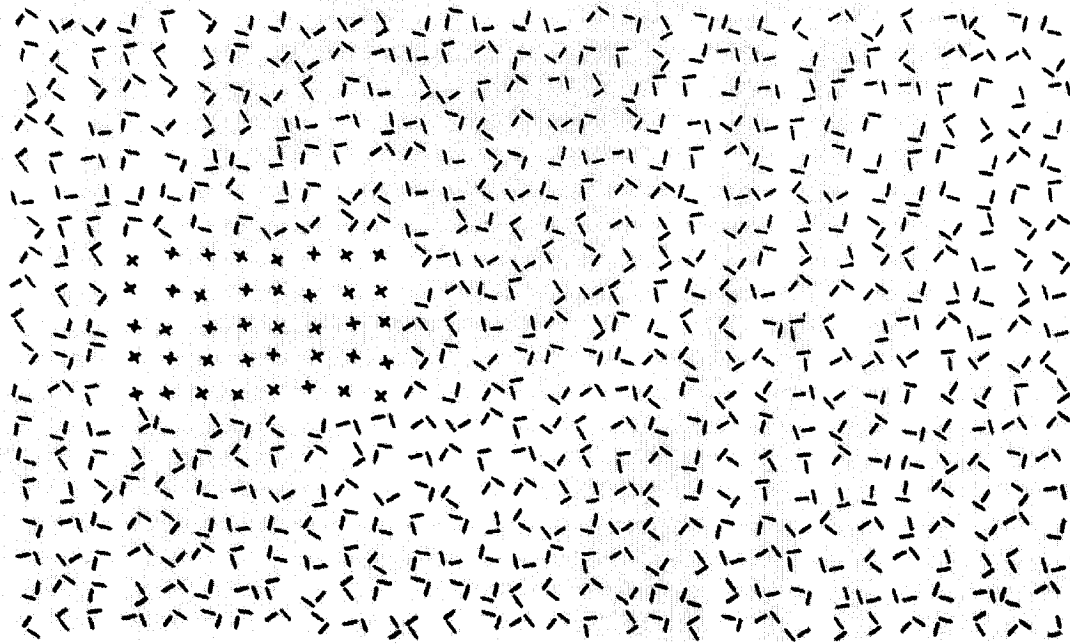


Figure 1.4 Examples of microelement pairs that produce or fail to produce spontaneous texture segmentation. The "+"s segment easily from the "L's while distinguishing the "T's from the "L's requires an examination of individual elements. (adapted from Julesz and Bergen (1983)).

search of individual elements in the display. The preattentive process was considered to occur instantaneously across the entire visual field (Julesz, 1962; Neisser, 1967; Treisman & Gelade, 1980). In figure 1.4, the effortless separation of "+" and "L" micropatterns is an example of preattentive texture perception while the separation of the "T" and "L" micropatterns requires serial processing. More recent studies suggest that visual processing occurs along a continuum (e.g. Duncan & Humphreys, 1989; Wolfe, 1998) in which preattentive and attentive processing represent the extreme ends. This thesis examines phenomena that fall towards the preattentive end of this continuum.

Similarity between texture segmentation and visual search

Visual search is a paradigm that has largely been used to examine the visual attention dichotomy described above. In a visual search task, the observer scans the visual display looking for an object defined by specified features or combinations of features. (e.g. color, size, orientation). Search types are classified as being one of two types based on the reaction time to find the target as a function of the number of distracters. In a serial search, response time increases with the number of distracters present in the display. In parallel search, the target appears to “pop-out” from the background elements and reaction time is independent of the number of distracters in the display.

There are a number of similarities between “effortless” texture segmentation and “pop-out” in visual search experiments. In both cases, a target is easily distinguished from its background. In many cases, a particular characteristic of a stimulus will lead to both pop-out and effortless texture segmentation. Such is the case for tilted targets embedded in a background of vertical line segments of the same size. However, texture element pairs that lead to pop-out in a visual search paradigm do not necessarily lead to easy texture segmentation and vice versa. Wolfe (1992) demonstrated that the two paradigms may lead to different results when the stimulus is made up of a conjunction or combination of features. For example, parallel search occurred for red vertical targets or green horizontal targets within a background of red horizontal and green vertical distractors but this contrast did not elicit effortless texture segmentation.

Commonly these two paradigms differ in terms of stimulus exposure duration and microelement density/inter-element distance. For example, in the

visual search task the stimulus is presented until a response is made, whereas many segmentation tasks are presented with short exposure durations to limit eye movements. Few studies have examined the differences between these two paradigms directly. When stimulus duration was limited in a visual search task, Meinecke and Donk (2002) found that variations in element density (which they referred to as display size, ranging from 2 elements to 81 elements) accounted for the resulting search pattern. In their study, all displays contained a single line target oriented at $\pm 45^\circ$ embedded in a background of lines with the orthogonal orientation. For relatively small display sizes that were similar to standard visual search displays, target detection declined when the display size was increased and when the target was presented at further eccentricities. As the number of elements in the display was further increased and the display more closely resembled a visual texture, target detection increased along with display density while performance varied across eccentricity. Performance initially increased from the fovea to approximately 4 deg of eccentricity and then declined as the target was moved to further eccentricities. As shown by the results of Meinecke and Donk (2002), texture segmentation and visual search paradigms can lead to different results. One must be cautious in generalizing the results obtained in one paradigm to the other.

Theories of Texture segmentation

A recurring theme in texture perception involves the search for stimulus attributes that give rise to rapid effortless segregation as opposed to attributes that result in a slow effortful processing. It is not always obvious which textures will segregate easily and which will not. For example, Beck (1966) found that an upright letter T was judged to be more similar to a T figure tilted at 45° than to an

upright L. However, when he used these three microelements to form textures, upright Ts and Ls did not produce strong texture segmentation while upright Ts and tilted Ts did. Theories of texture segmentation fall into three main categories; those that attribute texture segmentation to (i) differences between image statistics, (ii) to differences in basic “features” in the image and (iii) differences in the responses of “spatial frequency channels.”

Image Statistics

The early development of texture segmentation theories was dominated by the work of Bela Julesz (Julesz, 1962; Julesz, Gilbert, Shepp, & Frisch, 1973). Julesz (1962) attempted to use statistical analysis of black and white random dot textures to define global properties that allowed for texture segmentation. He distinguished textures on the basis of their n th order joint probability distributions; i.e., the probability that randomly thrown n -gons will fall on particular combinations of black and white points (dots) of the figure. A needle and a triangle are respective examples of 2-gons and 3-gons. The first-order statistics of an image referred to the dot density in the image and represented a measure of overall intensity (or luminance levels). Second-order and higher statistics were related to distributions of intensity within a texture. For example, images with iso-second-order statistics contain identical dot densities and identical probability distributions for pairs of dots at a specified distance from each other within the image but they may differ in probability distributions for dot triplets. Julesz et al. (1973) asserted that effortless texture discrimination was possible when textures differed in first- or second-order correlations but that textures that differed in higher-order statistics could only be segmented on the

basis of effortful serial search. The mechanism by which texture segmentation was accomplished was alluded to but not clearly provided.

Counterexamples provided evidence against this theory. For example, Martin and Pomerantz (1978) demonstrated patterns with identical second-order statistics created by the 180-degree rotations of letter micropatterns that were more discriminable than similar patterns created using mirror reversals that differed in their second-order statistics. They also demonstrated dot patterns differing in second-order statistics that could not be easily separated. Effortless texture discrimination has also been shown in response to quasi-collinear dot patterns (Caelli & Julesz, 1978), "corner" and "closure" texture patterns (Caelli, Julesz, & Gilbert, 1978) with identical second-order statistics. It appears that differences in second order statistics are neither necessary nor sufficient to explain texture segmentation. Julesz, Gilbert, and Victor (1978) found an instance in which a two-dimensional texture with identical third-order statistics could be easily discriminated calling into question whether the conjecture holds for patterns with higher order-statistics.

Image Features

A second approach suggests that effortless texture segregation occurs when neighboring regions differ in elementary features or primitives. For example, Beck (1972, 1982) considered the perception of texture as a synthetic process in which texture elements are grouped using simple properties such as color, brightness, size, and slopes of the texture elements and their parts. According to Beck, the properties that produced similarity grouping were the properties that are easily discriminated in peripheral vision without the use of focal attention. Beck was one of the first to come up with a feature-based theory

but other researchers independently came up with similar feature-based approaches.

This body of research appears to have influenced Julesz's later work. After finding that his statistical analysis of textures did not sufficiently account for texture segmentation Julesz (1981) developed the "texton" theory. He defined textons as simple local textural features that include elongated blobs (with specific color, orientation, width, and length), line terminators, and line crossings. According to texton theory, texture regions are segmented when they differ in texton density. Julesz examined what divided texture regions. One major drawback to a feature-based texture segmentation approach is that it is based upon a "verbal description of image features" (Bergen & Adelson, 1988) and does not place much emphasis upon a neural mechanism by which texture segmentation occurs.

Another drawback of a feature-based texture segmentation approach is the absence of a universal definition of what constitutes an elementary feature or primitive to the texture segmentation process. For example, Vorhees and Poggio (1988) supported the use of blobs as textons but not the line crossings or terminator textons suggested by Julesz. Furthermore, counterexamples to the claims of texton theory indicate that it cannot fully explain texture segmentation. For example, Gurnsey and Browse (1987) demonstrated that differences in terminator and line crossing densities did not result in effective texture segmentation when stimulus configuration differences were controlled. They found that textures that differed in overall size and shape were the most easily segmented regardless of whether or not these textures contained the same density of terminator and line crossing textons.

Despite the drawbacks of feature-based theories as described above, texton theory continues to be explored and improved upon. For example, Von Tonder and Ejima (2000) showed that the variability of anti-textons (i.e., the spaces between micropatterns) may also represent an elementary feature of a texture that can be used in segmentation. Another example is the dual mechanism promoted by Barth, Zetsche and Rentschler (1998) that segments textures using a spatial filtering process tuned to micropattern size at low resolutions but that is sensitive to texton properties such as line endings and line crossing at higher resolutions. Their model suggests how this mechanism may be accomplished using end-stopped neurons, thereby linking the detection of textons to the functions of cells within the visual pathways.

Spatial Filtering

The third type of texture segmentation theory involves the use of spatial filtering to detect texture boundaries. In an attempt to show how texton detection could be accomplished in the human visual system, certain researchers that support a feature-based theory incorporated spatial filtering into their texture segmentation algorithms as a process that occurred prior to feature extraction (e.g. Vorhees & Poggio, 1988; Marr, 1982). For example, Vorhees and Poggio (1988) first divided grey-scale images into “blob” patterns through the use of center-surround filters. Marr (1982) similarly used low-level filters to derive the “raw primal sketch” that divided the image into features such as “bars”, “blobs” and “edges”. Once these primitive features were derived, attributes of these features such as orientation, length and density are derived. These verbal categories of features were similar to those described as textons above. Similar to

the texton theory, changes in feature attribute density occurred across texture boundaries.

Alternatively, it has been proposed that texture discrimination could be explained by simple low-level mechanisms in the visual system, such as a mechanism tuned to differences in micropattern size (Bergen & Adelson, 1988; Gurnsey & Browse, 1987, 1988) without resorting to the use of feature-like properties that were difficult to define. That is, a mechanism using local energy measures derived from the output of oriented filters may underlie texture segmentation. Such models will be reviewed in the section below.

Filter-based Models of Texture Segmentation

A number of researchers have proposed texture segmentation mechanisms that involve at least two levels of filtering of the visual image and include a non-linear component (e.g. Bergen & Adelson, 1988; Gurnsey & Browse, 1989; Landy & Bergen, 1991). The filtering process uses local scale and orientation selective units that are based on properties of cells within the visual pathway. These schemes have been shown to reliably segment a number of textures.

Many computational models of texture segmentation are based upon a filter-rectify-filter mechanism (FRF; e.g., Gurnsey & Browse, 1989; Bergen & Adelson, 1991). A fundamental aspect of these models is the assumption that at least two successive layers of spatial filtering are required. First, the image is filtered using localized linear filters that are tuned to a number of spatial frequencies and orientations (e.g. a Gabor filter, whose impulse response

function is created by the multiplication of a sine wave grating by a Gaussian envelope). The first layer filters perform an analysis of the image at a local level.

The output of this stage is rectified to eliminate negative responses. Methods that have been used to achieve rectification include squaring or taking the absolute values of the outputs of the first filter. The rectification is performed so that all outputs will not be cancelled out during the pooling operation performed during the second filtering stage. The output of this stage results in a number of filtered images, each representing the information available within specific orientation and spatial frequency bands.

A second stage of filtering is performed using lower resolution bandpass filter units with larger receptive fields than those of the first layer filters. One filter that can accomplish this function is the classical center-surround difference of gaussian (DOG) filter. This stage is used to average the outputs of the first layer filters across space and results in a "texture energy" measure. Gradient detection is used to identify image regions where the texture energy changes. It is implied that all filter maps are combined in the process. Lastly, a decision stage determines the boundary of each texture. This process converts texture differences into a form that can be analyzed by conventional edge detection mechanisms. The second layer filters operate over larger regions of the image than first layer of filters. An example of a FRF model is presented in Figure 1.5.

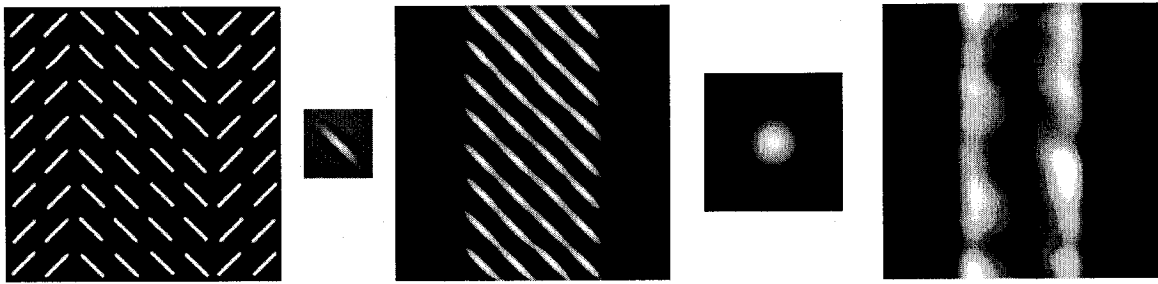


Figure 1.5 FRF model. The texture boundary defined by differences in microelement orientation that represents the input (I) to the FRF model is shown in the leftmost panel. In the next step, I is convolved with the spatial frequency selective filter oriented to 135° seen to the left of I. The middle panel represents the output of this process after the output of the first filtering stage has been rectified. A second stage of filtering is accomplished using the bandpass Gaussian filter represented in the next panel. Boundaries between image regions are clearly illustrated in the output of the second filtering stage seen in the rightmost panel.

Gurnsey and Laundry (1992) distinguished between texture segmentation that occurs on the basis of classifying property differences between regions versus texture segmentation that occurs through edge detection. An edge-based mechanism implies that a clear boundary exists between two adjacent textures while a region-based mechanism implies that textures can be distinguished even when there are intervening regions between textures or when textural properties vary gradually across the visual space. Although texture experiments conducted prior to the 1990s involved the study of adjoining or embedded textures, psychophysical evidence supports the existence of a mechanism that can distinguish separated textures. For example, Gurnsey and Laundry (1992) demonstrated that blurring the boundaries of textures comprising "X" and "L" micropatterns by inserting "transition regions" between the texture regions resulted in a ten percent decline from performance with abrupt boundaries. They found little difference in performance between textures separated by a blank as compared to adjoining textures with an abrupt boundary.

Wolfson and Landy (1998) supported a distinction between edge-based and region-based texture segmentation mechanisms. To examine edge-based and region-based mechanisms, they used two types of textures composed of randomly placed, short, oriented line segments. The first type of textures differed in mean orientation while the second texture type had identical mean orientation with a large variability of line orientation within a texture. For textures with different mean orientations, they found that textures in adjoining regions were easier to discriminate than textures that were separated by a blank region. For textures that differed in microelement orientation variability but not mean orientation, performance was similar when the textures were presented side-by-side or separated by a blank space. Wolfson and Landy (1998) concluded that both edge-based and region-based segmentation mechanisms exist in the visual system.

This recognition of a distinction between two underlying mechanism of texture has significant implications for the study of textures. Computational models of texture segmentation are generally divided into edge-based or region-based approaches. Visual texture models suggest a mechanism for texture segmentation rather than prove that such a mechanism exists. Different approaches have been used to develop FRF models. Therefore, it is not surprising that different models (i.e., different mechanisms) have been used to explain identical phenomena. For example, some models rectify the stimulus by squaring the outputs of the first layer filters while other models assume a half-wave rectification in which negative filter outputs are removed but positive filter outputs remain intact. Depending upon the particular phenomenon being

studied, additional steps may be added to the process. For example, Gurnsey and von Grünau (1997) used an FRF model to explain the perception of subjective contours and included an endstopping mechanism between the two filter layers.

Segmentation models attempt to specify a biologically plausible mechanism by patterning the model after known properties of the visual system. Common to many of the FRF texture models is the suggestion that the first layer filters approximate the function of simple cells in V1 while the second layer filters represent the function of cells in V2 (see for example, von der Heydt & Peterhans, 1989). Evidence that the FRF model can be used to explain a number of visual phenomena provides support of its biological plausibility. Variants of the FRF model have been successfully used to model or explain texture segmentation based on differences in orientation (Bergen & Landy, 1991; Kingdom, Prins, & Hayes, 2003; Landy & Bergen, 1991; Malik & Perona, 1990), contrast (Sutter, Beck, & Graham, 1989), or element arrangement (e.g. striped versus checkerboard patterns; Graham, Beck, & Sutter, 1992; Graham, Sutter, & Venekestan, 1993). FRF-type models have also been applied to the detection of spatial or spatio-temporal variations in non-Fourier stimuli. (Here, Fourier stimuli refers to stimuli defined by variations in mean luminance levels. Non-Fourier stimuli refers to images defined by variations on a dimension other than mean luminance level.) For example, a FRF mechanism has been used to predict the perceived direction of moving plaids (Wilson, Ferrara & Yo, 1992) and moving contrast patterns (Chubb & Sperling, 1988). The model has also been used to explain the detection of illusory contours (Gurnsey & von Grünau, 1997;

Song & Baker, 2006) and detection of global form structure exhibited in glass patterns (Wilson & Wilkinson, 1998).

Limitations on Visual Processing Across the Visual Field

Images of the physical world must be converted into neural signals that can be understood by the visual system in order for an observer to understand the content of the scene. Collections of cells in the retina, lateral geniculate nucleus and the striate cortex form neural arrays that provide the foundation for pattern discrimination. Variations in architecture and function across the visual system result in inhomogeneity in resolution of visual stimuli across eccentricity and impose limits on performance of spatial discrimination tasks. Visual processing can be constrained in a number of ways through means such as optical blur, density and regularity of the photoreceptor mosaic and sampling apertures of individual cones.

Neural response to the visual image begins with the transformation of light energy into changes of the membrane potentials of retinotopically organized light-sensitive neurons. The neural response represents measurements of discrete units of the visual image taken at regular intervals. The response of an individual photoreceptor can be considered as one sample of the image.

The ability to resolve fine detail may be limited by the density or spacing of the photoreceptors that sample the image. According to Sampling theory, to faithfully reproduce a visual stimulus of a particular spatial frequency each cycle of the grating must be sampled at least twice. For example successful measurement of a 50 cycle per degree sine wave requires a sampling rate of 100 cycles per degree or greater. The highest spatial frequency that a neural array can

represent is called the Nyquist limit. When the spatial frequency exceeds the Nyquist limit, the observer may misinterpret the signal as being composed of lower frequencies that fall below the Nyquist limit. This phenomenon is called aliasing (see Wilson et al, 1990, for a review).

The ability to resolve sine wave gratings has been used as a reliable measure of the spatial capabilities across the visual field. The contrast sensitivity function (CSF) measures the visibility of a sine wave grating as a function of its spatial frequency. That is, a contrast detection threshold is determined for each spatial frequency. Sensitivity for gratings of each spatial frequency is defined as the reciprocal of the threshold contrast required to detect the grating. Visual acuity is the spatial resolving capacity of the visual system. Acuity may be defined in terms of the highest spatial frequency resolvable. The maximum resolvable spatial frequency of sinusoidal grating patterns declines rapidly as a stimulus is presented at increasing eccentricities (Thibos, Cheney & Walsh, 1987).

There are optical limits on the signal that reaches the retina. Due to optical factors, no contrast will be registered on the retina in response to high frequency gratings after a certain limit. In foveal vision, optical factors appear to be the limiting factor in visual acuity. Campbell and colleagues (Campbell & Green, 1965; Campbell & Gubish, 1966) showed a close correspondence exists between central visual acuity and the Nyquist limit of approximately 50 to 60 c/deg imposed by the optics of the eye. Optical limits remain relatively constant at 50 c/deg over the central 20 to 30 deg (Campbell & Gubish, 1966, Jennings & Charman, 1981).

In the periphery, visual acuity falls below this limit indicating that factors other than optical limitations may affect visual resolution outside the fovea. Retinal receptor properties are one factor known to limit visibility. The distribution of cone photoreceptors varies with eccentricity in humans and Rhesus monkeys. Merigan and Katz (1990) inferred that the major constraints to primate spatial vision may be present in the retina. They indicated that cone sampling density limits acuity in the central visual field while ganglion cell density has a stronger impact on peripheral acuity.

The highest concentration of cones is found in the fovea and reduces rapidly outside the fovea (Wikler, Williams & Rakic, 1990; Curcio, Sloan, Kalina, & Hendrickson, 1990; Curcio, Sloan, Packer, Hendrickson, & Kalina, 1987). At the fovea in humans, the density of cone spacing is sufficient to record spatial frequencies up to the limits imposed by the optics of the eye. That is, the cone Nyquist limit approximately matches the optical limits in central vision. However, outside the fovea, the cone Nyquist limit decreases rapidly and falls below the optical limits due to a rapid decline in cone density (Curcio, Sloan, Kalina, & Hendrickson, 1990; Marcos, Tornow, Elsner, and Navarro, 1997). Spatial frequencies above the cone Nyquist limit but below the optical limit will be transmitted to the retina but may be distorted due to spatial aliasing. Visibility is further constrained by the Nyquist limit for retinal ganglion cells (Curcio & Allen, 1990) that falls below the cone Nyquist limit. Thibos, Cheney, and Walsh (1987) suggested that grating resolution is limited by ganglion cell spacing whereas limits to pattern detection are related to individual cone size.

The properties of cortical cells are another factor that limit visibility. Physiological investigations have shown that average retinal field size of cortical cells increases with eccentricity (e.g. Hubel & Wiesel, 1974). Experiments that have examined contrast sensitivity suggest how this increase in receptive field size may relate to reduced visibility with increased eccentricity. Contrast sensitivity has been shown to decrease from fovea towards the periphery (Graham, 1981). That is, sensitivity to higher spatial frequencies declines in the periphery. Based on these findings, it has been proposed that visual processing is dependent upon the area of the cortex stimulated. The area of the visual cortex used to analyze a stimulus of constant size decreases as a function of eccentricity. Research showed that foveal and peripheral performance could be equated by magnifying the stimulus (Rovamo & Virsu, 1979; Rovamo, Virsu & Näsänen, 1978). This concept is known as the “cortical magnification factor.”

As described above optical or physical factors, retinal factors and cortical factors can limit pattern discrimination. Optical factors appear to constrain foveal discriminations while retinal and cortical limitations have stronger influences on peripheral vision.

The Central Performance Drop (CPD)

Based on the results of the physiological and psychophysical studies cited above, an observer’s ability to discriminate two textures would be expected to vary when the target texture is placed in different locations in the visual field. That is, target detection would be expected to deteriorate as it is moved to more peripheral locations. Therefore, Kehrer’s (1987) finding that texture discrimination improves as stimuli are moved from fovea to the periphery is

highly counterintuitive. Kehrner referred to this phenomenon as the central performance drop (CPD).

The initial CPD experiments (Kehrner, 1987, 1989) used very similar methodologies. In these experiments, the target is present on half of the trials and the subject is asked to indicate the presence or absence of the target on each trial. The stimulus background consisted of repeated line micropatterns oriented at 45 or 135 degree with a small target pattern consisting of orthogonally orientated lines. The disparate texture region was presented for short stimulus durations at random positions along the horizontal meridian. Stimulus presentation was followed by a backward mask. More recent studies have shown the CPD could be elicited along the vertical (Joffe & Scialfa, 1995) and oblique (Morikawa, 2000) meridians, texture micropatterns are not necessarily restricted to oriented lines (e.g. Meinecke & Kehrner, 1994a) and a backward mask may not be required to elicit the effect in all cases (Morikawa, 2000).

It might be thought that the CPD indicates that subjects use a more conservative criterion at or near fixation. For the CPD to be explained in terms of a more conservative criterion at fixation, subjects would have to show both a drop in hits and an accompanying decrease in false alarms at this location compared to other retinal locations. Using the standard CPD experiment methodology described above, Kehrner (1989) asked observers to indicate the target location on trials in which they indicated a target was present. His results showed that a lower hit rate at the fovea was accompanied by a higher false alarm rate at that location. That is, reduced hit rates reflected a reduced sensitivity at fixation rather than a criterion shift. Gurnsey, Pearson, and Day

(1996) came to the same conclusion based upon a d' analysis conducted across eccentricity. Their results showed that d' drops at fixation relative to the peak of the curve, indicating a real drop in sensitivity rather than a more conservative criterion at fixation.

Explanations of the CPD

A Temporal Explanation

An early explanation for this phenomenon attributed the CPD to differences in neural processing speed for stimuli presented at different locations in the visual field (Kehrer, 1989). Fiorentini (1989) demonstrated that the reaction time to detect targets in a visual search task was elevated for fine textures confined to foveal viewing as compared to a similar size-scaled stimulus presented in the parafovea. Kehrer (1989) also assumed that the processing speed associated with foveal processing is slower than the processing in more peripheral locations. Again, this is consistent with physiological evidence. Physiological evidence supports the existence of different processing speeds across the visual field. Two parallel pathways exist that are specialized for different aspects of visual processing: the magnocellular (M) and parvocellular (P) pathways. Parvocellular fibres respond well to higher spatial and lower temporal frequencies while magnocellular fibres respond better to lower spatial and higher temporal frequencies (Livingstone & Hubel, 1988). The ratio of parvocellular fibres to magnocellular fibres is higher in the fovea than in the periphery (Azzopardi, Jones, & Cowey, 1999; Connolly & Van Essen, 1984). Mechanisms selective for low spatial frequencies in the M pathway process

information faster than mechanisms specialized for high spatial frequencies in the P pathway (Schmolesky & al., 1998); again, consistent with Kehrers theory.

Kehrers theory required the additional assumption that the sensitivity for low spatial frequencies peaks in the periphery and declines towards the fovea. This assumption is somewhat questionable (De Valois & DeValois, 1988; Wright & Johnston, 1983).

At a very basic level, the CPD is dependent upon relatively short presentation times. When observers are allowed to view a visual texture for unlimited amounts of time, most textures would be discriminable. It has been demonstrated that increasing the stimulus duration from 40 to 80 or 120 ms leads to a weakening of the CPD (Kehrer, 1989). Psychophysical experiments have demonstrated that visual processing speed increases with eccentricity in target detection (Carrasco, McElree, Denisova, & Giordano, 2003) and visual search (Fiorentini, 1989) tasks, supporting Kehrers assumption of differences in processing speed across the visual field. However, according to a temporal explanation of the CPD, the effect should be elicited when processing time is limited by a stimulus mask. The fact that the CPD has been demonstrated in the absence of a mask (Morikawa, 2000) suggests that temporal factors alone are not sufficient to explain the CPD.

Another problem for a temporal account is the finding that, at least in some cases, the absolute level of performance dropped as the performance peak moved to greater eccentricities (Gurnsey et al., 1996; Kehrer, 1989). To be consistent with a temporal explanation for the CPD, overall performance should increase as the peak performance is moved towards the periphery because

processing speed is faster in the periphery while an opposite pattern would be seen when the peak is shifted towards the fovea (Kehrer, 1997).

A Spatial Explanation

Gurnsey, et al. (1996) attributed the CPD to a mismatch between the scale of the texture displayed at the fovea and the scale of the mechanisms responsible for encoding the texture differences at that location. It is also assumed that the scale of the spatial mechanisms varies with eccentricity. In effect, this theory suggests that a CPD occurs when cortical receptive fields receiving input from the fovea are too small to effectively analyze the texture while receptive fields receiving input from the far periphery are too large.

The spatial explanation is supported by evidence that the location of the performance peak associated with the CPD is dependent upon the spatial frequency content of a stimulus. Joffe and Scialfa (1995) observed that the eccentricity corresponding to peak performance was inversely related to spatial frequency. This has been studied in several ways. Kehrer (1989) manipulated inter-element spacing and found that the peak target detection moved further toward the periphery for increased inter-element spacing and more toward the fovea for decreased inter-element spacing. However, this manipulation also changed the texture gradient (or microelement density). Similar results were obtained for cases in which the frequency of the stimulus was altered independently of the texture gradient by changing the size of the stimulus while keeping the inter-element ratio constant (Joffe & Scialfa, 1995) or by changing the viewing distance (Gurnsey et al., 1996). The performance peak moves to greater

eccentricities at near viewing distance, indicating that the effect is not retinally specific.

In a study of the effect of attention on the CPD Yeshurun and Carrasco (1998) found that attentional manipulations can produce effects similar to those found by directly altering the spatial frequency of the stimulus. According to their “resolution hypothesis” attention alters performance by increasing spatial resolution at the attended area in spatial resolution and orientation discrimination tasks (Carrasco, Penpeci-Talgar, & Eckstein., 2000; Yeshurun & Carrasco, 1999). Precuing target location in a texture segmentation task that elicits the CPD led to a shift in the performance peak to a further eccentricity (Yeshurun & Carrasco, 1998). They suggested that cueing changes the size of the mechanism analyzing the stimulus, thereby leading to a decrease in filter size. That is, the cue results in an analysis by a higher frequency selective mechanism at the attended location.

Furthermore, computational models based on spatial factors have successfully approximated the responses obtained in psychophysical experiments (e.g. Kehrner, 1997, 2003; von Berg, Ziebell, & Stiehl, 2002). Using a filter-rectify-filter model of the type described above Kehrner and Meinecke (2003) attributed the CPD to the second-filter layer. When they tested their model against psychophysical results, they set the parameters of their first layer filters in a way that resulted in a performance peak in central vision. The response to the second layer of filtering resulted in a performance decrement in central vision.

Yeshurun and Carrasco (2000) used textures composed of narrow-band Gabor patches in an attempt to determine whether the first or the second filter layer underlies the CPD. They considered the first layer of filtering to provide a local analysis of spatial frequency and orientation while the second filter layer was tuned to lower spatial frequencies that provide an analysis of image structure over a larger region. Using Gabor patches of different spatial frequency, they expected that if their attention manipulation influenced the first filter layer, they would find that performance peaks at a further eccentricity for the lower frequency Gabor patches. When they demonstrated results that were largely independent of the spatial frequency of the Gabor patch, they argued that the CPD is attributable to the influence of the second filtering layer. In summary, two explanations that concentrate on either temporal factors or spatial factors have been used to explain the CPD.

Texture Discrimination Asymmetries

Many recent studies show that texture discrimination may depend on which texture makes up the foreground (target) and which makes up the background (larger visual field). For example, texture A embedded in texture B may be easier to detect than texture B embedded in texture A. This is referred to as a visual texture discrimination asymmetry. Such asymmetries have been noted in a number of texture discrimination studies (e.g. Gurnsey & Browse, 1987, 1989; Meinecke, 1989; Meinecke, & Kehrner, 1994; Meinecke, Kimchi, & Grandegger, 2002; Rubenstein & Sagi, 1990, 1996; Williams & Julesz, 1992). Similar asymmetrical performance had been shown in visual search tasks (e.g. Treisman & Gormican, 1988; Treisman & Souther, 1985). Figure 1.6 shows an example of

textures composed of “L” and “X” micropatterns that give rise to an asymmetry (Gurnsey & Browse, 1987). Under conditions of short exposure durations, their subjects found the L in X textures much easier to segment than the X in L textures.

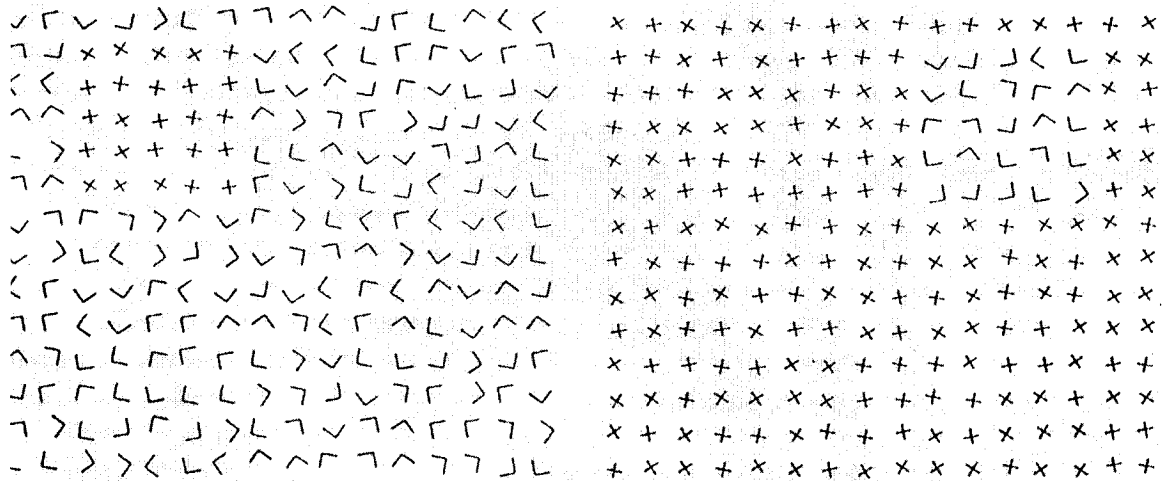


Figure 1.6 Example of visual texture asymmetry taken from Gurnsey and Browse (1988). The left panel shows a region of Ls embedded in a background of Xs. The right panel is the resulting texture when micropattern positions are reversed.

The existence of asymmetrical detection might seem to pose a problem for linear filter models because micropattern distribution would not change across the texture border. If texture segmentation relied on the analysis of local features exclusively, asymmetries would not occur. This suggests that the procedure that underlies texture discrimination is not limited to the distribution of “features” in the neighborhood of the texture boundary. A comprehensive account of asymmetries does not yet exist, however, three candidate explanations will be discussed below.

Weber-type explanations

One of the first explanations of discrimination asymmetries comes from experiments using the visual search paradigm. Anne Treisman and colleagues

developed the Feature Integration Theory (e.g. Treisman & Gormican, 1988; Treisman & Souther, 1985) that attributed visual search asymmetries to core feature properties present or absent in the target and distractor elements. They assumed that visual images are first decomposed into elementary features such as color, orientation and size and that these are represented in separate “feature maps.” The feature map indicated the presence of a feature in a display. They asserted that a search asymmetry occurs when a single feature is present in either the target or the distractors but is absent or reduced in the other. A target will be easily detected when it contains a unique feature; i.e., a feature that is absent (or of lower magnitude) in the distractors. A target will be much harder to detect when the background contains a feature that is absent (or of lower magnitude) in the target. Consider a pair of circles, one with an intersecting line and one without an intersecting line. A circle with an intersecting line embedded in a background of plain circle elements is easier to detect than the obverse case. According to this theory, the target with the unique stimulus feature activates a prototypical channel common to both target and background elements while also activating its own channel. When the target and the context elements are reversed, it is hard to detect the target because there is little difference in the activation rates of the two channels when the target is present versus when it is absent.

To explain asymmetries between element features that vary along a quantitative dimension (e.g. shorter versus longer lines), Treisman and Gormican (1988) extended their theory to suggest that an application of Weber’s Law would determine the discriminability between the target and background

elements. According to Weber's law, the size of a just noticeable difference between the target and the background would be a constant proportion of the background elements. To decide whether the target is present in a display, the observer would compare the activity generated in that feature channel in response to a display containing the target with an identical size display containing only distractors. An asymmetry occurs when there is a difference between the activity level generated by the target and background elements. It is easier to detect targets that generate a higher level of activity in a background of distractors that generate a lower level of activity than *vice versa*.

Gurnsey and Browse (1987, 1989) expanded the study of detection asymmetries to visual textures. Their displays had the structure shown in Figure 1.6 above and they required subjects to identify the disparate quadrant in the display. They preferred to explain the asymmetry in terms of general image properties that could be measured by mechanisms that perform simple computations rather than resorting to the use of highly specific features. They indicated that it would have been difficult for them to apply Treisman and Souther's explanation relating to asymmetries based on feature differences to their experiments. Since target location is not a direct output of the feature map, Feature Integration Theory may not be able to predict the results of a target detection task in which the target was identified by location. However, they supported Treisman and Gormican's (1988) Weber-type explanation for the emergence of asymmetries.

Gurnsey and Browse (1989) suggested that asymmetries arise when the responses of local visual operators or simple receptors are normalized according

to the degree to which similarly tuned cells are responding within an image. In other words, targets that produce a strong signal relative to the context signal will segment more easily.

Signal Detection (Noise-based) Explanations

Rubenstein and Sagi (1989) discussed how asymmetrical texture discrimination is related to “distinct noise characteristics” contained in all texture stimuli that are essentially caused by spatial-variability within the stimulus. For example, if we examined rotated “L” and “X” shaped patterns, there would be more orientation variability in the Ls than the Xs because the Xs are symmetrical but the Ls are not. They proposed that it would be more difficult to detect a texture boundary within a noisy background than it would be to detect the same boundary with a less noisy background. Using a two-stage filtering model, they demonstrated a good correlation with the psychophysical results of Gurnsey and Browse (1987). Rubenstein and Sagi limited their examination solely to the study of orientation variability as the noise factor; no circular or curved patterns were examined. Using the space between microelements, Von Tonder and Ejima (2000) found similar results. Their subjects reported stronger texture segmentation for regions containing irregular anti-textons embedded in regions containing more regular spaces between microelements than vice versa.

A Subjective Completion Explanation

Williams and Julesz (1992) disagreed that asymmetries were attributable to Weber’s Law or orientation variability based on their demonstration of asymmetries in two-element textures comprising open and closed circles. They used a display containing only two elements to examine whether an asymmetry

could be attributed to specific element features. One element served as the target and the other served as the distractor. Observers were required to indicate whether the stimulus contained a target and a distractor or two distractor elements. They asserted that according to Weber's Law texture discriminability will be independent of the number of targets and distractors when the number of target and background elements are equal. They rejected the Weber explanation after they found that discriminability decreased when the number of targets and distractors were increased in equal proportions. The orientation variability explanation was rejected because they were able to show that asymmetries can be present in stimuli in which spatial variability is largely absent within the stimulus. Williams and Julesz (1992) posited that this particular asymmetry was explained by subjective closure.

Studies of visual texture asymmetries have usually presented target displays at or near the center of the visual field. Meinecke, Kimchi, and Grandegger (2002) is one of the only studies to examine the effect of visual texture across eccentricity. They studied several effects related to texture discrimination asymmetries including element density, spatial jitter of the elements and distance of the target from the fovea. In the experiment where texture elements were densely distributed and jitter was absent, a CPD occurs in one stimulus of an asymmetrical stimulus pair but not the other. However, they were not specifically examining this effect they gave little explanation for why this may have occurred. Given that little is known about how texture asymmetries change across the visual field, it may be useful to further examine how texture asymmetries change as a function of eccentricity using

micropatterns known to elicit asymmetries and to verify whether there are common factors between the CPD and texture asymmetries.

Cross-Frequency Inhibition

Cross-frequency inhibition or cross-frequency interference refers to a condition in which information in one spatial frequency band interferes with access to information in another spatial frequency band. Cross-frequency interference has been used to explain the perception of quantized images. Harmon and Julesz (1971) modified a portrait of Abraham Lincoln by coarse quantization of the gray-levels. This transformation made the picture unrecognizable even though the transformed image retained the lower spatial frequencies of the original image that were sufficient to recognize the subject (Lincoln). They claimed that the spurious higher spatial frequencies introduced by this transformation effectively masked the lower spatial frequencies that were present. Recognition of the image was recovered by blurring the stimulus. This effect is illustrated in Figure 1.7

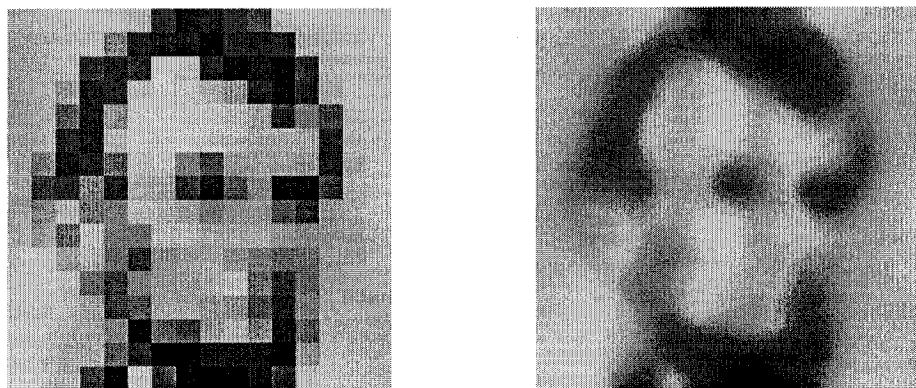


Figure 1.7: Illustration of the effects of cross-frequency inhibition, In the left panel, a block portrait of Lincoln similar to that used in Harmon and Julesz (1973) is shown. Blurring the image makes the face easier to recognize as can be seen in the panel on the right.

Morrone, Burr, and Ross (1983) argued against the cross-frequency inhibition hypothesis because they were able to demonstrate that the recognition of a similarly transformed portrait of Mona Lisa can be improved without resorting to low-pass filtering of the image. Instead they added further high-frequency noise to the quantized image. While it was true that recognition of the portrait did not require removal of the high frequency information in the transformed image, the added high frequency noise served as a mask to the spurious high frequency information in the image. That is, attenuating the high frequency information by masking allowed the image to be processed by a mechanism that employed lower spatial frequency tuning.

Cross-frequency inhibition was also demonstrated in grating induction (McCourt & Foley, 1985). They found that the presence of a higher frequency grating in the inducing field reduced the contrast of lower frequency inducing gratings that co-existed in the same field. Conversely, grating induction was enhanced when interfering gratings of lower spatial frequencies were also present in the visual field. They suggested that each spatial frequency channel inhibits all channels tuned to lower spatial frequencies and may represent a mechanism which involves the suppression of redundant low-frequency information.

Meinecke and Kehrner (1994b) showed that the addition of equally spaced dots to a visual texture made of angular element micropatterns enhanced the CPD while performance in the periphery was improved. They argued that the higher frequency elements of the stimulus (i.e., the dots) masked responses to low- frequencies in the display and resulted in reduced texture segmentation that was largely restricted to a small region of the fovea. This would be consistent

with the fact that the ratio of fibers that respond preferentially to higher spatial frequencies (parvocellular fibers) to fibers that respond preferentially to lower spatial frequencies (magnocellular fibers) is higher in the fovea than in the periphery (Connolly & Van Essen, 1984). Their low pass filtering of these images clearly showed there could be an inconsistency between the information carried by the higher frequencies in the image and the lower frequencies.

Research indicates that sensitivity to high spatial frequencies degrades with distance from the fovea while sensitivity to low spatial frequencies remains constant across the visual field (e.g. DeValois & DeValois, 1988; Wright & Johnston, 1983). This indicates that high frequency mechanisms are well represented at the fovea. An electrophysiological study by DeValois and Tootell (1983) demonstrated a preference for high over low spatial frequencies in neurons of the striate cortex of the cat. In their study almost all of the simple cell responses measured showed significant inhibition of their preferred spatial frequency in the presence of a grating of a different spatial frequency. Of the cells that showed inhibition, approximately 90% were maximally inhibited following the addition of a grating that was two to three times higher than their optimal spatial frequency. Only 16% of the cells were inhibited by the addition of lower spatial frequency information. Taken together these two studies support the possibility that cross-frequency inhibition may influence the processing of information at the fovea. A normalization process such as a process that divides the responses of individual neurons by the total response from a set of neurons may explain the difference in sensitivity patterns of different spatial frequency mechanisms across the visual field (Heeger, 1992, Graham & Sutter, 2000). As the

neurons responsive to high spatial frequencies are concentrated at the fovea, this mechanism would have more of an effect at or near that location.

Yeshurun and Carrasco (2000) suggested that attention may serve to enhance higher spatial frequency information at the attended location by selectively increasing the sensitivity of the smallest receptive fields there. They further suggested that the enhancement of the smallest receptive fields could serve to inhibit sensitivity to lower spatial frequencies at the same location. Yeshurun and Carrasco (2000) indicated that a normalization process as described above may be responsible for this cross-frequency interference and could also be used to explain the CPD found in studies using line stimuli. Stimuli composed of line elements that were used in many of the early CPD studies are broadband stimuli that activate filters of different scales. Some of the filters activated would be higher spatial frequency filters that are not optimal for the task. According to this line of reasoning, the high frequency filters would obscure the low frequency information present in the image.

Some researchers have directly examined whether the inhibition of low spatial frequency mechanisms by high spatial frequency mechanisms at the fovea is responsible for the CPD (e.g. Carrasco, Loula & Ho, in press; Gurnsey & al., 1996; Morikawa, 2000). A cross-frequency inhibition explanation for the CPD represents an elaboration of a spatial explanation for the CPD. In addition to a mismatch between the texture scale and the texture segmentation mechanism, this theory assumes that non-optimal high-frequency filters contribute to the normalization process.

When low-pass filtering was used to remove high-frequency information from the stimulus, the results were equivocal. Gurnsey et al. (1996) found that

overall performance generally declined and there was no improvement in foveal performance as more high-frequencies were filtered out. Using a texture composed of a single line of micropatterns, Meinecke (1989) found that defocusing the stimulus led to increased performance near the fovea. However, overall performance appeared to decrease. Morikawa (2000) found that the CPD was eliminated with low pass filtering of the stimulus. Recently, Carrasco, Loula and Ho (in press) reduced the influence of the high-frequency signal by having the subjects adapt to sinusoidal gratings of different spatial frequencies before the test stimulus was presented. Their results suggest that the CPD is markedly reduced after adaptation to high- but not to low-frequency adaptation. Because the results of all these studies are not consistent, a re-examination of whether cross-frequency inhibition underlies the CPD appears justified.

Overview of the thesis

The series of research projects described in this thesis builds on previous research that attempted to explain how the human visual system segregates two-dimensional image textures across eccentricity.

Chapter 2 presents three experiments that examine the necessity of backward masking in eliciting the CPD. A temporal explanation asserts that the CPD will not occur in the absence of a backward mask. However, a spatial account for the CPD suggests that the backward mask serves as a source of spatial noise. We used an alternative method to introduce spatial noise into the stimulus that does not require the use of a backward mask to limit performance.

Chapter 3 presents two experiments examining visual discrimination asymmetries across the visual field for visual textures previously demonstrated to elicit asymmetrical texture discrimination. Most asymmetry experiments have

restricted stimulus location to the fovea which does not allow for a determination of whether the asymmetry remains invariant across the visual field. For texture pairs that have been previously shown to elicit asymmetries, we examined whether that the asymmetry is dependent upon stimulus location and whether either or both of the asymmetrical texture pairs give rise to the CPD.

Chapter 4 presents three experiments in which the effect of cross-frequency inhibition on the CPD is reexamined. Three previous studies considered the effect of the removal or attenuation of high-frequency components of a stimulus on the CPD. However, the results were equivocal due to inconsistencies in the results across studies and procedural ambiguities within two of the studies. We attempted to address the confounds presented in the previous studies to determine whether CFI is an underlying factor in the CPD.

Chapter 5 provides a summary of the empirical results and suggestions for future research.

CHAPTER 2

**BACKWARD MASKING IS NOT REQUIRED TO ELICIT
THE CENTRAL PERFORMANCE DROP.**

by

CINDY POTECHIN AND RICK GURNSEY

**DEPARTMENT OF PSYCHOLOGY
CONCORDIA UNIVERSITY**

ABSTRACT

In some circumstances, texture discrimination performance peaks in the parafovea rather than at the fovea. Kehrner (1987) referred to this phenomenon as the central performance drop (CPD). In most studies showing the CPD, task performance has been limited by a backward mask. Morikawa (2000) has argued that in these studies the backward mask was critical to the emergence of the CPD. In three studies, we use textures comprising left and right oblique line segments and limit performance by manipulating the orientation variability within the foreground and background textures. Using this method we demonstrate that significant CPDs emerge whether or not there is a backward mask. We conclude that in past studies of the CPD the backward mask functioned primarily as a source of spatial noise and that its temporal relation to the texture display is not critical to the emergence of the CPD.

INTRODUCTION

Psychophysical studies have demonstrated that visual performance generally deteriorates as a target of fixed size appears at greater eccentricities (Rovamo & Virsu, 1979). This is referred to as the eccentricity effect. Explanations of the eccentricity effect have referred to changes in cone density and receptive field size with eccentricity and cortical magnification (see Wilson et al., 1990 for a useful review).

Kehrer (1987) showed a striking counter-example to the usual eccentricity effect using a texture discrimination task. He found that the detection of oblique lines of a particular orientation embedded in a larger background of orthogonally oriented oblique lines improves as the target texture is moved away from the fovea. Kehrer coined the term 'central performance drop' (CPD) to denote the sub-optimal detection performance at foveal or near-foveal locations.

Kehrer (1989) argued that the CPD could be understood on the assumption that the visual system responds more quickly to low frequencies than to high frequencies. He suggested that a texture boundary presented at the fovea is segmented on the basis of differences in high frequency content between the disparate and background regions. A mask presented at a stimulus onset asynchrony (SOA) of 50 ms (for example) could interfere with the completion of segmentation based on higher frequencies at the fovea. However, segmentation based on lower frequencies available in the periphery might be completed prior to the onset of the mask. The existence of the CPD leads to the further assumption that low frequencies are not processed as effectively in the fovea as in the periphery. Therefore, Kehrer posited an association between the frequency

selectivity of spatial filters, their sensitivity at different eccentricities and their speed of operation.

Gurnsey, Pearson and Day (1996) argued that the CPD could be understood without appealing to differences in the processing speed of frequency selective mechanisms. Like Kehrner, they suggested that textures are segmented based on the responses of high frequency information at the fovea and low frequency information in the periphery. They further assumed that the effective region over which textures are compared is tied to the scale of the frequency selective mechanisms involved. Thus, at the fovea smaller regions are compared than in the periphery. In other words, segmentation at the fovea is based on the responses of small mechanisms tuned to high frequencies whereas segmentation in the periphery is based on the responses of large mechanisms tuned to low frequencies. Consequently optimal performance will occur when the scale of the texture (in this case defined by inter-element spacing) is matched to the scale of the available segmentation mechanism. At the fovea the segmentation mechanisms are actually too small relative to the textures whereas in the far periphery they are too large. However, at some intermediate eccentricity the texture and mechanism are optimally matched thus yielding a performance peak.

The spatial account of the CPD has been supported by results showing that segmentation performance peaks at different eccentricities when the texture scale is modified through changes in texture element size (Joffe & Scialfa, 1995), inter-element distance (Kehrner, 1989), or viewing distance (Gurnsey & al., 1996; Yeshurun & Carrasco, 1998). As well, the assumptions of the spatial theory can be used to model data from several experiments showing the CPD (Kehrner, 1997;

von Berg, Ziebell & Stiehl, 2002). Furthermore, Yeshurun and Carrasco (1998) demonstrated that the texture discrimination performance peak can be shifted further into the periphery by drawing attention to the location of the disparate region with an exogenous cue. The observed shift in the performance peak was predicted from physiological results showing that attention reduces the size of cortical receptive fields (e.g., Desimone & Duncan, 1995; Moran & Desimone, 1985).

Kehrer's temporal theory suggests that the CPD should not occur in the absence of a backward mask whereas the spatial theory treats the mask as a source of spatial noise. Simply eliminating the backward mask, however, does not allow us to distinguish between the two theories because doing so leads to ceiling performance at all eccentricities (e.g., Joffe & Scialfa, 1995). Morikawa (2000) attempted to distinguish between these two theories. He employed a four alternative forced choice (4AFC) task in which subjects were to identify the quadrant containing a disparate texture (left and right obliques as in the top panel of Figure 2.1). When performance was limited by a backward mask there was a clear CPD. However, when a simultaneous noise mask (single pixel noise dots having a density of 6 - 7%) was used to limit performance no CPD was obtained; i.e., the usual eccentricity effect was observed. As well, when performance was limited by reducing the length of the lines comprising the textures the usual eccentricity effect was again found.

A backward mask was not necessary in all cases, however. When micropatterns comprised elements whose orientation was conveyed by the virtual line connecting two dots (or very short line segments) then textures differing in the orientations of these virtual lines produced a very robust CPD

without a backward mask (Morikawa, 2000, Experiment 4). These results demonstrate very clearly that a backward mask is not required to elicit the CPD in all cases.

When the 'virtual line' stimuli were filtered and contrast normalized to enhance the low frequency components of the display the CPD was eliminated (Morikawa, 2000, Experiment 5). These filtered stimuli no longer resembled the the virtual line stimuli from which they were derived. Rather, they looked more like the line segment textures used in previous studies demonstrating the CPD (e.g. Kehrner, 1987, 1989; Joffe & Scialfa, 1995; Gurnsey et al., 1996; Yeshurun & Carrasco, 1998). Therefore, Morikawa argued that the weight of evidence from his experiments supports the idea that texture comprising line segments (e.g. Kehrner, 1987, 1989; Joffe & Scialfa, 1995; Gurnsey et al., 1996; Yeshurun & Carrasco, 1998) do not elicit a CPD unless a backward mask is employed. From this he argued that the temporal theory provides a better account of the data from previous experiments.

We note a few points that may undermine this conclusion. First, it is not necessarily the case that all textures produce a CPD. For example, consider the textures comprising very short line segments (Morikawa, 2000, Experiment 3). These results can only be used to argue for the importance of a backward mask if the stimuli involved elicit the CPD in the presence of a backward mask. Unfortunately, this condition was not tested. On the other hand, one could argue that reducing the length of the lines produced a very difficult task. In fact, performance reached only 75% correct (in a 4AFC task) at an exposure duration of 106 ms. For longer lines (e.g., Figure 2.1) this would have produced a ceiling effect. Given the greater difficulty of the task, subjects may have been forced to

search element by element through the display in order to locate the target region. In this situation one might well expect the normal eccentricity effect rather than the CPD (e.g., Carrasco & Frieder, 1997).

Morikawa's second experiment employed lines of length and density comparable to those in Figure 2.1 but performance was limited by a sparse noise mask. Although the mask has a flat power spectrum it may have been more effective in the periphery than at fixation. That is, because the mask comprised relatively sparse dots the failure to find a CPD may indicate that subjects found it easier to segment the mask from the texture at fixation, where spatial resolution is high, than in the periphery where spatial resolution is low. This argument would be easily refuted if the sparse noise mask had produced a CPD when used as a backward mask. Unfortunately, this condition was not run so it is not known if this combination of stimulus and mask would produce a CPD in the usual testing conditions.

We conclude that the question of whether a backward mask is necessary to elicit the CPD is still open. Our purpose in this paper is to derive an alternative method of limiting performance in a texture discrimination task without the use of a backward mask. Our method attempts to avoid the confounding mask/stimulus properties across eccentricities.

In all three experiments reported here, foreground and background textures were composed of lines with a mean orientation of $\pm 45^\circ$. Within each texture region individual texture elements were chosen at random from a flat distribution of orientations. The range of sampled orientations is referred to as "orientation bandwidth." Examples of stimuli of different bandwidths are shown in the bottom four panels of Figure 2.1; note, in all cases the two textures have

the same bandwidths. A bandwidth of 1 means that all lines have the same orientation. A bandwidth of 180 means all orientations are equally probable. The expectation is that as the orientation bandwidth increases the textures would become harder to discriminate. This method of limiting performance has been used previously in texture and symmetry studies (e.g., Wolfson & Landy, 1998; Kingdom, Keeble & Moulden, 1995; Dakin & Hess, 1997; Motoyoshi & Nishida, 2001).

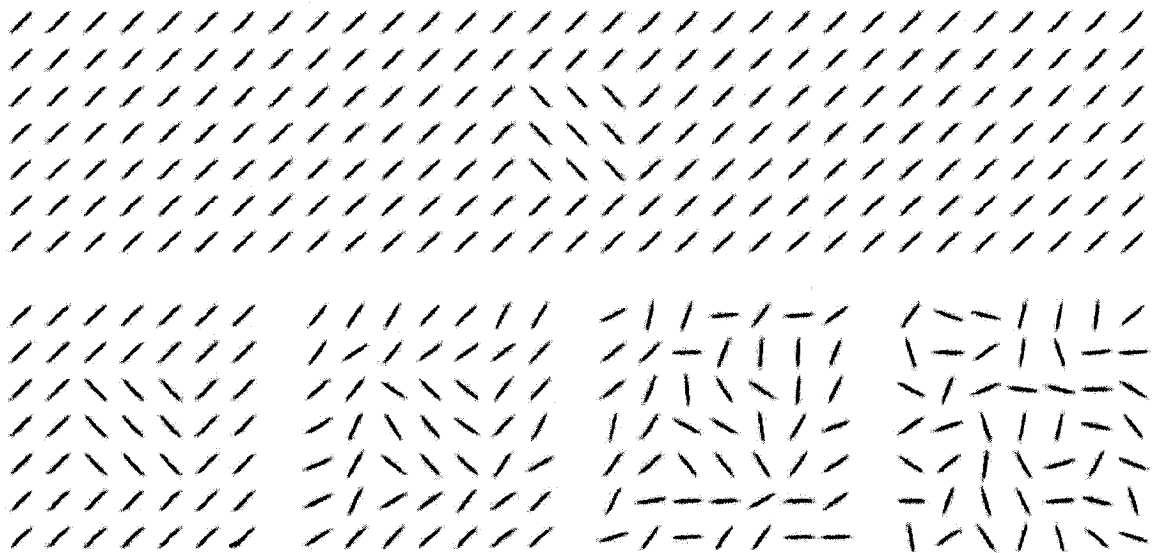


Figure 2.1. Top. Stimulus set-up used in Experiment 1 and 2. The average orientation of the line elements of the foreground is 135° and the average orientation of the line elements of the background is 45° . Bottom. Examples of different bandwidths. Starting with the texture at the left and moving to the right, these patches show increasing bandwidths in the range of 1 to 170.

EXPERIMENT 1

The purpose of Experiment 1 is to assess the utility of the bandwidth manipulation to limit performance in conjunction with a backward mask. Percent correct responses in a 2AFC task were measured at each eccentricity for a range of orientation bandwidths. The bandwidth eliciting 75% correct responses was defined as the threshold bandwidth.

METHOD

Subjects

Four subjects participated in the experiment. Three subjects were experienced psychophysical observers and one was naïve. All reported normal or corrected to normal vision.

Apparatus

The stimuli were presented on a Macintosh G4 computer attached to a 21" monitor having a frame rate of 85 Hz and a resolution of 1600 X 1200 pixels. The stimulus elements were presented in black (0.11 cd/m²) against a white background (89 cd/m²). The experiment was conducted under low ambient lighting conditions. A viewing distance of 120 cm was maintained through the use of a chin rest.

Stimuli

The stimulus display consisted of 350 (7 rows x 50 columns) patches of 32 pixels squared each. Each patch contained one line element of an approximate length of 0.14° of visual angle. The lines were smoothed to eliminate aliasing. On each trial, a nine-element target (3 rows x 3 columns) was embedded in the background. Within each texture, the average orientation of elements was either 45° or -45° from vertical drawn from distributions having bandwidths 30, 40, 53, 71, 95, 127 and 170°. Clockwise and counterclockwise rotations of the elements were varied from trial to trial so that the detection of a line element of a particular orientation could not be used to determine the presence of the target.

A slight positional jitter (± 6 pixels horizontally and vertically) was introduced into the placement of the texture elements to minimize the

contribution of long range grouping phenomena. The stimulus display subtended 17.61° in the horizontal and 2.54° in the vertical direction. The size of the target texture was 1.09° in both the vertical and horizontal directions.

Procedure

Each trial consisted of a fixation screen, the presentation of two masked textures in succession and a response screen. One of the textures contained a disparate region having a mean orientation 90° different from the background texture and the other contained no disparate region. Subjects indicated whether the disparate region appeared in the first or second interval by clicking the mouse once or twice respectively. The duration of the stimulus presentation ranged from 83.3 to 200 ms and was adjusted for each subject individually so that the range of bandwidths tested covered a performance range from chance to 100% accuracy. For each subject the exposure duration was constant throughout the experiment. Each stimulus was followed by a mask comprising randomly rotated "+" elements presented for 333 ms. There was a 667 ms interval following the offset of the mask in the first interval and the onset of stimulus in the second interval.

Prior to each trial two vertical bars (3 pixels wide by 75 pixels high) appeared 1.7° from the left-hand edge of the stimulus display above and below the region in which the stimulus was to appear. Subjects were instructed to fixate midway between these two bars. On the initial trial of a block the appearance of the fixation bars signaled the subject to press the spacebar to initiate the first trial. The fixation bars were colored blue during the stimulus presentation and changed to red when the subject was required to provide a response. On all

subsequent trials, the fixation bars appeared immediately after the response on the previous trial. On these trials the first texture display appeared 1000 ms after the onset of the fixation bars.

A single bandwidth was tested in each block and the disparate regions were placed at one of eleven positions along the horizontal meridian ranging from 0° to 12.31° to the right of fixation (0.00, 0.27, 0.55, 0.81, 1.19, 1.76, 2.61, 3.86, 5.70, 8.39, and 12.31°). Eccentricities were chosen randomly on each trial subject to the constraint that each eccentricity was presented only once in each sequence of eleven trials. Each eccentricity was presented 25 times per block for a total of 275 trials per block and all subjects completed 2 blocks per bandwidth. Therefore each subject participated in 3850 trials in the experiment (11 eccentricities \times 7 bandwidths \times 25 replications \times 2 blocks).

RESULTS AND DISCUSSION

The probability of correct detection was calculated for each bandwidth at a number of eccentricities. At each eccentricity, the data were fit using a best fitting cumulative Gaussian that was normalized to a range of .5 to 1. Figure 2.2 shows the percentage of correct responses as a function of orientation bandwidth for one subject at 3.86° eccentricity. The best fitting curve (solid line) was used to determine threshold bandwidth. Threshold bandwidth was defined as that corresponding to 75% correct detection performance. In this case, the threshold bandwidth was 93.

Threshold bandwidth indicates the level of noise that a subject can tolerate in a particular texture. A higher threshold bandwidth indicates that the subject has more tolerance for noise in that stimulus; in other words, greater noise tolerance indicates greater sensitivity to texture differences. A CPD is

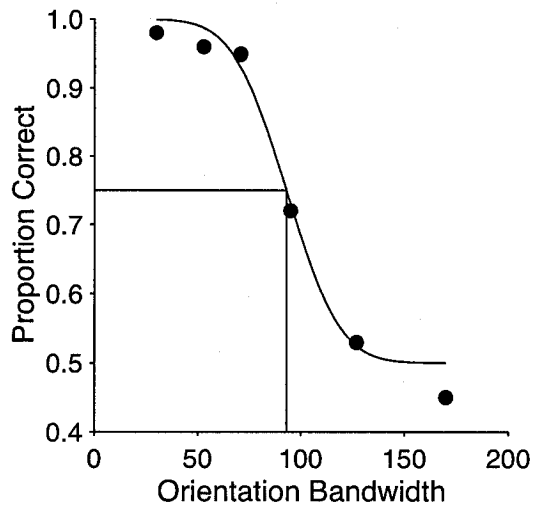


Figure 2.2. The percentage of correct responses is shown as a function of orientation bandwidth. The resultant curve shown here represents data obtained for one subject at one eccentricity. In this case, the threshold bandwidth was 93.

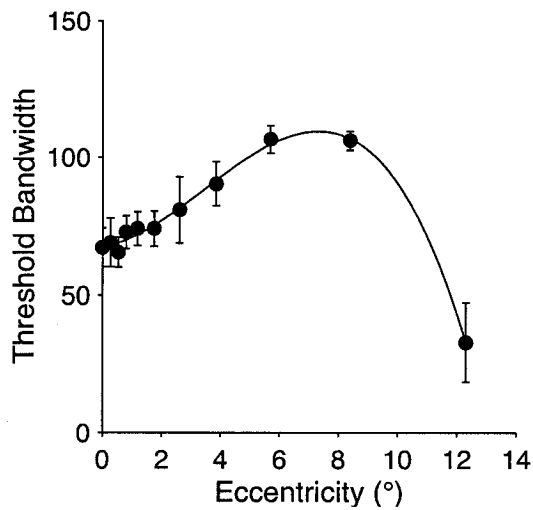


Figure 2.3. Results of Experiment 1. Orientation bandwidth is shown as a function of eccentricity. Bandwidth threshold levels peaked in the parafovea, with reduced thresholds occurring towards both the fovea and the periphery. That is, a CPD was demonstrated.

demonstrated when threshold bandwidth increases with eccentricity.

For each subject, the threshold bandwidths were found at each eccentricity. The results are summarized in Figure 2.3. A one way ANOVA was used to analyze the data, using threshold bandwidth as the dependent measure.

Detection performance peaked in the parafovea, with reduced performance occurring towards both the fovea and the periphery [$F(3, 10) = 6.273, p < 0.01$]. A linear trend analysis showed that there was an increase in hit rate from the fovea to 8.39° from fixation [$F(1, 3) = 60.346, p < 0.01$].

The temporal account of the CPD might suggest that there should be some relationship between exposure duration and the magnitude of the CPD. One way to quantify the magnitude of the CPD is to calculate the slope of the threshold as a function of eccentricity from fixation to the peak of the performance curve. The correlation coefficient between slope and exposure duration was -0.68 , indicating a tendency for the magnitude of the CPD to increase at shorter exposure duration. This then might be consistent with the temporal account.

EXPERIMENT 2

The bandwidth manipulation in conjunction with a backward mask produces a significant CPD. The question addressed in Experiment 2 is whether the CPD depends on the presence of the mask.

METHOD

The apparatus and procedures used in this experiment were identical to those used in Experiment 1 with the following exceptions.

Subjects

Four subjects participated in the experiment. Three subjects participated in Experiment 1. The other subject was naive. All reported normal or corrected to normal vision.

Stimuli

The bandwidths tested were 60, 69, 79, 91, 104 and 120°. These changes were made to eliminate ceiling and floor effects respectively.

Procedure

The textures were not followed by a mask and the inter-stimulus interval was 1000 ms between the offset of the first texture and the onset of the second. Stimulus exposure varied within a range of 83.3 to 150 ms as determined individually for each subject. When the target was presented, it was randomly placed in one of eight positions across the horizontal meridian ranging from 0 to 12.31° away from fixation (0.00, 0.70, 1.76, 2.61, 3.86, 5.70, 8.39, and 12.31°). Again, each eccentricity was presented 25 times per block. Therefore, each block consisted of 200 trials and all subjects completed 2 blocks per bandwidth. Therefore each subject participated in 2400 trials in the experiment (8 eccentricities x 6 bandwidths x 25 replications x 2 blocks).

RESULTS AND DISCUSSION

Bandwidth thresholds were calculated as in Experiment 1 and the results are summarized in Figure 2.4. Detection performance peaked in the parafovea, with reduced performance occurring towards both the fovea and the periphery [$F(3, 7) = 72.083, p < 0.01$]. A linear trend analysis showed that there was an increase in hit rate from the fovea towards the periphery [$F(1, 3) = 11.408, p < 0.05$] to the performance peak at 8.39° away from fixation.

We again calculated the correlation coefficient between slope and exposure duration. In contrast to Experiment 1, this correlation coefficient was 0.89, indicating a tendency for the magnitude of the CPD to decrease at shorter

exposure durations. In other words, the results are opposite from Experiment 1. In our view, the relationship between the magnitude of the CPD and presentation duration is not particularly information. The essential point is that a CPD was demonstrated in Experiment 2. It is clear that a backward mask is not needed to elicit the CPD.

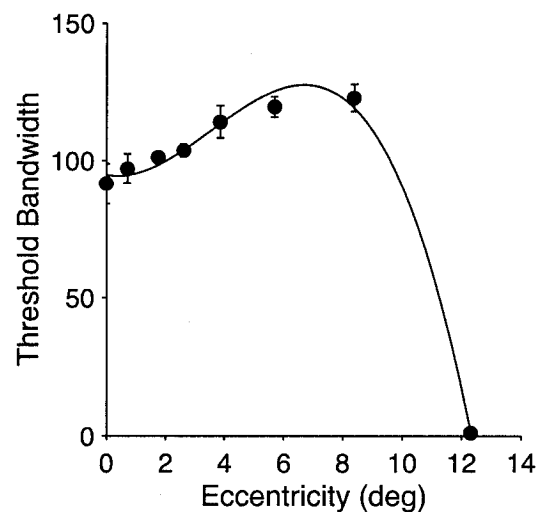


Figure 2.4. Results of Experiment 2. Orientation bandwidth is shown as a function of eccentricity.

EXPERIMENT 3

Experiment 3 combines the bandwidth manipulation of Experiments 1 and 2 with the 4AFC task used by Morikawa (2000). Rather than measuring orientation bandwidth thresholds at each eccentricity, bandwidth was fixed across all trials. In effect this adds a constant level of noise to the task to limit performance. In this case, the orientation variability serves the same function as the simultaneous mask in Morikawa's second experiment, without its attendant limitations.

METHOD

The apparatus and procedures used in this experiment were similar to those used in Experiment 2 with the following exceptions.

Subjects

Five subjects participated in the experiment. Three subjects participated in Experiments 1 and 2, one of the new subjects was an experienced psychophysical observer and the other was naive and inexperienced. All reported normal or corrected to normal vision.

Apparatus

The experiment was conducted under ambient lighting conditions for all but one who ran the experiment with the overhead fluorescent lights on because he experienced discomfort under ambient lighting conditions. However, this subject's results fell within the range of results of the other subjects.

Stimuli

The target patches were presented at seven eccentricities (0.68, 1.00, 1.47, 2.16, 3.16, 4.64, and 6.79°) along each of the four oblique meridians for a total of 28 positions. The stimulus field subtended 17.61° in the horizontal and vertical directions. The size of the target texture was 1.09° in both the vertical and horizontal directions. An example stimulus display is shown in Figure 2.5. In all conditions the orientation bandwidth was fixed at 100°.

Procedure

On the initial trial, a central blue fixation dot signaled the subject to press the spacebar to initiate the experiment. On each trial, the stimulus was presented for 83 ms. The disparate region appeared in a randomly chosen quadrant and at

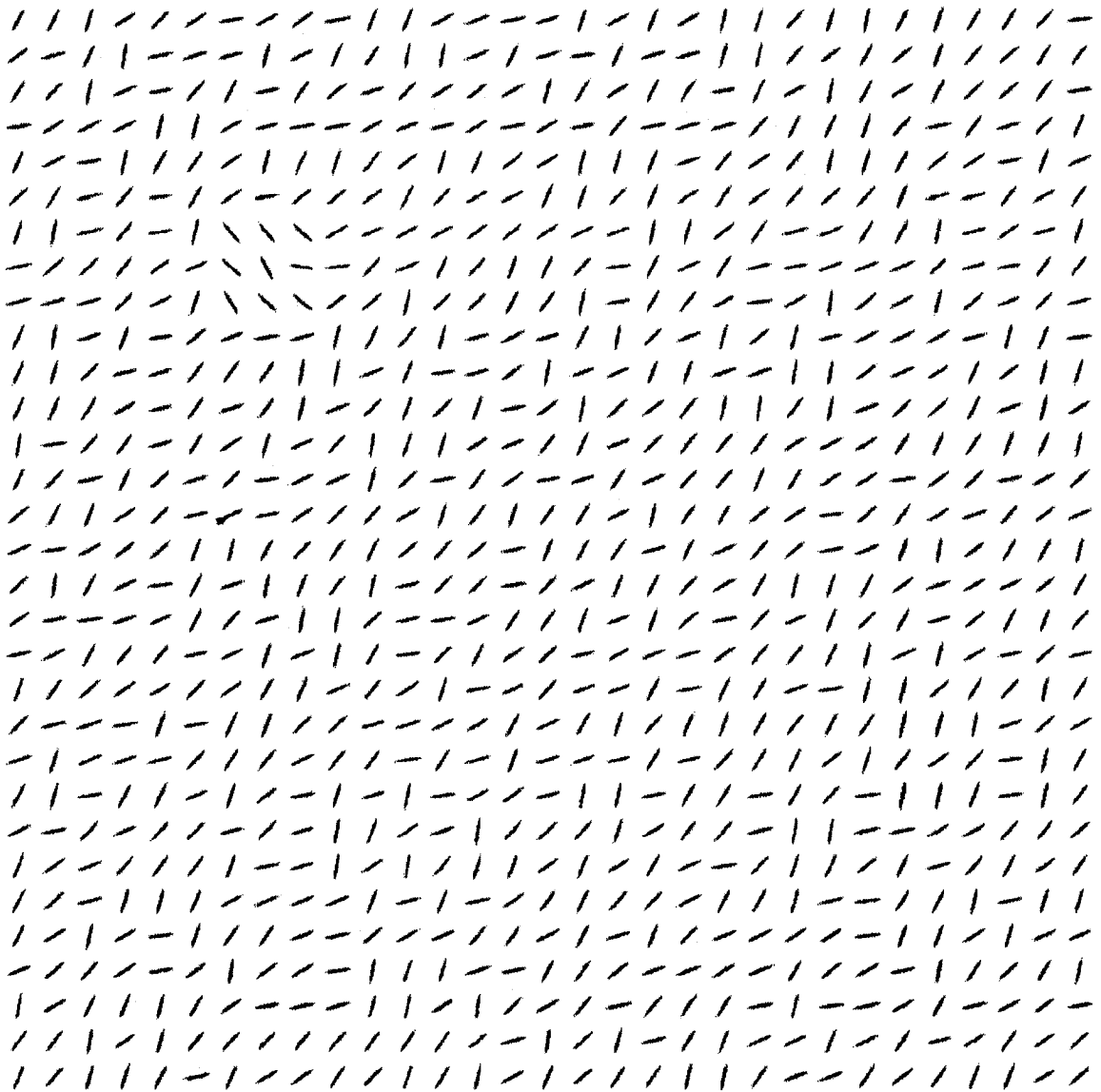


Figure 2.5. Stimulus pattern used in Experiment 3. The target is presented in one quadrant on each trial. The subject's task is to correctly locate the target. In this stimulus, the target is presented in the upper left quadrant.

a randomly chosen eccentricity. The stimulus presentation was followed by a red fixation dot centered in an otherwise blank screen. Subjects pressed predetermined numbers on the computer keypad to indicate the quadrant in which the disparate region had appeared. There was a delay of 1000 ms between

the onset of the fixation dot and the onset of the texture display. Each stimulus position was presented 25 times in each quadrant at each eccentricity. Therefore, there were 100 responses at each eccentricity, for a total of 700 trials per subject.

RESULTS AND DISCUSSION

The probability of a correct response was calculated at each eccentricity (collapsed over quadrants) and the results submitted to a one way ANOVA. The results are summarized in Figure 2.6. Detection performance peaked in the parafovea, with reduced performance occurring towards both the fovea and the periphery [$F(4, 6) = 46.157, p < 0.01$]. A linear trend analysis of responses from fixation to 3.16° eccentricity (the performance peak) showed a significant increase [$F(1, 4) = 84.998, p < 0.01$]. Once again, a CPD was demonstrated.

We note that peak performance in this task occurred at about 4° from fixation whereas in Experiments 1 and 2 the performance peak was at about 7° from fixation. The most likely explanation for this difference has to do with the position of the disparate region on the screen. In Experiments 1 and 2 a disparate region at a position corresponding to the performance peak (7°) would be close to the center of the screen, a long way from the screen boundary and surrounded by many background texture elements. In Experiment 3, by contrast, a disparate region 7° from fixation would be very near the screen boundaries and surrounded on two sides by very few background texture elements. This is an important methodological consideration when trying to relate the experimental results to quantitative models of texture segmentation because the exact location of the peak would have implications for the nature of the mechanisms determining performance. In the present case the difference in the performance

peak across paradigms is not so critical given that the qualitative question was whether or not the CPD would obtain without a backward mask; it clearly does.

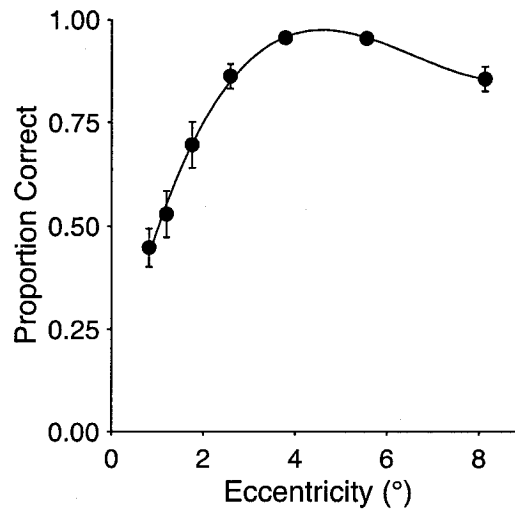


Figure 2.6. Results of Experiment 3. Percentage of correct responses is shown as a function of eccentricity.

GENERAL DISCUSSION

The bandwidth manipulations used in the present study provide a useful way of limiting performance without a backward mask. Similar methodologies have been used in the past in a wide array of circumstances. This method has several advantages over the backward masking paradigm, which is widely used in the texture literature. First, backward masking introduces the possibility that temporal factors determine task performance. This leads to the question of whether a backward mask is critical to the emergence of the CPD. There may be important temporal factors determining texture discrimination (e.g., Motoyoshi & Nishida, 2001) but if one is interested in the spatial factors determining texture discrimination it would be desirable to minimize or eliminate uncontrolled temporal contributions to performance. We expect that in most cases the bandwidth manipulation will mimic the effects of the 'X-type' backward mask,

because we believe that in most cases it is simply a source of spatial noise. Nevertheless, the bandwidth manipulation completely eliminates temporal factors from consideration.

A second advantage of the bandwidth manipulation is that it provides for finer control over performance. In a backward masking paradigm the SOA between stimulus and mask is typically determined by the frame rate of the host computer. Although special purpose video boards may provide for temporal resolution on the order of 1 ms, it is more common to have frame rates of 60 to 100 Hz, which permit SOAs that are multiples of 10 to 15 ms. These relatively large time intervals may make it difficult to control performance precisely because performance may jump from floor to ceiling over two frames. The bandwidth manipulation (and variants, e.g., Kingdom, Keeble & Moulden, 1995; Dakin & Hess, 1997; Wolfson & Landy, 1998; Motoyoshi & Nishida, 2001) provides finer control over stimulus discriminability leading to more stable performance

The bandwidth manipulation has wide application and we have used it to examine the interaction of eccentricity with discrimination asymmetries. For example, it is well known that texture discrimination is frequently asymmetrical; texture A embedded in texture B may be more easily discriminated than texture B embedded in texture A (Gurnsey & Browse, 1987, 1989; Rubenstein & Sagi, 1990, 1996). One such texture pair showing this kind of asymmetry comprises vertical and tilted lines (e.g., Treisman & Gormican, 1988; Foster & Ward, 1991). Potechin and Gurnsey (2001) showed that bandwidth thresholds are greater when tilted lines are embedded in vertical lines than vice versa. This asymmetry showed an interesting dependence on eccentricity. Bandwidth thresholds

increased with eccentricity for the tilted in vertical stimuli (i.e., the CPD) whereas a decrease in bandwidth thresholds with eccentricity was found for the vertical in tilted stimuli (i.e., the typical eccentricity effect). This result is consistent with those of Carrasco et al. (1998) who found that orientation discrimination asymmetries in a visual search task increased with eccentricity of stimulus presentation.

We have argued elsewhere for a purely spatial account because of its simplicity and connection to existing eccentricity dependent spatial discriminations (Gurnsey et al., 1996). The spatial account requires only a consideration of variations in spatial sensitivity across eccentricities. Therefore the spatial account is more parsimonious than the spatiotemporal account originally suggested by Kehrner. There are numerous data and models consistent with this account. We argued that Morikawa's data do not show definitively that a backward mask is required to elicit the CPD. We reviewed the limitations of these studies in the introduction. Experiments 2 and 3 show clearly that the CPD emerges in the absence of a backward mask for stimuli that are closely related to those that have been widely used in previous studies of the CPD (Kehrner, 1987, 1989; Joffe & Scialfa, 1995; Gurnsey et al., 1996; Morikawa, 2000). We conclude that in past studies of the CPD the backward mask functioned primarily as a source of spatial noise and that its temporal relation to the texture display is not critical to the emergence of the CPD.

CHAPTER 3

TEXTURE DISCRIMINATION ASYMMETRIES ACROSS THE VISUAL FIELD

by

**CINDY POTECHIN AND RICK GURNSEY
DEPARTMENT OF PSYCHOLOGY,
CONCORDIA UNIVERSITY**

ABSTRACT

Texture discrimination is sometimes asymmetrical; texture A embedded in texture B is more easily detected than texture B embedded in texture A. Furthermore, texture discrimination often improves as the disparate texture is moved into the periphery; this has been referred to as the central performance drop (CPD). The interaction of these interesting and counter-intuitive aspects of texture discrimination has received very little attention. Using four stimulus pattern pairs that were previously shown to elicit asymmetrical texture discrimination, we examined texture discrimination asymmetries as a function of eccentricity. We found three patterns of results; (i) both texture arrangements (A in B, and B in A) elicit a CPD but do not show an asymmetry, (ii) both texture arrangements elicit a monotonic decrease in performance with eccentricity (i.e., no CPD) but an asymmetry is seen at each eccentricity and (iii) discrimination asymmetries are minimal at fixation and in the far periphery and maximal about 3° from fixation with a CPD generally shown for the 'stronger' member of the pair. These results emphasize that one cannot talk about the 'discriminability' of a particular texture pair without reference to the arrangement of the two textures and the eccentricity of presentation.

Visual textures have been used for many years to probe the sensitivity of the visual system to differences in local spatial structure (e.g., Julesz, 1981, Beck, 1982). Current theories suggest that differences in local energy responses of filters tuned to orientation and spatial frequency explain sensitivity to texture differences; e.g. Malik and Perona (1990), Rubenstein and Sagi (1990), Bergen and Landy (1991), and Gurnsey, Pearson and Day (1996), among many others. Many models of texture segregation involve two stages of spatial filtering (e.g., Gurnsey & Browse, 1989; Landy & Bergen, 1991). In the first stage the input image is convolved with a set of band-pass filters, creating a set of “neural images” (Robson, 1980). The responses within each neural image are rectified and filtered again to detect local differences in first-layer responses. Texture segregation will be difficult if the first-layer filters are not sufficiently stimulated or if there is a poor match between the content of a rectified neural image and the properties of the second-layer filter. Such Filter-Rectify-Filter (FRF) models provide a way of thinking about a number of texture discrimination phenomena.

Over the years a number of interesting, and seemingly counter-intuitive findings have emerged. First, texture discrimination is frequently asymmetrical; i.e., Texture A embedded in Texture B is often easier to detect than Texture B embedded in Texture A (Gurnsey & Browse, 1987, 1989; Gurnsey & Laundry, 1992; Rubenstein & Sagi, 1990, 1996). The result is counter-intuitive because the local difference between A and B is the same regardless of which is the embedded texture. A second unusual result was first reported by Kehrner (1987). He showed that the detection of oblique lines of a particular orientation embedded in a larger background of orthogonally oriented lines improves as the

target texture is moved away from the fovea. Kehrner coined the term “central performance drop” (CPD) to denote the sub-optimal detection performance at foveal or near-foveal locations.

The purpose of the present study is to examine further the eccentricity dependence of texture discrimination asymmetries for a number of textures that have been previously reported to elicit discrimination asymmetries. We begin with a brief review of the issues in the asymmetry and CPD literatures.

Texture Discrimination Asymmetries

There have been many reports of asymmetries in the texture literature (e.g. Gurnsey & Browse, 1987, 1989; Meinecke & Kehrner, 1994; Meinecke, Kimchi, and Grandegger, 2002; Rubenstein & Sagi, 1990, 1996). In one of the first reports, Gurnsey and Browse (1987) studied the classic LX textures of Julesz (1984, see also, Bergen & Julesz, 1983; Bergen & Adelson, 1988) using a four-alternative forced choice procedure in which subjects had to indicate the quadrant containing the disparate region. They found that randomly rotated Ls embedded in randomly rotated Xs were detected more easily than Xs in Ls. Such asymmetries suggest that the segmentation procedure cannot be restricted to local information because the texture difference at a texture boundary is the same regardless of which is the embedded region.

Gurnsey and Browse (1989) suggested two explanations for the LX-type asymmetry. First, they noted that in some sense Ls are larger than Xs; e.g., their minimum enclosing circles differ in diameter by 40%. If one were to assume that the size contrast measured at a texture boundary is somehow normalized by the average micropattern size in the display, then the contrast will be greater when small patterns make up the background; i.e., because there are more

micropatterns in the background than foreground they will produce a lower average (normalizing constant) than in the obverse case. Indeed, Gurnsey and Browse (1989) found that for textures comprising large and small circles, large circles in small circles were more easily detected than vice versa. [This explanation is generally in line with the explanation given by Treisman and Gormican (1988) for a number of asymmetries found in the visual search task. It is also consistent--but not identical--with the explanation given by Foster (e.g., Foster & Ward, 1991; Foster & Westland, 1998) for orientation discrimination asymmetries.] Rubenstein and Sagi (1996) reported a similar result, although they offered a different explanation for it. Interestingly, they also found that the asymmetry reversed when the circles involved became sufficiently large.

In addition to being larger than Xs, Ls also generate more variable textures. For example, the Fourier amplitude spectrum of a texture comprising randomly rotated Ls has a broader distribution of energy than a texture comprising randomly rotated Xs (see Rubenstein & Sagi, 1990). Gurnsey and Browse (1989) argued that variability differences per se might produce an asymmetry. Indeed, Gurnsey and Browse (1989) found that textures comprising circles differing only in the variability of their placement (jitter) produced strong asymmetries such that the texture with greater jitter was more easily detected in a background of less jitter than vice versa. Rubenstein and Sagi (1990, 1996) made similar suggestions. They pointed out that within a "neural image" Ls would elicit more variable responses than Xs.

The Central Performance Drop

Several early results showed that sensitivity to texture differences decreased with eccentricity. For example, Saarinen, Ravamo, and Virsu (1987)

used texture pairs differing in minimum inter-dot distances and found that textures of constant retinal size could be discriminated easily in central vision but these same textures were not resolvable with peripheral viewing, presumably because of decreased visual acuity. Nothdurft (1985) demonstrated a similar dependence of texture segregation on visual acuity using textures consisting of lines with differing orientations.

In contrast to the results cited above, Kehrner (1987) demonstrated that the detection of a small patch of oblique lines oriented ± 45 deg from vertical embedded within a much larger background of orthogonal lines actually improved with eccentricity. Kehrner's paradigm involved a backward mask to limit performance and Kehrner (1989) argued that a difference in the processing speed of spatial-frequency selective filters across the visual field was the underlying factor resulting in texture discrimination variability at the fovea versus more peripheral locations; processing speed was assumed to increase with eccentricity and hence the segmentation process would be more advanced in the periphery than at the fovea before the arrival of the mask. This proposal has been the subject of some debate (Gurnsey, Pearson & Day, 1996; Kehrner, 1998; Morikawa, 2000; Kehrner & Meinecke, 2003; Potechin & Gurnsey, 2003; Gurnsey, di Lenardo & Potechin, 2004). Gurnsey et al. (1996) argued that texture segmentation in the fovea involves mechanisms tuned to high spatial frequencies that operate over a small spatial extent whereas peripheral segmentation involves mechanisms operating over a larger spatial extent tuned to low spatial frequencies. Optimal detection of a disparate texture occurs when the scale of the texture matches the spatial frequency selectivity of the mechanism involved (see Bergen (1991) for similar arguments). Although a role for temporal factors cannot

be conclusively ruled out, it is clear that backward masking is not a necessary condition for the emergence of the CPD (Morikawa, 2000; Potechin & Gurnsey, 2003) and it is quite likely that backward masks serve mainly as a source of spatial noise (Gurnsey et al., 2004).

Very little is known about the types of textures that elicit the CPD. In all but one published report of the CPD the textures comprised line segments differing in orientation by 90° ¹. The exception is the study by Meinecke and Kehrner (1994) that used chevrons comprising lines of the same length but differing in the angle at which they meet. Some chevron contrasts produced a CPD and others did not.

Texture Discrimination Asymmetries and the CPD

Both texture discrimination asymmetries and the CPD can be explained in terms of FRF models (Rubenstein & Sagi, 1990, 1996; Gurnsey et al., 1996; 2004) and both phenomena impose constraints on theories of texture discrimination. However, to this point there has been little attention paid to how these two phenomena interact and how they might depend on the particular textural contrasts involved. An illustration of these potential interactions may be seen in the work of Meinecke and Kehrner (1994). In one experiment they presented right facing chevrons with an interior angle of 70° embedded in left facing chevrons with an interior angle of 50° . In a second experiment the roles of the two textures were reversed so that the left facing chevrons were embedded in the right facing

¹Meinecke (1989) used a stimulus pattern consisting of "H" and "O" elements equally spaced on a horizontal plane. Each stimulus configuration consisted of 29 identical distractor elements and one target element. Although this stimulus differs from what is typically considered a texture, Meinecke's (1989) results demonstrated that such "textures" could elicit a CPD and resulted in detection asymmetries when the target and background elements were reversed.

chevrons. Hit rate was measured as a function of eccentricity for these two conditions. Figure 3.1 replots the data from their experiments (note, Meinecke & Kehrner did not explicitly compare these two conditions). Filled circles represent 70 in 50 and unfilled circles represent 50 in 70 (data have been collapsed across the right and left visual field). The results demonstrate an intriguing complexity. There are two different asymmetries. Between 0 and 3° eccentricity hit rate is greater for 70 in 50 and beyond 3° hit rate is greater for 50 in 70. In other words, the asymmetry is eccentricity dependent. Furthermore, there is a pronounced CPD for the 50 in 70 condition (unfilled circles) but not for the 70 in 50 condition.

In a more recent study closely related to the present one, Meinecke et al. (2002) considered the interaction between asymmetries and retinal eccentricity in a number of segregation tasks. Their stimulus elements were outline squares (closed squares) and squares with the top bar missing (open squares). In the conditions most similar to the standard texture discrimination task they found results somewhat like those shown in Figure 3.1. At fixation open squares were easier to detect in closed squares than vice versa and in the periphery this pattern was reversed. In other words, the asymmetry reversed with eccentricity. Furthermore, there was a clear CPD for closed squares in open squares but a classical eccentricity dependent sensitivity loss for open squares in closed squares.

The example shown in Figure 3.1 and the results of Meinecke et al. (2002) suggest that there may be a relatively complex relationship between texture discrimination asymmetries and eccentricity. In this paper we examine four texture types that have been reported to produce discrimination asymmetries. The textures studied are the LX pair (Bergen & Julesz, 1983; Gurnsey & Browse;

1987; Rubenstein & Sagi, 1990; Gurnsey & Laundry, 1992), the jitter-differing textures (Gurnsey & Browse, 1989) and the size-differing textures (Gurnsey & Browse, 1989; Rubenstein & Sagi, 1996). Finally, orientation discrimination asymmetries have been widely reported in the literature (e.g., Treisman & Gormican, 1988; Foster & Ward, 1991a, 1991b; Foster & Westland, 1995, 1998; Poirier & Gurnsey, 1998). A single tilted line within a background of vertical lines is more easily detected than the obverse arrangement. Therefore, in a fourth condition we examine orientation discrimination asymmetries within the texture discrimination paradigm.

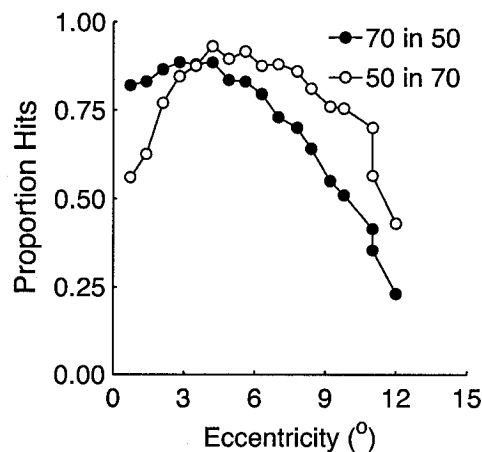


Figure 3.1. Data replotted from Meinecke and Kehrner (1994) showing differences in asymmetries across the visual field. Unfilled circles represent narrow angle chevrons embedded in wide angle chevrons and the filled circles represent the opposite relationship.

As noted earlier, several explanations of the texture discrimination asymmetry have been provided in the literature and there are no data in the literature suggesting whether either or both elements of a texture pair would produce a CPD. Therefore, the range of possible outcomes in this experiment is very large. The objective of the experiment is to examine texture discrimination

asymmetries across the visual field to gain further insight into the internal representation of textures.

EXPERIMENT 1

METHOD

Stimuli

The stimuli used in the experiments are a generalization of those used by Potechin and Gurnsey (2003). To limit performance without a backward mask a continuum of micropatterns is created, permitting a continuous degradation of the strength of the texture contrast. Examples of the four stimulus continua are shown in Figure 3.2.

LX-Stimuli. The top panel shows the LX continuum. The leftmost column shows perfect L stimuli in four of 16 possible orientations. Each line was drawn with a Gaussian cross section having a standard deviation of 1.3 pixels. The two lines were approximately 19.24 pixels in length and drawn within a 32 x 32 pixel window. Progressing from left to right the stimuli morph from Ls to Xs and back to Ls. (This may be thought of as one cycle of a texture modulation.) There were 31 linear *steps* between a perfect L and a perfect X; each step corresponded to a difference in the position at which the two lines met. There were 496 different micropatterns in the stimulus set; 31 (steps) x 16 (equally spaced orientations per steps).

The strength of a texture contrast was manipulated by varying the bandwidth of the micropatterns contained within a region. Consider the top left panel of Figure 3.3 in which Ls are embedded in Xs. We refer to this as a bandwidth of 1 step because there is only one type of micropattern type within

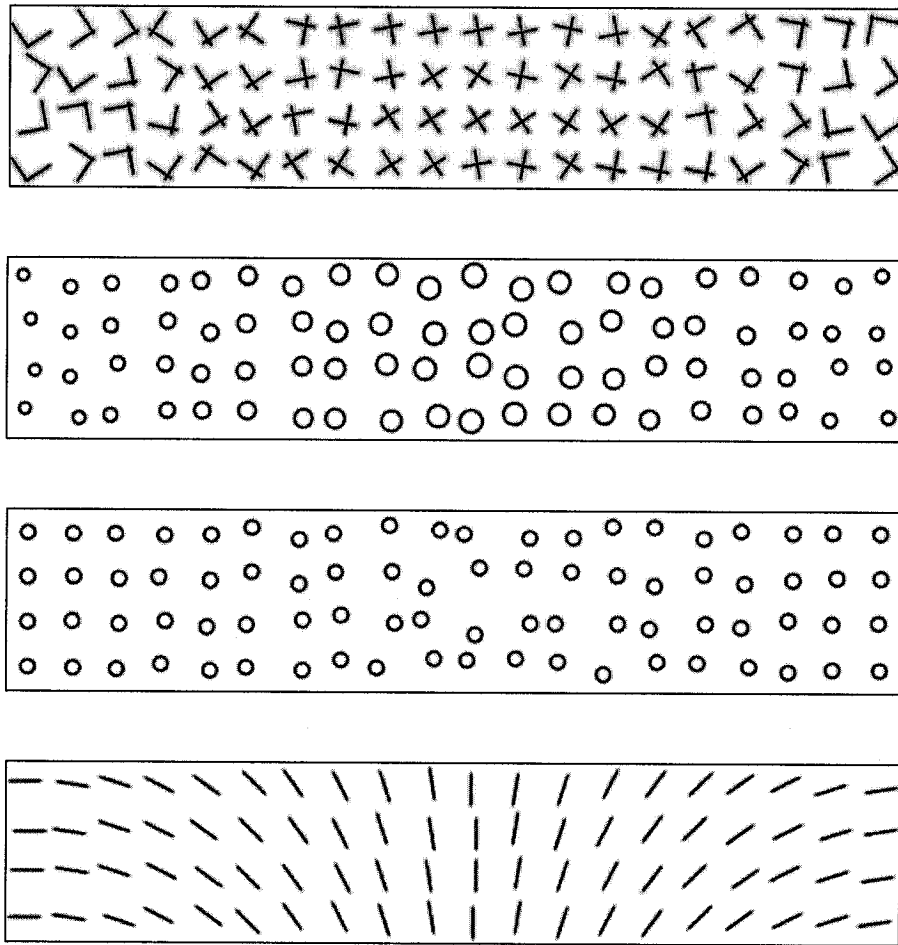


Figure 3.2. Examples of the four stimulus continua used in the experiments. The four panels from top to bottom show, respectively, one full cycle of a pattern modulation for the LX continuum, the Size continuum, the Jitter continuum and the Orientation continuum.

each region. The two texture regions in the top right panel of Figure 3.3 are both described as having a bandwidth of 15. The region of Xs, for example, samples the LX continuum from a region centred on the X and includes seven steps on either side of the X. The region of Ls is sampled from a region of the LX continuum centred on the L and includes seven steps on either side of the L; the seven steps to the right are achieved by wrap-around. Within these bounds each micropattern has an equal probability of being chosen; i.e., stimuli were sampled from a flat distribution. As the width of the stimulus space being sampled

increases, the texture becomes more difficult to discriminate, as can be seen in the bottom left and right panels of Figure 3.3 which show bandwidths of 30 and 60 respectively.

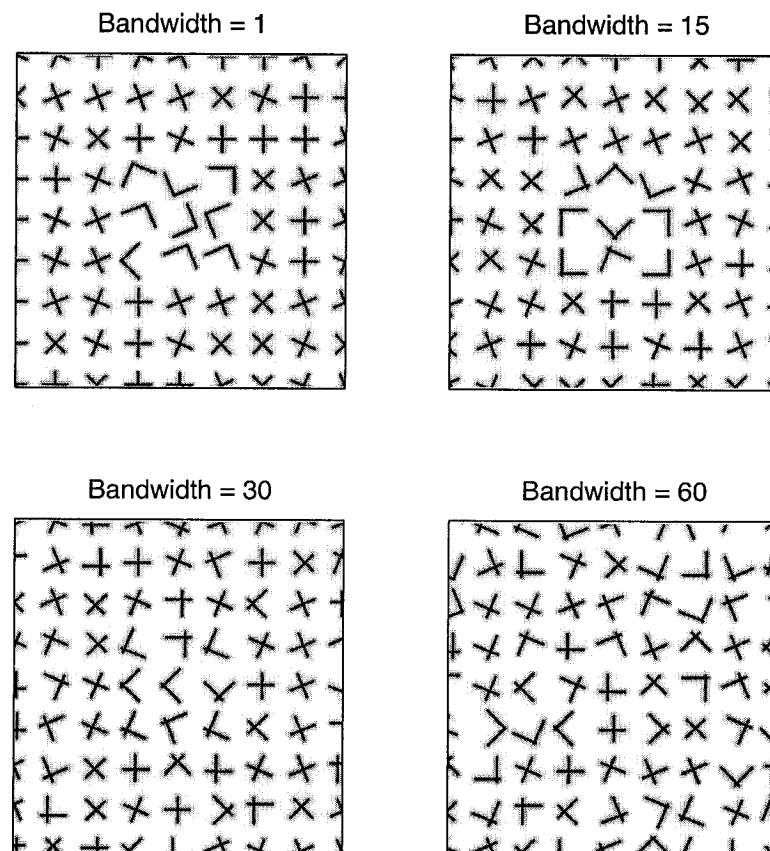


Figure 3.3. Examples of changing texture contrasts for the LX continuum as bandwidth increases from 1 to 60.

The stimulus field subtended 17.61 X 13.45 deg in the horizontal and vertical directions, respectively. Each stimulus display contained 50 x 37.5 micropatterns as shown in Figure 3.4. The disparate region was composed of a 3 x 3 sample of micropatterns and could appear at one of seven distances from fixation (0.69, 1.01, 1.48, 2.18, 3.19, 4.69, and 6.86 deg) along each of the four diagonal axes. Note that the bandwidth of the textures in the two regions is the

same. The construction of all other stimuli followed the same principles as those for the LX textures. The main differences had to do with the stimulus continuum.

Size Stimuli. The second panel in Figure 3.2 shows the size continuum. The leftmost column shows a circle having a radius of 4 pixels; the local cross section (perpendicular to the tangent) was Gaussian with a standard deviation of 1.3 pixels. From left to right the circles progress from a radius of 4 to 8 pixels and back to 4; again one cycle of a texture modulation. In the actual stimulus set there were 31 steps between the 4- and 8-pixel circles. The centre of each circle was shifted two pixels from the centre of the 32 x 32 pixels region in which it was drawn. For each stimulus size, 16 different circles were created, each at a different orientation from the centre of the 32 x 32 region. This introduced a spatial jitter within all textured regions.

Jitter Stimuli. The third panel in Figure 3.2 shows the jitter continuum. All stimuli in this set are circles having a radius of 6 pixels; again the local cross was Gaussian with a standard deviation of 1.3 pixels. In the first column all stimuli are centred within the 32 x 32 micropattern window. Jitter was introduced by shifting the centre of the circle away from the centre of the window. There were 31 "jitter-radii" ranging from 0 to 8 pixels in linear steps. For each non-zero jitter 16 different circles were created, each at a different orientation from the centre of the 32 x 32 region.

Orientation Stimuli. The fourth panel in Figure 3.2 shows the orientation continuum. All stimuli were lines having a Gaussian cross-section. The standard deviation of the Gaussian was 1.3 pixels and the length was approximately 19.34 pixels. A continuum of stimuli was created with orientations ranging from 0°

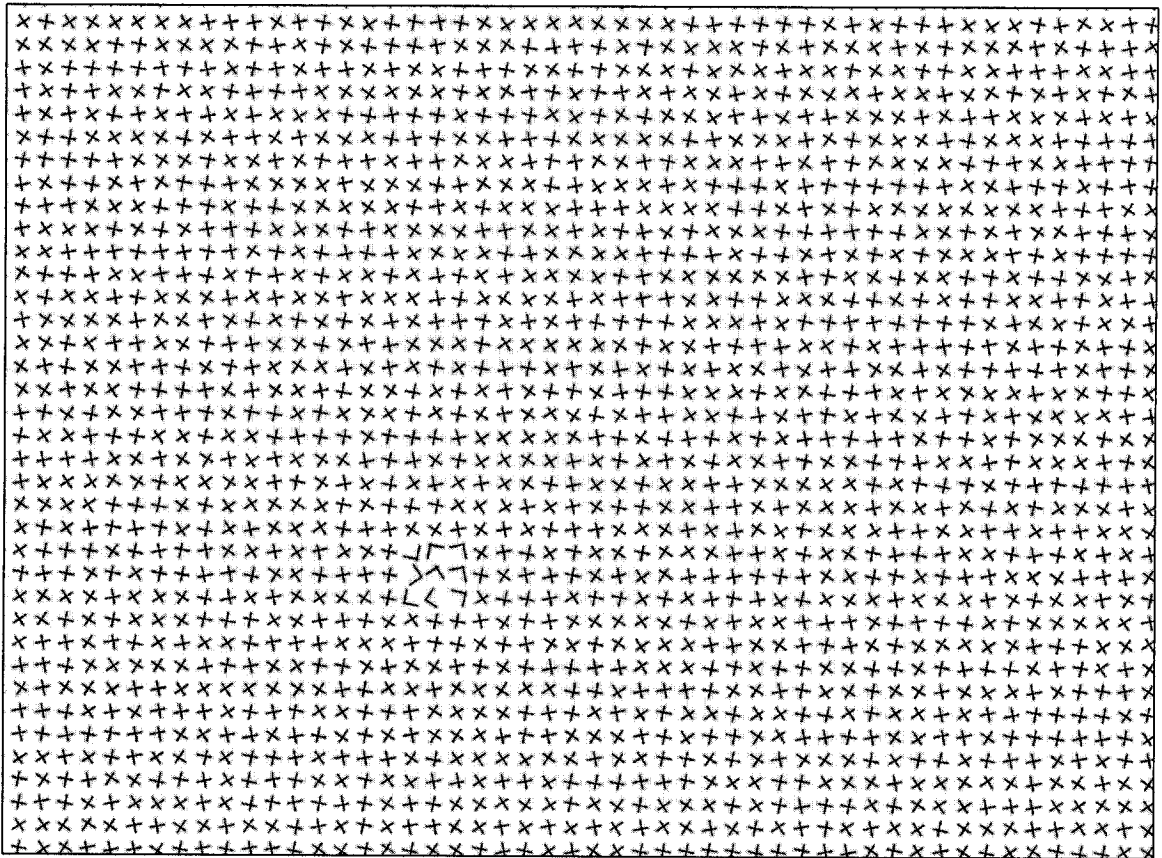


Figure 3.4. An example display showing L-type micropatterns embedded in X-type micropatterns

(vertical) to 179° . For each orientation, stimuli were shifted up to 3 pixels from the centre of the 32×32 micropattern window.

Subjects

Four subjects participated in all four conditions of the experiment. An additional two subjects participated in the LX condition and one of these subjects also participated in the Jitter condition. All reported normal or corrected to normal visual acuity.

Apparatus

The stimuli were presented on a G4 Apple computer attached to a 21" monitor with a frame rate of 85 Hz and a resolution of 1600×1200 pixels. The

stimulus elements were presented in black (0.1 cd/m^2) against a white background (89 cd/m^2). The experiment was conducted under ambient lighting conditions, provided by a shielded 40-watt incandescent bulb placed out of view of the subject. A viewing distance of 120 cm was maintained through the use of a chin rest.

Procedure

The four conditions of the experiment involved the four stimulus types shown in Figure 3.2. For the LX continuum the two texture types were centred on the Ls and Xs with a bandwidth of 35. For the Size continuum the two texture types were centred on the smallest and largest circles with a bandwidth of 40. For the Jitter continuum the two texture types were centred on the smallest and largest jitters with a bandwidth of 30. For the Orientation continuum the two texture types were centred on 0° and $\pm 18^\circ$ with a bandwidth of 33. Pilot testing showed that these bandwidths produced a good range of performance variation across eccentricities.

At the beginning of each trial a blue fixation dot appeared. Subjects initiated the trial by pressing the space bar on the computer keyboard. The fixation screen was immediately replaced by a stimulus display that remained on screen for a time that was determined individually for each subject. The durations ranged from 67 ms to 150 ms to ensure that the subject's ability to segment the texture at fixation was not at a ceiling or floor level. The subject's task was to identify the quadrant containing the target texture by pressing one of four computer keys that represented each quadrant. At the end of each trial in which the subject made an error, feedback was provided in the form of a beep.

All texture stimulus types (e.g., Ls in Xs and Xs in Ls are different stimulus types) were presented within separate experimental sessions. Each session consisted of 10 blocks of trials. Within each block the disparate region was presented 8 times at each eccentricity (i.e., twice in each quadrant). Therefore, a session consisted of 7 (eccentricities) * 4 (quadrants) * 2 (replications) * 10 (blocks) = 560 trials.

RESULTS

The results are summarized in Figure 3.5. Within each stimulus type (e.g., Ls in Xs) data were collapsed across quadrants resulting in 80 trials at each eccentricity. Proportion of correct responses was the dependent measure. The data were submitted to a 2 (stimulus types) by 7 (eccentricities) within subjects ANOVA. Effect size was calculated as a partial ϵ^2 (h_p^2) The effects of eccentricity for each target type were then examined separately using trend analysis to determine whether a CPD had been demonstrated. The trend analysis was limited to data positions representing eccentricities 0.69° to 3.19°

LX Condition. The top left panel of Figure 3.5 summarizes the LX data. The main effect of stimulus type [$F(1,5) = 115.77, p < 0.05$] was statistically significant indicating better performance for Ls in the foreground than Xs in the foreground. There was also a statistically significant effect of eccentricity [$F(6, 30) = 5.71, p < 0.05$], which was, qualified by a statistically significant interaction of target type by eccentricity [$F(6, 30) = 14.67, p < 0.05$]. The effect size of the interaction was 0.746. As shown in the top left panel of Figure 3.5, performance peaked in the parafovea when Ls were embedded in Xs, with reduced performance occurring towards both the fovea and the periphery for all subjects.

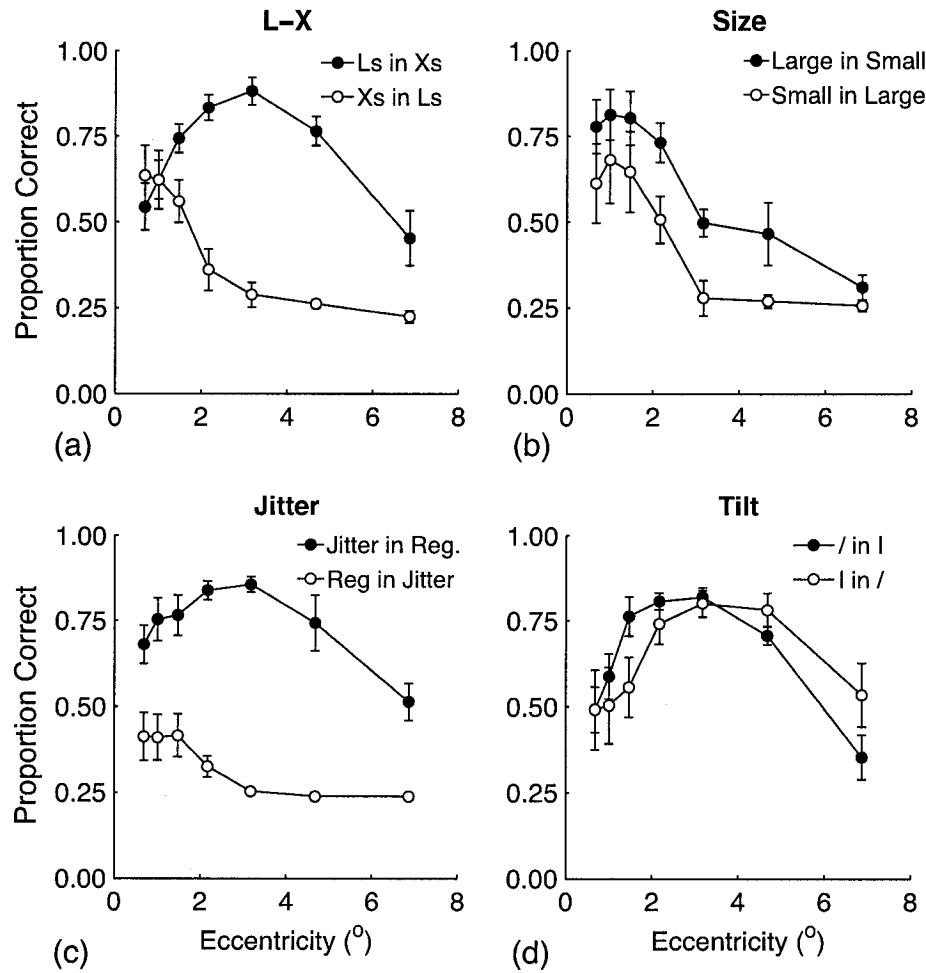


Figure 3.5. Summary of the results of Experiment 1. Each panel shows the probability of a correct detection as a function of eccentricity for the two possible arrangements of the textures.

When Xs were embedded in Ls performance dropped off sharply as the target was moved away from the fovea. The trend analysis revealed a statistically significant increase in accuracy over eccentricities 0.69° to 3.19° when Ls formed the disparate texture [$F(1, 5) = 16.84, p < 0.05$] but the opposite occurred when Xs formed the disparate texture [$F(1, 5) = 10.99, p < 0.05$]. That is, a CPD was demonstrated in response to the L-micropattern target but the normal

eccentricity effect is demonstrated in response to the stimulus containing the X-micropattern target.

Size Condition. The data from the size experiment are summarized in the top right of Figure 3.5. The ANOVA revealed a statistically significant main effect of stimulus type [$F(1,3) = 58.84, p < 0.05$] indicating that large circles were more easily detected in small circles than vice versa (consistent with Gurnsey & Browse, 1989). The effect size was 0.951. There was also a statistically significant main effect of eccentricity [$F(6, 18) = 14.87, p < 0.05$] with an effect size of 0.832. The interaction of target type by eccentricity was not statistically significant. It is clear from Figure 3.5 that there is no tendency towards a CPD; in both cases performance falls off with eccentricity. The trend analysis supported a statistically significant decrease in accuracy from the fovea towards the periphery when the target texture comprised either the large circles [$F(1, 3) = 10.61, p < 0.05$] or the small circles [$F(1, 3) = 37.07, p < 0.01$].

Jitter Condition. The data from the jitter experiment are summarized in the bottom left of Figure 3.5. There was a statistically significant main effect of stimulus type [$F(1, 4) = 506.51, p < 0.05$] with an effect size of 0.99 indicating that jittered in regular is more easily detected than regular in jitter (consistent with Gurnsey & Browse, 1989). The main effect of eccentricity [$F(6, 24) = 4.94, p=0.052$] and the interaction [$F(6, 24) = 5.54, p=0.053$] approached but did not reach significance. The jitter data resemble the LX data (Figure 3.5 top left) in that there is a trend towards a statistically significant improvement in accuracy over eccentricities 0.69° to 3.19° [$F(1, 4) = 7.32, p =0.054$] but a decrease with eccentricity for the regular in jitter that was not significant [$F(1, 4) = 4.64, p > 0.05$].

Line Orientation Condition. For the stimuli composed of tilted and vertical lines there was a statistically significant main effect of target location [$F(6, 18) = 9.95, p < 0.05$] with an effect size of 0.77 but no statistically significant effect of stimulus type or interaction of stimulus type by eccentricity. For both conditions there was an increase in performance as the target was moved from the fovea to the parafovea and then performance dropped off in the periphery. The trend analysis showed that there was an increase in accuracy from the fovea towards the periphery for the target texture comprising tilted lines embedded in vertical lines [$F(1, 3) = 15.87, p < 0.05$] but the trend was not statistically significant for texture comprising vertical lines embedded in tilted lines [$F(1, 3) = 5.07, p = 0.155$]. In other words, there appears to be a CPD in both cases but for vertical lines embedded in tilted lines the trend was not quite statistically significant, which is probably attributable to the low power of the test.

DISCUSSION

In three of the four conditions, a clear asymmetry was demonstrated. In the LX and jitter conditions the asymmetry was most pronounced at approximately 3° eccentricity whereas in the size condition the asymmetry was more or less uniform across eccentricities (see Figure 3.5). In contrast to these three conditions, no overall asymmetry was found for vertical and tilted line textures. In this case, between 0 and 3° eccentricity accuracy was greater in response to tilted targets presented in a field of vertical background elements. Beyond 3° accuracy was greater for vertical targets in a background of tilted elements. However, these differences were not significant.

In three of the conditions, a CPD or CPD-like tendency was demonstrated. The exception was the size condition. In this case, performance dropped off as

either of the two target textures was moved toward the periphery. In two of the three conditions in which, a CPD or CPD-like pattern was demonstrated, this pattern was elicited in response to the stimuli eliciting higher overall performance while the normal reduction in performance with eccentricity was demonstrated in response to the stimulus eliciting lower overall performance.

EXPERIMENT 2

Experiment 2 replicates Experiment 1 with a minor procedural modification. In Experiment 1 stimulus bandwidth was fixed and exposure duration was calibrated on a per subject basis to keep performance within a useful range. In Experiment 2 exposure duration was fixed at 67 ms and stimulus bandwidth was adjusted on a per subject basis prior to running the experiment itself.

METHOD

The apparatus and procedures used in this experiment were identical to those used in experiment 1 with the following exceptions:

Subjects

Six subjects participated in all four conditions of the experiment. All reported normal or corrected to normal visual acuity.

Procedure

Calibration. Each subject underwent a four-alternative forced choice calibration procedure used to determine the threshold bandwidth to be used during the experiment. Separate calibrations were used for each of the four experimental conditions. On the initial trial, a central fixation dot signalled the subject to press the spacebar to initiate the calibration. Each trial consisted of a

fixation screen followed by the presentation of a full-screen display containing a target within one of the four quadrants. The disparate region was presented at 3 eccentricities (0.69, 1.48, and 4.69 degrees of visual angle) to ensure that subjects did not restrict their field of view exclusively to the most central regions of the display. Target eccentricity was varied randomly on each trial with the constraint that each eccentricity was presented only once per block of trials. The bandwidths were determined in identical fashion to that used in Experiment 1. Bandwidth values ranged from 15 to 55 in increments of 10 units. In cases in which the subject performed at chance levels, these bandwidth values were lowered below 15 units, resulting in stimuli that were easier to discriminate.

On each trial, the stimulus was presented for 67 ms, followed by a blank screen. The centrally placed fixation dot was blue prior to each stimulus presentation then changed to red with stimulus onset and remained so until the subject made a valid response. Each response triggered the next trial.

In each calibration procedure, the probability of correct detection was determined for each bandwidth. Bandwidth thresholds were determined for the “stronger” end of the stimulus continuum for the target position nearest to fixation (0.84°). Separate thresholds were computed for each condition. The data were fit using a cumulative Gaussian that was normalized to a range of .25 to 1. Threshold was defined as the bandwidth that elicited 67% correct detections.

Experiment. The procedure for Experiment 2 was identical to that used in Experiment 1 with the following exceptions: 1) the stimuli were presented for 67 ms for all subjects, and 2) within each of the four conditions stimulus bandwidth was set to that determined in the calibration procedure described above. The average values of the bandwidths used in the LX, Size, Jitter and Orientation

conditions were 34.79 ± 9.37 , 38.48 ± 7.76 , 35.52 ± 7.99 , and 15.66 ± 3.04 , respectively. In LX, Size, and Jitter conditions, the average bandwidth was highly influenced by the performance of one subject. When the results of this subject were excluded, the mean bandwidths of the other five subjects in the LX, Size, and Jitter conditions were 38.18 ± 5.18 , 41.21 ± 4.4 , and 38.6 ± 1.2 respectively.

RESULTS

The data were analysed using a procedure identical to that used in Experiment 1. The results of Experiment 2 can be seen in Fig. 3.6.

LX Condition. Similar to the results obtained in the LX condition of Experiment 1, the main effects of stimulus type [$F(1,5) = 30.87$, $p < 0.05$] and target location [$F(6, 30) = 9.39$, $p < 0.05$] were both significant, as was the interaction of these two factors [$F(6, 30) = 16.28$, $p < 0.05$]. The effect size of the interaction was 0.77. However, in Experiment 2, in response to the L-shaped micropattern target embedded in a background of X-shaped micropatterns, detection performance was relatively stable until it dropped off at the most peripheral eccentricities. In response to the X embedded in L stimulus type, performance dropped off sharply as the target was moved from the fovea. Once again, overall detection performance was better for L micropattern targets than for X micropattern targets. The trend analysis indicated that there was a significant decrease in performance for the X in L type stimulus [$F(1, 4) = 15.58$, $p < 0.05$] but no significant trend was noted in the L in X stimulus. That is, an eccentricity effect was demonstrated in response to the patterns with X-micropattern targets but no CPD was demonstrated in response to in the L in X stimulus.

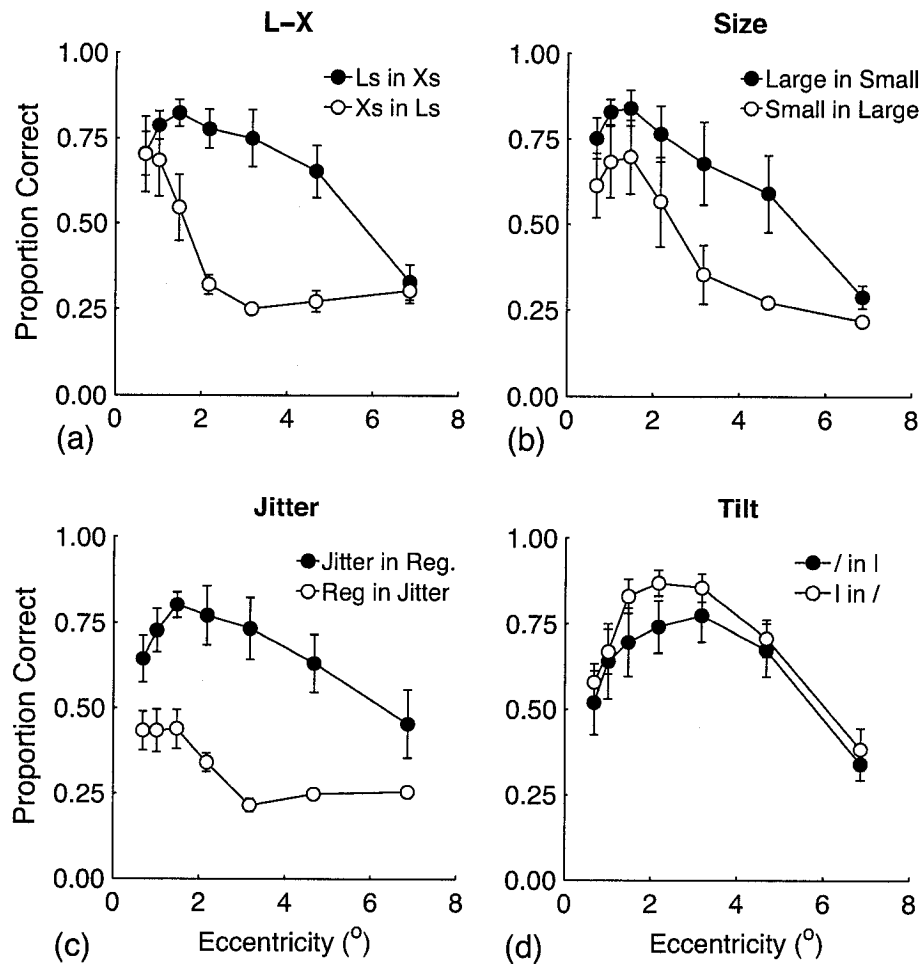


Figure 3.6. Summary of the results of Experiment 2. Each panel shows the probability of a correct detection as a function of eccentricity for the two possible arrangements of the textures.

Size Condition. For the stimuli composed of small and large circles, the main effects of stimulus type [$F(1,5) = 7.34, p < 0.05$] and target location [$F(6, 30) = 26.07, p < 0.05$] were both significant. The effect sizes in the stimulus type and target location conditions were 0.60 and 0.84, respectively. The interaction was non-significant. In both stimuli comprising small and large circle micropatterns, performance remained relatively stable near the fovea and then dropped off sharply as the target was moved further from the fovea. Overall, detection

performance was better when a large circle target was embedded in a background of small circles than vice versa. These results were similar to the results obtained in the corresponding condition in Experiment 1. The trend analysis indicated that there was a significant decrease in performance for the large circle targets embedded in a smaller circle background over the first five eccentricities [$F(1, 5) = 14.945, p < 0.05$] but no significant trend was noted in the other case. No CPD was demonstrated in response to stimuli created using these micropattern pairs.

Jitter Condition. For the stimuli composed of jittered and more regularly spaced circles, the main effects of stimulus type [$F(1,5) = 14.35, p < 0.05$] and target location [$F(6, 30) = 5.32, p < 0.05$] were both significant. The effect sizes in the stimulus type and target location conditions were 0.74 and 0.52, respectively. The interaction was non-significant. In response to regularly spaced circles embedded in jittered circles performance declined as the target was moved away from the fovea. For jittered circles presented in a background of regularly spaced circles, accuracy increased slightly from the fovea to the third eccentricity position and then dropped off as the target was moved further away from the fovea. Overall, detection performance was better when a jittered circle target was embedded in a background of more regularly spaced circles than vice versa. The trend analysis showed that there was a decrease in accuracy from the fovea towards the periphery when the target texture comprised regularly spaced circles embedded within a jittered background [$F(1, 5) = 7.15, p < 0.05$] that approached significance. No CPD was demonstrated in response to either stimulus pattern created using this micropattern pair.

Line Orientation Condition. For the stimuli composed of tilted and vertical lines, only the main effect of target location [$F(6, 30) = 32.25, p < 0.05$] was significant with an effect size of 0.866. In response to both stimuli, performance increased from the fovea towards the parafovea and declined in the periphery. The main effect of stimulus type and the interaction were not significant. The trend analysis further supported a significant increase in accuracy from the fovea towards the periphery for the target texture composed of vertical lines embedded in a background of tilted lines [$F(1, 5) = 30.82, p < 0.01$] only. That is, a CPD was demonstrated in response to vertical line targets embedded in a tilted background. When the micropattern locations were reversed, the demonstrated CPD pattern was not significant [$F(1, 5) = 5.07, p > 0.05$].

DISCUSSION

Similar to Experiment 1, in three of the four conditions a clear asymmetry was demonstrated and this asymmetry was more pronounced in the parafovea than in the fovea or the far periphery. The asymmetry effect noted for the vertical and tilted line targets was not significant.

With respect to eccentricity, performance in the size condition again dropped off as the stimulus was moved from the fovea towards the periphery. This eccentricity effect was also noted in the LX and Jitter conditions for one stimulus pattern only, the stimulus that elicited lower overall performance. In Experiment 1, a CPD or CPD-like tendency was demonstrated in three conditions. In Experiment 2, a CPD was only demonstrated in the case of a vertical line target embedded within a background of tilted lines.

GENERAL DISCUSSION

In two experiments we examined texture discrimination asymmetries across the visual field using a paradigm that manipulates foreground/background texture contrast. There were generally more similarities than differences in the results of the two experiments. Therefore, in most of what follows we average the results of Experiments 1 and 2.

To interpret the results we rely on the signal detection model used by Rubenstein and Sagi (1990). According to this model the ease with which two textures (1 and 2) can be discriminated depends on the distribution of difference signals (from a second-layer filter) at a texture boundary, and by the distribution of difference signals in the background. Assuming that the distribution of difference signals at a texture boundary is the same regardless of which is the embedded texture, then signal detection theory (SDT) implies that detection accuracy should be greater when the less variable texture is in the background.

Performance can be modelled using two distributions to represent the two textures in question. The distributions are assumed to be normal with means μ_1 and μ_2 and standard deviations σ_1 and σ_2 . The distribution of response differences, $p_{fb}(x)$, at a texture boundary will have a mean of $\mu_1 - \mu_2$ and standard deviation $(\sigma_1^2 + \sigma_2^2)^{1/2}$. The distribution of absolute differences at the texture boundary (the probability density function) can be described as $p_{fb}(|x|) = p_{fb}(x) + p_{fb}(-x)$. The distribution of response differences, $p_{bb}(x)$, within a texture will have a mean of $\mu_i - \mu_i = 0$, and standard deviation $(\sigma_i^2 + \sigma_i^2)^{1/2}$. The distribution of absolute differences can be described as $p_{bb}(|x|) = p_{bb}(x) + p_{bb}(-x)$ and will have a distribution function (cumulative distribution function, CDF) of $P_{bb}(|x|) = P_{bb}(x)$

- $P_{bb}(-x)$. This corresponds to the distribution of difference signals arising in the background region. Combining these terms allows us to express the probability of a correct detection in an N -alternative forced choice task (for given values of μ_1, μ_2, σ_1 and σ_2) as follows

$$pc = \int_0^{\infty} p_{fb}(|x|)P_{bb}(|x|)^{N-1} dx \quad [1]$$

For textures 1 and 2 performance depends on $\delta = |\mu_1 - \mu_2|, \sigma_1$ and σ_2 . Asymmetrical discrimination occurs in texture pairs for which $\sigma_1 \neq \sigma_2$. For each texture pair, we fit experimental data at each eccentricity using equation 2 with $\delta = 1$. That is we found σ_1 and σ_2 that fit the data. The results place constraints on the underlying representation upon which discrimination is based, assuming a signal detection framework. We describe results from simplest to most complex.

Line Orientation Textures

The Oriented Line conditions produced similar results in Experiments 1 and 2 so the results were averaged to simplify the analysis. Figure 3.7(a) shows these averaged results. (Of course, in all cases the model perfectly fits the data.) These averaged data show no asymmetry but a strong CPD. Figure 3.7(c) shows σ values that produced the fit (again assuming that $\delta = 1$). The σ values are essentially the same at each eccentricity and have values that complement the accuracy data. These fits indicate that the relative difference between the two textures is greatest at about 3° and decreases towards the fovea and greater eccentricities. If we had fixed $\sigma_1 = \sigma_2$ and varied δ to fit the data then we would find that δ is greatest at 3° and falls off towards the fovea and the periphery. This reveals the standard explanation for the CPD as discussed in the introduction;

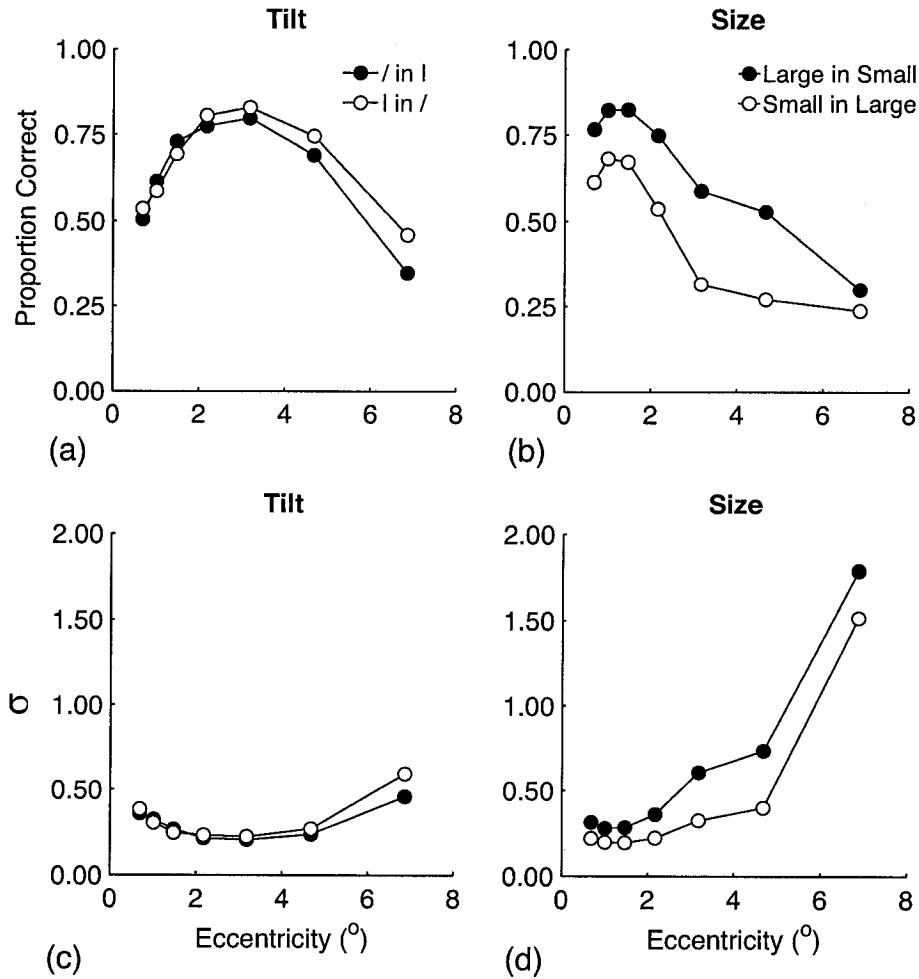


Figure 3.7. Averaged data from the orientation (a) and size (b) experiments and σ values that fit the orientation data (c) and size data (d).

i.e., that as eccentricity increases from fixation to the periphery the match between the scale of the stimulus and mechanism improves and performance increases, but beyond the performance peak performance decreases (δ drops) because of resolution loss (Gurnsey et al., 1996).

Size Textures

Figure 3.7(b) shows the averaged results for the size stimuli. These averaged data show an asymmetry but no CPD. Figure 3.7(d) shows σ values that produced the fit. The σ values increase monotonically with eccentricity and

at all eccentricities the large circles are associated with larger σ values. Therefore, within a signal detection framework it would be argued that the larger circles engage mechanisms that for some reason produce a noisier response than the smaller circles. In fact, this is exactly the argument used by Rubenstein and Sagi (1996) to explain texture discrimination asymmetry for certain size-differing textures (Gurnsey & Browse, 1989). Roughly similar results would be obtained if we had fixed variability difference ($\sigma_1 - \sigma_2 = k$) and varied δ to fit the data. In this case δ would drop more or less monotonically with eccentricity. In either case the explanation would be essentially the same. That is, the two textures give rise to unequal variability and the relative differences between the means decreases with eccentricity.

LX and Jitter Textures.

The LX and Jitter conditions produced very similar results in Experiments 1 and 2. Both the LX and Jitter conditions produced very large asymmetries consistent with past research. However, the size of the asymmetry is eccentricity dependent and particularly so in the case of the LX pair. In fact, the LX pair produced no asymmetry at fixation and an extremely large asymmetry at about 3.19° from fixation. This eccentricity dependent asymmetry might explain why texture discrimination asymmetries had not been a focus of study before 1987. Previous experiments by Julesz (1981, 1984) and Bergen and Julesz (1983) used displays in which the disparate texture was centred in the display. In contrast, Gurnsey and Browse (1987, 1989; see also Rubenstein & Sagi, 1990, 1996) positioned the disparate texture in one of four quadrants putting the centre of the disparate region well into the periphery. The present results suggest that when a

disparate texture is centred on fixation an asymmetry is much less likely to emerge than when it is placed in the periphery. The same general comments are true for the jitter stimuli however, the asymmetry, while attenuated at fixation is not completely eliminated.

For these two texture pairs the change in asymmetry with eccentricity goes hand in hand with a divergence in performance across eccentricity for the members of the pairs. For the LX pair there is a CPD (in Experiment 1) for Ls in Xs but a standard eccentricity dependent sensitivity loss for Xs in Ls. The same general pattern is seen for the Jittered and non-Jittered stimuli, although the CPD is not significantly present in Experiment 2. Figure 3.8(a) plots the averaged results for the LX and Figure 3.8(b) plots the averaged results for jitter stimuli. Figure 3.8(c) and Figure 3.8(d) plot the σ values that fit the accuracy data. As before, the σ values complement the accuracy data. For the LX pair the σ values are identical at fixation, diverge as eccentricity increases then converge again beyond the performance peak for the Ls at 3.19°. At fixation the lack of asymmetry is explained by equal variance in the response distributions governing performance. As eccentricity increases the variances diverge in the manner described by Rubenstein and Sagi (1990). At the furthest eccentricities the relative difference in variance decreases; this would be equivalent to a reduction in mean response difference (δ).

The results of the two experiments reveal the complexities of texture discrimination. It is not uncommon for models of texture discrimination to attempt to match existing psychophysical data. Often such models focus on the average discrimination of a texture pair (e.g. Malik and Perona, 1990),

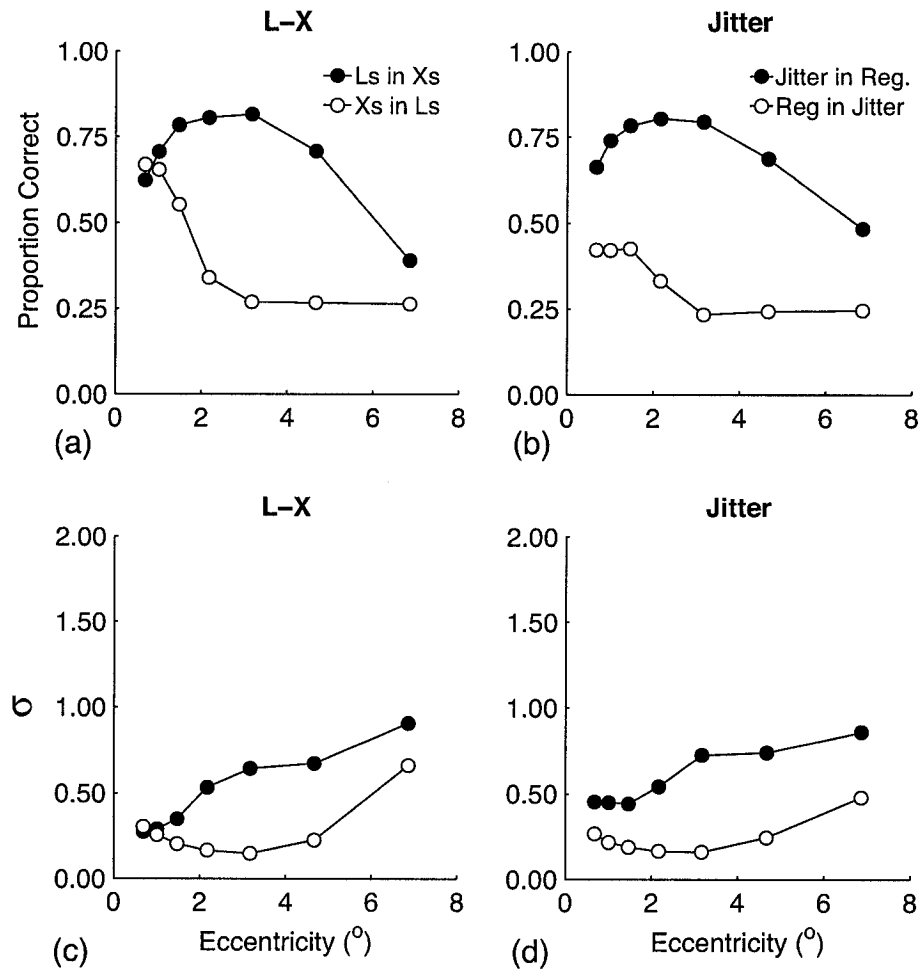


Figure 3.8. Averaged data from the orientation (a) and size (b) experiments and σ values that fit the orientation data (c) and size data (d).

whereas others consider the potential asymmetrical discrimination of texture pairs (e.g., Liu & Wang, 2002; Rubenstein & Sagi, 1990, 1996). The current results demonstrate the need to consider asymmetries within the context of eccentricity. Clearly, one cannot talk about the discriminability of two textures without referring to both eccentricity and the arrangement of the two textures.

We have discussed the results within the context of signal detection theory. Such an analysis places constraints on the mechanisms involved but does

not uniquely specify the representations or processes that give rise to texture discrimination. Perhaps the easiest results to explain are those from the Oriented Line experiment. When the results are averaged over the two experiments both tilted-in-vertical and vertical-in-tilted give rise to a CPD with little evidence of an asymmetry. (We are inclined to attach little importance to the differences in the orientation results from Experiments 1 and 2. We feel that the average data capture the most important aspects of the data. Perhaps a more sensitive analysis would reveal a principled difference that we are missing.) As noted already, computational models by Kehrer and Meinecke (2003) and Gurnsey et al. (2004) are in good agreement with this kind of result.

The failure to find consistent asymmetries in the orientation experiment is puzzling because asymmetries have been previously reported for these stimuli in the visual search task (e.g. Treisman & Gormican, 1988; Foster & Ward, 1991a, 1991b; Foster & Westland, 1995, 1998; Poirier & Gurnsey, 1998). Nothdurft (1985) pointed out that stimulus element density can affect texture segmentation performance. Differences in stimulus density and orientation of individual line elements differs between the images used in previous asymmetry experiments and those used here. Visual search experiments normally use a single target element in a multi-element background and it is not uncommon for there to be a relatively small number of elements in the displays. The density of such stimuli is reduced as compared to the textures used here and may explain the different pattern of results.

Furthermore, asymmetries between vertical and tilted lines have been demonstrated in stimuli where the orientations of microelements were bimodal (i.e. the orientation of tilted and vertical lines represented two standard values).

We were previously able to demonstrate an asymmetry in textures where the line elements were oriented at either 0 or 18 degrees (Potechin & Gurnsey, 2001); i.e., no within-region orientation variability. It is possible that orientation discrimination asymmetries arise only when there is little noise in the displays.

The size differing stimuli elicit an asymmetry that is relatively constant across eccentricities. As mentioned above, this is consistent with reduction in the mean difference between responses as eccentricity increases accompanied by a greater variance in the distribution of responses associated with the larger stimuli (Rubenstein & Sagi, 1996). However, these data do not permit us to distinguish this explanation from that given by Gurnsey and Browse (1989), which suggested that the strength of a texture contrast at a texture boundary is normalized by the summed activity within the relevant channel; in this case a fixed texture contrast is strongest when the background region produces the least activity. It is interesting, however, that there is no evidence of a CPD, meaning that the match between texture and mechanism does not improve with eccentricity. In other words, performance is optimal at fixation. Because the Size differing textures are alone in showing no hint of CPD for either member, it seems that they might be discriminated in virtue of quite different mechanisms than the remaining three.

The similarity of the LX and Jitter textures suggest that quite similar mechanisms might be involved. Specifically, with increasing eccentricity the Xs and regular circles become increasingly difficult to detect among Ls and Jittered circles, respectively. The unequal variance explanation seems particularly apt in this case. As mechanisms (presumably) increase in size with eccentricity a small region with low variability will become increasingly difficult to detect within

disorder than vice versa. This is consistent with the idea that variability is principally responsible for the LX asymmetry [although Sezikeye & Gurnsey (2005) found statistically significant asymmetries for Ls among Xs even when orientation variability was eliminated.] It is interesting, however, that the jittered and non-jittered stimuli never become equally discriminable at fixation, as do the LX textures. It may be that the L- and X-type contrast offer useful information to an attentional mechanism at fixation whereas the circles in the jitter contrast do not. That is, discrimination in the case of jitter is based on purely relational properties between micropatterns whereas assessment of individual micropatterns might lead to correct responses in the case of Ls and Xs.

The LX and Jitter results are similar in many ways to the results reported by Meinecke et al. (2002) who asked subjects to detect closed squares among open squares and vice versa. Performance depended on which elements formed the foreground and background, eccentricity and density. In low density displays open squares were easier to detect in closed squares at all eccentricities and performance fell off monotonically with eccentricity. In dense displays this asymmetry was reversed and in all but one condition performance fell off monotonically with eccentricity. (Unfortunately performance was on the ceiling at fixation for most dense displays making it impossible to determine if one or the other condition produced a CPD.) In the dense condition that did not produce ceiling level performance at fixation, a CPD was found for closed in open squares. These results seem quite similar to the LX results reported in Figures 3.5 and 3.6 and might be interpreted in a similar way. That is, there may be a change in strategy from fixation to the periphery. It may be that at fixation the properties of individual micropatterns provide the basis for discrimination

(e.g., terminators or line crossings) whereas in the periphery differences in textural properties (i.e., properties of regions) provide the basis for discrimination. This seems to be generally in line with the explanation Meinecke et al. (2002) give for their data.

In conclusion, we have replicated a number of previously reported asymmetries and extended the findings to incorporate the effects of eccentricity on texture discrimination. We found that there is a relatively complex array of dependencies on texture arrangements and eccentricity; it is clearly not reasonable to talk about the discriminability of two textures without referring to eccentricity or the arrangement of the two textures.

CHAPTER 4

**CROSS-FREQUENCY INHIBITION AND
THE CENTRAL PERFORMANCE DROP.§**

by

CINDY POTECHIN AND RICK GURNSEY *

**DEPARTMENT OF PSYCHOLOGY
CONCORDIA UNIVERSITY**

ABSTRACT

The central performance drop (CPD) refers to the phenomenon whereby peak texture discrimination performance occurs with parafoveal viewing and deteriorates as the disparate texture is moved towards either the fovea or the periphery. There is a question of whether cross frequency inhibition (CFI) (i.e., the inhibition of low spatial frequency information by high frequency information) contributes to the CPD. Previous examinations of the CFI by Gurnsey, Pearson and Day (1996), Morikawa (2000) and Carrasco, Loula and Ho (in press) led to different conclusions. In three experiments, we examined how the attenuation of high frequency information in texture displays influences texture discrimination. Two experiments showed that low-pass filtering of the stimulus improved target detection at the fovea (Experiment 1) and other locations in the visual field (Experiment 2). In the third experiment, attenuation of the high frequency components by adaptation had no effect on target detection. These results suggest that CFI may play an important role in the CPD.

Spatial resolution declines with eccentricity (Graham, 1989; DeValois & DeValois, 1988). Therefore, it is not surprising that our ability to segment texture and to detect and discriminate visual targets typically declines as stimuli of fixed size are presented at further eccentricities (e.g. Carrasco & Frieder, 1997; Nothdurft, 1985; Saarinen, Ravamo, and Virsu, 1987). Kehrler (1987) reported an exception to this pattern in the case of texture discrimination. He showed that the detection of oblique lines of a particular orientation embedded in a larger background of orthogonally oriented lines improves as the target texture is moved away from the fovea. This “central performance drop” (CPD; i.e. sub-optimal texture performance at foveal or near-foveal locations) has been replicated a number of times in a variety of paradigms (e.g. Gurnsey, Pearson, & Day, 1996; Joffe & Scialfa, 1995; Morikawa, 2000; Potechin & Gurnsey, 2003, 2006; Yeshurun & Carrasco, 1998).

Kehrler originally attributed the CPD to differences in the processing speeds of the spatial-frequency selective filters that underlie texture discrimination. His theory assumed that the visual system responds more quickly to low frequencies than to high frequencies and that sensitivity to low spatial frequencies is greater in the periphery than at the fovea. Psychophysical results have demonstrated an increase in processing speed as the target is further removed from the fovea (Carrasco, McElree, Denisova, & Giordano, 2003; Fiorentini, 1989). Kehrler (1989) suggested that texture discrimination at fixation is determined by differences in high frequency content within target and background regions. Taken together these assumptions imply that a backward mask (as used in Kehrler’s experiments) should have a greater effect at fixation than in the periphery. In the

periphery, faster mechanisms tuned to lower spatial frequencies may achieve segmentation prior to mask onset.

Demonstrations of the CPD in the absence of backward masking (Gurnsey, di Lenardo & Potechin, 2004; Morikawa, 2000; Potechin & Gurnsey, 2003; Potechin & Gurnsey, 2006) indicate that a temporal account by itself cannot fully explain the CPD. Nonetheless, Morikawa (2000) found support for the temporal hypothesis after finding that a CPD was not elicited in two experiments in which a backward mask was not used. However, in both of these experiments, Morikawa (2000) made changes to the spatial structure of the mask or the stimulus in addition to eliminating the backward mask. In the first case, the line micropatterns comprised in the stimulus were shortened and the mask was eliminated. In the second case, the mask was (i) changed from an X-type pattern to a random dot noise pattern, and (ii) presented simultaneously with the stimulus rather than following it. Gurnsey et al. (2004) argued that the temporal theory could only be supported if a CPD was elicited when a backward mask was used along with the short line stimulus and if the noise mask was used as a backward mask instead of a simultaneous mask. They showed that the shortened line stimulus was difficult to detect and did not elicit a CPD when a backward mask was used. Although a modest CPD was found when the noise mask was used as a backward mask, Gurnsey et al. (2004) used a simple filter-rectify-filter model of texture segmentation to show that this result would be expected when spatial factors alone are considered. That is, evidence that was adduced to support the temporal theory is in fact also consistent with a spatial account. The inability to elicit a CPD in both these cases could be attributed to factors other than the absence of a backward mask.

A purely spatial account of the CPD (Gurnsey et al., 1996, Kehrner, 1997) has been more widely accepted (e.g. Kehrner & Meinecke, 2003; Gurnsey, Di Lenardo & Potechin, 2004). Gurnsey et al. (1996) argued that texture segmentation in the fovea involves mechanisms tuned to high spatial frequencies that operate over a small spatial extent whereas peripheral segmentation involves mechanisms tuned to low spatial frequencies operating over a larger spatial extent. According to their logic, peak segmentation performance would occur when the scale of the texture to be detected matches the spatial frequency selectivity of the detection mechanism involved, likely at some intermediate eccentricity. At the fovea the segmentation mechanisms are too small relative to the textures whereas in the far periphery they are too large (Gurnsey et al., 1996).

Both explanations for the CPD noted above require an assumption that low spatial frequencies are not processed as effectively in the fovea as in the periphery. There are two possible reasons why this might be so. The first possibility is that no low spatial frequency filters are present in the fovea. However, De Valois and De Valois (1988) reported that the entire range of spatial frequencies is detected within the fovea. Additionally, sensitivity to many spatial frequencies has been reported to be highest in the fovea (Robson & Graham, 1981; Wright & Johnston, 1983). Therefore, it appears unlikely that low spatial frequency filters are absent at the fovea.

Alternatively, in some situations, low frequencies may not be processed effectively in foveal vision because filters tuned to high spatial frequencies are given preference over low-spatial frequency filters, whether or not these filters are optimally matched to the task. Sensitivity to high spatial frequencies declines markedly with eccentricity while a drop in sensitivity to low spatial frequencies

with eccentricity is much less pronounced. (De Valois & De Valois, 1988; Wright & Johnston, 1983). A sharp decline in high-frequency sensitivity with eccentricity is likely due to the much higher concentration of cells responsive to high spatial frequencies in the fovea than in the periphery (Connolly & Van Essen, 1984). One would expect any high-frequency influences to be strongest in the fovea. The inhibitory or interfering effect of the high frequency signal on low-frequency information in an image has been called cross-frequency inhibition or cross-frequency interference (Carrasco et al., in press; Gurnsey et al., 1996; Morikawa, 2000).

Mechanisms tuned to high spatial frequencies may only exert an indirect effect over mechanisms tuned to lower spatial frequencies. It has been proposed that the responses of local visual filters or simple receptors are normalized according to the degree to which similarly tuned cells are responding within an image (Graham & Sutter, 2000; Gurnsey & Browse, 1989; Heeger, 1992). Carrasco, et al. (in press) suggested that the CPD is caused by the influence of the high-frequency filters in the normalization process. That is, the responses of high-frequency filters that are non-optimal for the task obscure the outputs of lower frequency filters that are better matched to the stimulus.

Cross frequency inhibition has been used to explain other visual phenomena. A well known example is the difficulty observers have in recognizing a block portrait of Abraham Lincoln created by Harmon and Julesz (1973). The coarsely sampled image was constructed by first scanning a high-resolution photograph and creating a digitized image that was divided into a number of small square size patches or blocks. To create the block portrait, each

block was converted to a uniform brightness level that matched the average brightness value of that region within the original photograph. Discontinuities in the image produced by the high spatial frequencies in the block edges make the portrait unrecognizable. Blurring such images improves recognition because it eliminates high spatial frequency interference and reveals the lower spatial frequency information. In this case, when high and low frequency information compete, the higher-frequency information appears to take precedence².

Gurnsey et al. (1996) were the first to examine a cross-frequency explanation for the CPD. The experiment involved the detection of a disparate texture at a range of eccentricities across the horizontal meridian. Subjects were required to detect a 3 x 3 element target composed of lines with mean orientations of $\pm 45^\circ$ ($\pm 10^\circ$) embedded within a much larger background of orthogonally oriented lines. Five levels of low pass filtering were used to systematically attenuate the high frequency content of their stimuli, and a backward mask was used to limit performance. Both their stimuli and mask were filtered with the same Gaussian filter. Overall performance was negatively correlated with degree of blurring. No improvement in segmentation performance at the fovea was found for any of the blurring conditions. Gurnsey et al. concluded that cross-frequency inhibition could not explain the reduced foveal performance that is characteristic of the CPD.

In contrast to the results of Gurnsey et al. (1996) Morikawa (2000) reported improved performance at the fovea when textures were low-pass filtered

² Morrone, Burr, and Ross (1983) examined a similar block portrait and argued against a cross-frequency hypothesis after finding that by further increasing the

(blurred). His micropatterns comprised line pairs that differed in the direction of their vertical offsets. Subjects were required to locate a 3 x 3 element target presented in one of the four quadrants of the display. In the target region, pairs of vertical lines were connected by a left or right oblique *virtual* line. In the other region, they were connected by orthogonally oriented virtual lines. When blurred with a Gaussian filter, the oblique lines became apparent as luminance contours. Because low pass filtering reduces image contrast, Morikawa (2000) increased the image contrast of the filtered stimuli presented to subjects. In effect, Morikawa made two changes to his stimuli, making it difficult to determine whether his results were a consequences of the altered spatial frequency content of the stimulus or the increased contrast in low-frequency bands. Although Morikawa's (2005) results appear consistent with a CFI explanation of the CPD, there remains a question of which of the two manipulations used in this experiment resulted in increased performance at the fovea.

Carrasco et al. (in press) used a selective adaptation procedure to examine the effect of spatial frequency on the CPD. Subjects were required to detect a 3 X 3 element target composed of lines oriented at either $\pm 8^\circ$ from vertical embedded within a much larger background of vertical lines. Before the test stimulus was displayed, subjects adapted to three types of patterns: a homogenous gray field, a low frequency vertical sine wave grating or a high frequency sine wave grating. The purpose of the adaptation was to attenuate sensitivity to high spatial frequencies. Performance was limited through the use of a backward mask. Their results showed that (i) a CPD was present after adaptation to a homogenous gray

high-frequency content of an image, in this case a representation of the Mona Lisa, also resulted in better recognition of the face presented in the image.

field, (ii) a CPD was absent after adaptation to a high frequency grating and (iii) performance at central locations was in between these two conditions after adaptation to the low frequency grating. An important confound exists in this study. The orientation of the adapting stimulus was identical to that of the background elements and differed from the orientations of the target elements of the test stimulus. Therefore, increased performance at the fovea following adaptation to the high frequency grating may be a consequence of reduced sensitivity to the background elements (as compared to the foreground elements) rather than a general attenuation of the high spatial frequencies as proposed by the authors. Carrasco et al. (in press) concluded that attenuating the high frequency content of the stimulus resulted in improved performance at the fovea and an elimination of the CPD. However, since the adaptation may have had different effects on the target texture versus the background texture it is not possible to show that improved performance at the fovea was a direct result of high frequency attenuation.

The Morikawa (2000) and Carrasco et al. (in press) examinations of the CFI hypothesis suggest that high frequency information inhibits texture segmentation at and near the fovea but both studies involved confounds that make the results ambiguous. To examine the cross-frequency hypothesis further, the experiments reported here attempt to isolate the effects of high spatial frequency information on the detection of texture targets across the visual field. Experiment 1 presents a replication of Gurnsey et al. (1996, Experiment 2). However, in the present replication performance is limited through a manipulation in orientation variability within the texture and background regions rather than a backward mask. Because backward masking is not required

to elicit a CPD (Potechin & Gurnsey, 2003, 2006), this manipulation is not expected provide different results from those of Gurnsey et al. (1996). Experiments 2 and 3 addressed the confounds present in the Morikawa (2000) and Carrasco et al. (in press) studies. In Experiment 2, Morikawa's (2000) low-pass filtering of virtual line stimuli was repeated without a renormalization of contrast level of the stimulus after filtering; if the elimination of the CPD in Morikawa's study was a consequence of normalization, then no improvement in foveal performance should be found in the present experiment. In Experiment 3, an adaptation procedure similar to that used by Carrasco et al. (in press) was used to attenuate sensitivity to the high-frequency components in the image. In this experiment subjects adapted to a left oblique, high frequency grating prior to discriminating textures comprising left and right oblique line segments. Reduced sensitivity to left oblique stimuli should introduce an apparent luminance difference between foreground and background textures (as we assume occurred in the Carrasco et al. study). Therefore, detection accuracy at fixation following adaptation to the high frequency grating should be greater than adaptation to a homogenous field.

The CFI account predicts similar results in all three experiments. The previous examinations of the CFI discussed above have shown that a CPD is elicited in response to the unfiltered stimulus. Assuming that low-frequency information is suppressed in the presence of high-frequency information (i.e. the CFI hypothesis), then attenuation of the high frequency information through low-pass filtering and selective adaptation to high frequencies should lead to improved performance at the fovea. No difference in performance is expected in the periphery where sensitivity to high frequencies is already reduced. On the

other hand, if texture discrimination is not influenced by cross-frequency inhibition, performance at the fovea should not change significantly.

EXPERIMENT 1

Gurnsey et al.'s (1996) examination of the CFI hypothesis employed a backward masking procedure. However, the use of the backward mask creates the possibility of having a temporal influence on the task. Potechin and Gurnsey (2003, 2006) elicited the CPD without backward masking by limiting performance through the use of spatial noise within the stimulus. Experiment 1 re-examined the CFI experiment of Gurnsey et al. (1996) using a bandwidth manipulation (described further below) to limit performance rather than a backward mask.

The stimuli used in this experiment were based upon those used by Potechin and Gurnsey (2003). The foreground and background textures were composed of lines with mean orientations of $\pm 45^\circ$. Individual elements were chosen at random from a flat distribution of orientations. The range of orientations from which the line elements are sampled is referred to as the 'orientation bandwidth'. A bandwidth of 1 means that all line elements have the same orientation. A bandwidth of 180 is required to represent all possible orientations. In this experiment, a bandwidth of 100 was used.

METHOD

Subjects

Seven subjects participated in the experiment. All reported normal or corrected to normal vision.

Apparatus

The stimuli were presented on an Apple G4 computer attached to a 21" monitor with a frame rate of 85 Hz and a resolution of 1280 x 1024 pixels. The stimulus elements were presented in black against a white background. The experiment was conducted in the absence of any lighting except that provided by the computer screen. A viewing distance of 120 cm was maintained through the use of a chin rest.

Stimuli

The stimulus display consisted of 280 (7 rows x 40 columns) patches of 32 pixels squared each. Each patch contained one line element that was 0.63° of visual angle in length. All stimuli were lines having a Gaussian cross-section with a standard deviation of 1.3 pixels. On each trial, a nine-element target (3 rows x 3 columns) was embedded in the background. Within each texture, the average orientation of background elements was either 45° or -45° from vertical drawn from a flat distribution having a bandwidth of 100. Target elements were created in similar fashion except their mean orientation was orthogonal to the mean orientation of the background elements. The orientations of the foreground and background elements were varied randomly from trial to trial so that the detection of a line element of a particular orientation could not be used to determine the presence of the target. A slight positional jitter (± 2 pixels horizontally and vertically) was introduced into the placement of the line segments to minimize the contribution of discontinuity of element placement as the basis for texture segmentation. The stimulus display subtended 17.61° horizontally and 3.18° vertically. The size of the target texture was 1.36° in both the vertical and horizontal directions.

The stimuli were submitted to three levels of Gaussian blurring. In Conditions 1, 2 and 3 stimuli were blurred with isotropic Gaussian filters having standard deviations (σ) of 1, 3 and 5 pixels respectively. Examples of the stimuli are shown in Figure 4.1.

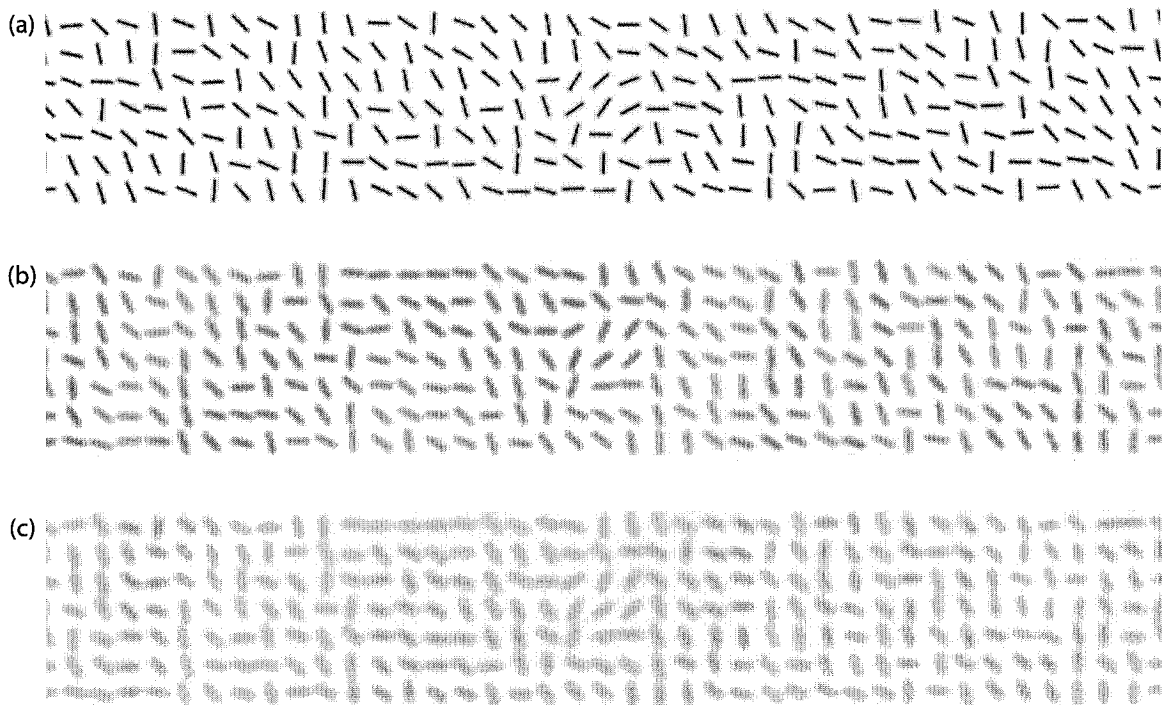


Figure 4.1. Examples of the stimulus patterns used in Experiment 1. The average orientation of line elements is 45° in the foreground and 135° in the background. Starting with the panel and moving downward, the images have been convolved with isotropic Gaussian filters having standard deviations (σ) of 1, 3 and 5 units.

Procedure

A 2AFC task was used. On the initial trial of a block a screen indicated the block number and signaled the subject to press the number “3” on the numeric keypad to initiate the first trial. Each interval of a single trial sequence consisted of the presentation of a central fixation dot followed by a stimulus display of 33 ms. A 5 x 5 pixel, black dot was used as the fixation stimulus. The two stimulus displays were separated by an inter-stimulus interval of 667 ms. In one interval

the stimulus contained the target region. A homogenous texture was presented in the other interval. The orientation of the background micropatterns was randomly chosen during each interval. The subject's task was to identify the interval containing the target texture by pressing one of two computer keys that represented each interval. At the end of each trial in which the subject made an error, feedback was provided in the form of a beep. A blank screen with a fixation dot remained until the subject provided a valid response. On subsequent trials, the subject's response initiated the next trial.

Within each block of trials the disparate regions were placed at one of fifteen positions along the horizontal meridian ranging from 0° to $\pm 7.77^\circ$ from fixation ($0.00, \pm 0.74, \pm 1.11, \pm 1.63, \pm 2.41, \pm 3.56, \pm 5.27, \text{ and } \pm 7.77^\circ$) for each of the three blurring conditions. Within a block trials were grouped by degree of blurring, such that all eccentricities were tested for one blurring condition before another blurring condition was tested. The order in which blurring conditions were tested was determined at random. Target eccentricity was chosen randomly on each trial subject to the constraint that each eccentricity was presented only once in each block of trials. The experiment consisted of twenty blocks of trials. Therefore, each subject participated in 900 trials in the experiment (15 eccentricities \times 3 blurring conditions \times 20 replications). Before the experiment, subjects were given 2 practice blocks.

RESULTS AND DISCUSSION

Data were collapsed across right and left visual field. The proportion of correct responses was calculated for each filter condition at each eccentricity. The data were submitted to a 3 (filter type) by 8 (eccentricities) within-subjects ANOVA. Effect size was calculated as a partial ϵ^2 (h_p^2). The effects of eccentricity

for each filter (blur) type were then examined separately using trend analysis to determine whether a CPD had been elicited. The linear trend analysis was limited to data positions representing eccentricities 0° to 2.41°. The results are summarized in Figure 4.2.

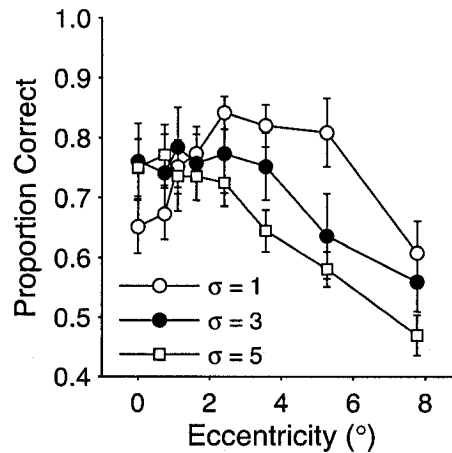


Figure 4.2. Results of Experiment 1. The proportion of correct target detections is shown as a function of eccentricity. This graph shows the probability of target detection for as a function of target eccentricity and degree of Gaussian blurring of the stimuli.

The main effect of eccentricity was statistically significant [$F(7, 42) = 15.81$, $p < 0.01$] whereas the main effect of filter type was not. The interaction of filter type by eccentricity [$F(14, 84) = 3.52$, $p < 0.05$] was also statistically significant. The effect size of the interaction was 0.369. As shown in Figure 4.2, performance peaked in the parafovea for Condition 1 ($\sigma = 1$), with reduced performance occurring towards both the fovea and the periphery. In Conditions 2 and 3 ($\sigma = 3$ and 5), performance was relatively stable in the fovea and parafovea and declined as the target was moved further into the periphery. In the periphery, overall performance declined in direct relation to the degree of high frequency attenuation. The trend analysis showed an increase in correct responses from the

fovea to the 2.41° position in Condition 1 [$F(1, 6) = 35.627, p < 0.01$]. The trends in Condition 2 [$F(1, 6) = 35.627, p > 0.05$] and Condition 3 [$F(1, 6) = 35.627, p > 0.05$] were not statistically significant. That is, a CPD was elicited in the stimulus with the least blurring whereas no CPD was elicited in the two conditions with a higher degree of blurring.

Overall these results indicate that performance varies across eccentricity and that this change in performance across eccentricity changes as a function of high frequency attenuation. Performance at peripheral locations was consistent with the results of Gurnsey et al. (1996). That is, performance in the periphery declined in direct relation to the amount of high frequency attenuation. As sensitivity to high spatial frequencies is reduced in the periphery, low-pass filtering should not have a marked effect on performance at these locations. The decrement in performance may be explained by the fact that removal of the high frequencies (or blurring the image) results in reduced overall contrast in the image.

To summarize, the results of Experiment 1 show that removal of high frequency information from a stimulus comprising oriented line elements using a Gaussian filter led to improved performance at foveal locations. These results appear to support a CFI explanation of the CPD. However, one has to rule out the possibility that an interaction between the bandwidth manipulation and the Gaussian filtering had no influence on the outcome of the experiment; see the General Discussion for further discussion.

EXPERIMENT 2

Morikawa (2000) examined the effects of high frequency attenuation on textures comprising vertically offset lines using a 4AFC in which subjects had to

identify a quadrant containing a disparate texture. As discussed in the introduction, his results could not be unambiguously interpreted because of a confound between the spatial frequency content of his displays and contrast of the low frequency components in the display.

Experiment 2 examines the same question using a 2AFC procedure (similar to Experiment 1) rather than the 4AFC employed by Morikawa (2000). Unlike Morikawa's (2000) procedure in which he increased the luminance energy levels on the stimulus after it was filtered, in this experiment the luminance levels of the filtered stimuli were not renormalized after the low-pass filtering. Therefore, any change in performance will be attributable to the effects of high frequency attention alone.

METHOD

The apparatus and procedures used in this experiment were identical to those used in Experiment 1 with the following exceptions:

Subjects

Seven subjects participated in all four conditions of the experiment. All reported normal or corrected to normal visual acuity. Five of the subjects had participated in Experiment 1.

Stimuli

The stimulus elements were presented in white (89 cd/m^2) against a black background (0.1 cd/m^2) as in the experiment of Morikawa (2000)³. A viewing distance of 60 cm was maintained through the use of a chin rest.

³ When the contrast of the stimulus elements and background was reversed the task became much more difficult and performance was generally at a floor level for most subjects.

The stimulus display consisted of 203 (7 rows x 29 columns) patches of 32 pixels squared each. Each micropattern consisted of a pair of 0.28° long vertical lines. Within each micropattern two short vertical lines were placed in diagonally opposite corners (e.g. one line placed in the upper-left and the other placed in the lower-right). The upper and lower lines had a horizontal offset of 0.34° and a vertical offset of 0.11° . Similar to Experiment 1, slight positional jitter (± 5 pixels horizontally and 4 pixels vertically) was introduced into the placement of the line segments to minimize the contribution of discontinuity of element placement as the basis for texture segmentation. The nine-element target (3 rows x 3 columns) contained lines that were left-right reversed versions of the background elements. The blurring procedure was identical to that used in Experiment 1. The stimulus display subtended 32.41° horizontally and 6.34° vertically. The size of the target texture was 2.72° in both the vertical and horizontal directions. Examples of the stimuli are shown in Figure 4.3.

Procedure

The procedure was identical to that used in Experiment 1 with the following exceptions. Each interval of a single trial sequence consisted of the presentation of a central fixation dot followed by a stimulus display of 66 ms. In each block, the disparate regions were placed at one of fifteen positions along the horizontal meridian ranging from 0° to 15.26° from fixation ($0.00, \pm 1.47, \pm 2.22, \pm 3.26, \pm 4.82, \pm 7.10, \pm 10.45, \text{ and } \pm 15.26^\circ$).

RESULTS AND DISCUSSION

The data analysis procedure was similar to that used in Experiment 1. The trend analysis was limited to data positions representing eccentricities 0° to 4.82° . The results are summarized in Figure 4.4.

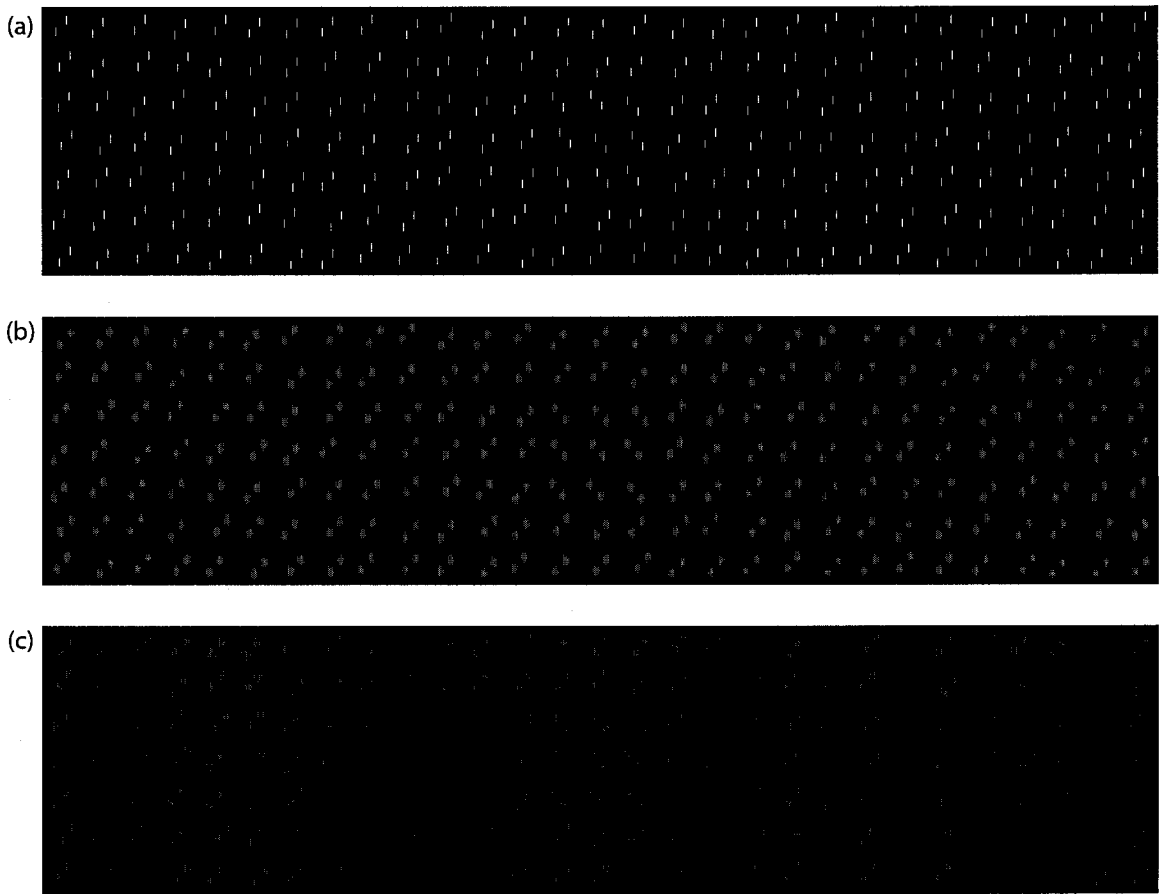


Figure 4.3. Examples of the stimulus patterns used in Experiment 2. In each micropattern, the lines are vertically offset by 10 pixels. Starting with the upper panel and moving downward, the images have been convolved with isotropic Gaussian filters having standard deviations (σ) of 1, 3 and 5 pixels.

The main effect of filter type was statistically significant, indicating that overall performance improved in direct relation to the level of high frequency attenuation in the stimulus [$F(2, 12) = 11.07, p < 0.01$] with an effect size of 0.648. The main effect of eccentricity and the interaction between filter type and eccentricity were not statistically significant. The trend analysis revealed the absence of a statistically significant linear effect from the fovea to 4.82° for all three conditions. That is, no CPD was demonstrated in any condition.

As was the case in Morikawa (2000), performance across eccentricity

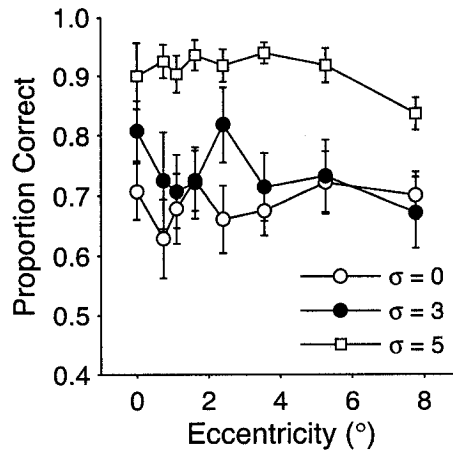


Figure 4.4. Results of Experiment 2. The proportion of correct target detections is shown as a function of eccentricity. This graph shows the probability of target detection as a function of target eccentricity and degree of Gaussian blurring of the stimuli.

changed as a function of the amount of high frequency information that was removed from the stimulus. On the other hand, Morikawa (2000) demonstrated a CPD in the unfiltered stimulus while performance was largely invariant across eccentricity in the unfiltered stimulus in this experiment. One factor that may underlie this difference is the level of sophistication of the observers. Morikawa used naïve subjects while most of our subjects were experienced psychophysical observers. Another possibility is that the large variability in subject's responses may have obscured a weak CPD if it was present.

In summary, these results show that using a Gaussian filter to attenuate high frequency information from a pattern of vertically offset lines led to improved texture detection. However, contrary to the results obtained in Morikawa (2000) a CPD for unfiltered stimuli was not found.

EXPERIMENT 3

As discussed in the introduction, Carrasco et al. (in press) employed a selective adaptation procedure to examine the CFI hypothesis. Given that the orientation of the adapting stimulus was identical to the background elements and differed from the orientation of the target elements of the test stimulus, the adaptation may have had different effects on the target texture versus the background texture. This confound made the results difficult to interpret. Here, we re-examine Carrasco et al.'s (in press) results using a similar high frequency adaptation procedure. Two stimulus displays mirroring each other in terms of the orientations of the foreground and background microelements were examined separately to ensure that the results were not due to a differential effect of the adaptation on foreground and background elements.

METHOD

The apparatus and procedures used in this experiment were identical to those used in Experiment 1 with the following exceptions:

Subjects

Four subjects participated in the experiment. All reported normal or corrected to normal vision. Three of the subjects had participated in Experiments 1 and 2. The fourth subject participated in Experiment 1 only.

Apparatus

The experiment was conducted under full lighting conditions. Lighting was provided by overhead fluorescent lights. A viewing distance of 60 cm was maintained through the use of a chin rest.

Stimuli

The stimulus display consisted of 168 (7 rows x 44 columns) patches of 44 pixels squared each. Each patch contained one line element of 0.51° of visual angle in length. The lines were smoothed to eliminate aliasing. On each trial, a nine-element target (3 rows x 3 columns) was embedded in the background. Within each texture, the orientation of background elements was either 45° or -45° from vertical. Target elements were created in similar fashion except their orientations were orthogonal to the orientation of the background elements.

The orientations of foreground (and background) elements varied from trial to trial so that the detection of a line element of a particular orientation could not be used to determine the presence of the target. A slight positional jitter (± 3 pixels horizontally and vertically) was introduced into the placement of the line segments to minimize the contribution of discontinuity of element placement as the basis for texture segmentation. The stimulus display subtended 32.41° horizontally and 6.34° vertically. The size of the target texture was 2.72° in both the vertical and horizontal directions.

Two types of stationary adapting patterns were used, a homogenous gray field (baseline condition) and a high-spatial frequency 100%-contrast sine wave grating of 8 cpd (test condition). The orientation of the adapting pattern was 45° and it was used to adapt to only one of the two microelements present in the test stimulus, either the target or the background elements depending upon the test stimulus. Examples of the stimuli and adapting patterns are shown in Figure 4.5.

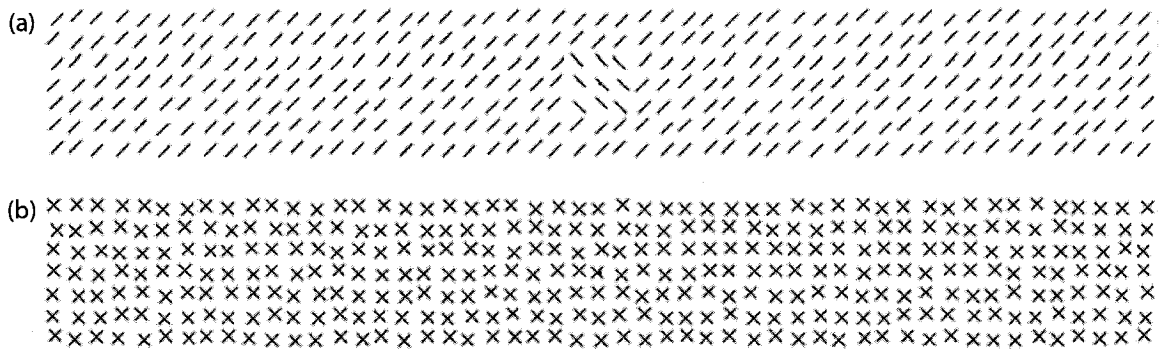


Figure 4.5. Examples of the stimulus and mask patterns used in Experiment 3. The average orientation of line elements is 45° in the foreground and 135° in the background.

Procedure

The two adaptation stimuli were run in separate conditions. In each block of a condition, the subject first adapted to the high-frequency grating or to the homogenous gray field for 120 s. On the initial trial of a block a screen indicating the number of the block signaled the subject to press the number “3” key on the numeric number pad to initiate the adaptation. During the adaptation, the subjects were asked to move their eyes continuously and steadily across the adaptation field. Following adaptation, subjects performed a 2AFC task in which they were asked to judge which interval contained a disparate region. The procedure was identical to that of Experiments 1 and 2 except that a mask (see Figure 4.5) was presented for after each stimulus. There were approximately 2 min of data collection after each 2 min of adaptation. Each subject participated in 600 trials in the experiment (15 eccentricities \times 2 target background directions \times 2 adaptation conditions \times 10 replications). In each block, the disparate regions were placed at one of fifteen positions along the horizontal meridian ranging from 0° to 13.12° from fixation ($0.00, \pm 1.90, \pm 3.80, \pm 5.69, \pm 7.60, \pm 9.46, \pm 11.30, \text{ and } \pm 13.12^\circ$). Before the experiment, subjects were given 2 practice blocks.

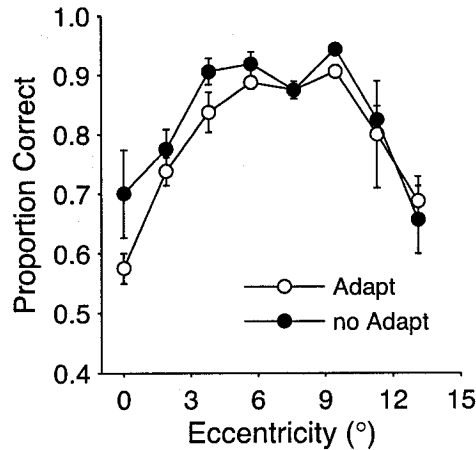


Figure 4.6. Results of Experiment 3. This graph shows the probability target detection with and without adaptation to a high spatial frequency grating as a function of eccentricity.

RESULTS AND DISCUSSION

The results are summarized in Figure 4.6. Data were collapsed across visual field. Proportion of correct responses was the dependent measure. The data were submitted to a 2 (adaptation type) by 8 (eccentricities) within subjects ANOVA. Effect size was calculated as a partial ϵ^2 . A one factor ANOVA was run to examine the effects of foreground/background orientation. The effects of eccentricity for each adaptation type were then examined separately using trend analysis to determine whether a CPD was present or absent. The trend analysis was limited to data positions representing eccentricities 0° to 7.60°.

There were no statistically significant differences when the adapting stimulus matched the orientation of the target microelements versus when the adapting stimulus matched the orientation of the background microelements. Detection performance peaked in the parafovea, with reduced performance occurring towards both the fovea and the periphery [$F(7, 21) = 5.65, p < 0.05$] with an effect size of 0.547. The main effect of adaptation type and the interaction

were not statistically significant. Trend analysis revealed a statistically significant improvement in performance from the fovea to 7.60° in the high-frequency adaptation condition [$F(1, 3) = 46.967, p < 0.01$]. In the no adaptation condition, the trend analysis came close to but did not reach significance [$F(1, 3) = 6.737, p = 0.06$]. That is, a CPD was clearly demonstrated in the adaptation condition and was merely suggested in the no adaptation condition.

Contrary to the results demonstrated in Carrasco et al. (in press), adaptation to a high frequency sine wave grating did not improve texture segmentation performance at the fovea. The adapting stimulus did not appear to have any statistically significant effect on either the background or the foreground elements. One might speculate that an adapting grating oriented at 45 deg is less effective than a vertically oriented adapting grating. Appelle (1972) determined that the visual system has a preference for vertical or horizontal orientations over oblique orientations, the so-called oblique effect. However, McMahan and McLeod (2003) demonstrated oblique gratings were comparable to horizontal gratings as adapting stimuli. Therefore, a lack of an effect in this case cannot be attributed to the orientation of the adapting stimulus.

GENERAL DISCUSSION

The experiments examined whether cross frequency inhibition could be used as an explanation for the CPD. Two methods were used to remove or attenuate high frequency information from the texture images.

In Experiment 1, blurring the stimulus resulted in improved performance at fixation and a decline in performance in the periphery. In Experiment 2, blurring improved discrimination accuracy more or less equally across the visual field. The results of these two experiments suggest that CFI plays some role in

the CPD. However, one would expect a manipulation that affects only high frequency information to have no effect at greater eccentricities where high frequency information becomes difficult to resolve. The results of Experiments 2 demonstrated that blurring a stimulus can improve performance outside the fovea in certain circumstances and Experiment 1 showed that blurring can harm performance in the periphery. These results suggest that blurring may perform a function in addition to the removal the high frequencies from the stimulus.

Experiment 3 represented an attempt to attenuate the influence of the high frequency components of the image through selective adaptation using an obliquely oriented sine wave stimulus. No such effects were seen. Possible reasons for this null result are discussed below.

The results of Experiment 1 raise two questions. First, why was evidence of CFI found in Experiment 1 but not in the earlier study of Gurnsey et al. (1996). Procedural differences may have influenced the outcomes of these experiments. Gurnsey et al. (1996) limited performance using a backward mask whereas performance was limited by a bandwidth manipulation here. The absence of a backward mask *per se* is not likely to be the sole explanation for the elimination of the CPD for filters with $\sigma = 3$ and 5. Potechin and Gurnsey (2003) showed that the bandwidth procedure can be used to elicit a CPD both in the presence and the absence of a backward mask. The absence of a mask led to a modest attenuation of the CPD. That is, when they used a bandwidth manipulation to elicit the CPD, the slope of the function was reduced if a backward mask was not used but the general shape of the function remained the same. Potechin and Gurnsey (2003, 2006) and Condition 1 ($\sigma = 1$) of Experiment 1 show compelling

evidence that, for textures differing in mean orientation, the CPD can be elicited without a backward mask. Nevertheless, it is possible that both CFI and backward masking make independent contributions to the CPD and that in the absence of one the CPD may still be obtained.

Another possibility is high-frequency attenuation through Gaussian blurring interacts with the bandwidth manipulation differently than with a backward mask. As there have been no previous attempts to combine these two manipulations, it remains to be determined whether these two manipulations do exert a combined influence on the stimulus and if any such interaction could explain these results.

A second question raised by both Experiment 1 and Gurnsey et al. (1996, Experiment 2) concerns why blurring should impair performance in the periphery, a result that is difficult to reconcile with CFI. Blurring the stimulus reduces the image contrast. Although this effect would apply to the entire image, it is possible that the effect of contrast reduction is more noticeable in the periphery than at fixation. That is, where performance is already degraded, a lower level of contrast leads to a noticeable difficulty resolving the image. At the fovea, where resolution is high, the effect of lower contrast in the image may be minimized and show a negligible effect on performance.

Experiment 2 showed evidence consistent with the CFI account of the CPD. However, the experiment failed to replicate the CPD reported by Morikawa (2000) in the unfiltered condition. Although there was a considerable amount of variability in subjects' responses (i.e. high standard deviations) this cannot explain the difference in the results. Small changes in procedure between may account for the difference. The size of the stimulus texture used the two

experiments was different. We used a horizontally oriented stimulus display that was 7 X 40 elements while Morikawa (2000) used a much larger 22 X 22 elements square display. Potechin and Gurnsey (2003) showed that a more compelling CPD was exhibited in response to square stimulus. Therefore, any CPD that we obtained might be expected to be of less magnitude than that of Morikawa (2000). Given the large variability in subject responses, any weak CPD that was present may have been obscured.

The results of Experiment 3 suggest that the adaptation procedure did not effectively remove or attenuate high frequency information in the image. This is unexpected, given that a similar procedure used by Carrasco et al. (in press) demonstrated differences in performance in response to stimuli presented with and without adaptation to stimulus composed of a similar high frequency vertical sine wave. We assumed that the two regions would have unequal apparent brightness after adaptation but we did not directly test the strength of the adaptation. Although the high frequency channels may have been successfully adapted during this procedure, the resulting contrast reduction between the two regions may not have been strong enough to improve performance at fixation.

Another possibility is that the adaptation was not directed towards the appropriate spatial frequency channels. In Experiment 2, relatively large Gaussian filters were required to show evidence of CFI. No significant effect was observed when smaller Gaussian filters were used. Therefore, our results may indicate that the frequencies we targeted with the adaptation were not broad enough.

One question that this paper did not address is whether texture segmentation is influenced by high frequency interference presented after the test stimulus. For example, could a mask containing high frequency noise alter discrimination performance? The experiments presented here appear to indicate that high frequency interference presented simultaneously with stimulus presentation may influence detection performance. Further study will be required to determine whether high frequency interference provided by a mask that is presented after the test stimulus results in a similar improvement in performance.

In summary, Experiments 1 and 2 demonstrate that directly removing high frequency information from the stimulus by low-pass filtering can improve texture segmentation in the foveal region and possibly other regions of the visual field. In Experiment 3, high frequency adaptation by selective adaptation to a high frequency grating did not appear to have much of an effect. However, we cannot rule out the possibility that selective adaptation can improve foveal performance under other experimental conditions. Considered together, the results of these three experiments suggest that CFI may play an important role in the CPD.

CHAPTER 5

Summary and Conclusions

In the Introduction, four questions were posed: 1) Is a mask required to elicit the CPD?, 2) Do texture discrimination asymmetries change across the visual field? 3) Will one or both textures of an asymmetrical texture pair produce a CPD? And 4) Does CFI play a role in the CPD? This section briefly summarizes the results of the studies that were undertaken to answer these questions. Suggestions for future research are also provided.

Eliminating temporal factors as an explanation for the CPD

As previously discussed, a temporal theory of the CPD attributes the CPD to differences in processing speed across the visual field. This theory suggests that a mask is required to elicit the CPD. The purpose of the first series of experiments (Chapter 2) was to demonstrate an alternative method in which the CPD obtains without a backward mask. More specifically, Potechin and Gurnsey (2003) employed a bandwidth manipulation that limited performance by the introduction of spatial noise into the stimulus. It was shown that performance declined as the degree of spatial noise in the image was increased.

The bandwidth manipulation was employed in a 2AFC procedure in which subjects were required to identify the interval that contained a texture target in a sequential presentation of two texture displays. The oriented line stimuli used in the first two of these three experiments were closely related to those that had been widely used in previous studies to reliably elicit the CPD. Results were obtained for stimulus presentations both with and without a backward mask. Although the magnitude of the effect was reduced when no

mask was present, in both cases a convincing CPD was elicited. The bandwidth procedure resulted in a more compelling CPD when the manipulation was extended to the 4AFC procedure employed by Morikawa (2000). In this case, subjects were required to identify the quadrant containing the disparate texture.

The experiments presented in Chapter 2 showed that a mask is not critical to the emergence of the CPD. Using the bandwidth procedure, Potechin and Gurnsey (2003) were able to eliminate temporal factors from consideration in task performance, thereby showing that the CPD could be explained using purely spatial factors.

Eccentricity dependence of texture discrimination asymmetries.

Texture discrimination is frequently asymmetrical. That is, texture A embedded in texture B may be more easily discriminated than texture B embedded in texture A (e.g. Gurnsey & Browse, 1987, 1989). However, little attention had been paid to whether texture discrimination asymmetries remain constant across the visual field. Both texture discrimination asymmetries and the CPD impose constraints on texture discrimination theories. These two phenomena were examined together to determine whether they have interacting effects on texture discrimination.

Using the bandwidth manipulation of Potechin and Gurnsey (2003), the second series of experiments examined variations in texture discriminations across eccentricity for a number of textures that had previously been shown to elicit texture discrimination asymmetries. Four different display types comprising stimuli made of up of the following patterns: L-X elements, circles differing in size, circles differing in amount of location variability or jitter, and oriented lines. Three different patterns of results emerged that indicate that a

texture discrimination asymmetry may be demonstrated in the absence of a CPD, a CPD may be demonstrated in the absence of a texture discrimination asymmetry, or both phenomena may be elicited in response to a stimulus. That is, there is no consistent relation between texture discrimination asymmetries and the CPD. For stimuli comprising texture pairs known to elicit discrimination asymmetries, either, both, or neither stimuli may produce a CPD. The results indicate that the discriminability of textures should be specified in terms of both eccentricity of presentation and in the relative locations of the micropatterns within the display.

The influence of CFI on the CPD

The few studies that have directly examined the influence of high spatial frequency attenuation of the stimulus on the CPD (Carrasco et al., in press; Gurnsey et al., 1996; Morikawa, 2000) have not provided a clear indication of whether CFI underlies the CPD due to ambiguities within some experiments and inconsistencies across studies. Morikawa (2000) used blurring to attenuate high frequencies. In addition to blurring the stimulus, he also increased the contrast of the blurred stimulus while the contrast level of the unblurred stimulus was unaltered. Carrasco et al.'s (in press) adaption procedure was meant to selectively attenuate the high frequencies within the image but it may have also had selective effects on the background elements in their texture.

In the experiments presented in Chapter 4, we attempted to bring clarity to the issue by re-examining the three previous CFI hypothesis studies together while addressing the confounds noted above in the Carrasco et al. (in press) and Morikawa (2000) studies. The first experiment re-examined the results of Gurnsey et al. (1996) using the bandwidth manipulation of Potechin and

Gurnsey (2003). The second experiment replicated the work of Morikawa (2000) without altering the contrast of either stimulus. In the third experiment, that was used to replicate Carrasco et al. (in press), the effects of the adaptation on both the foreground and the background elements were compared to determine whether the adaptation had specific effects in one texture region but not the other.

The results showed that removing the high frequency component from the stimulus by low-pass filtering did improve performance at fixation. This manipulation also had effects at more peripheral locations, which is counterintuitive. As discussed in the introduction, sensitivity to high spatial frequencies declines with eccentricity. Therefore, a manipulation that selectively attenuates high frequencies in an image would not be expected to influence performance in the periphery where high frequency sensitivity is low. This suggests that blurring may perform a function in addition to the removal the high frequencies from the stimulus. However, since blurring increased peripheral performance in one instance and decreased it in the other, it is difficult to determine a possible mechanism by which this method of high frequency attenuation influences peripheral performance.

The selective high frequency adaptation procedure we employed to examine the CFI did not appear to effectively attenuate high frequency information in the display. It is possible that adaptation effects were present but were not strong enough to affect the CPD. A more direct assessment would be required to examine whether the adaptation had any effects on the stimulus or whether another factor can explain these results.

Refining the bandwidth procedure

Our experience with using the bandwidth manipulation is quite limited and refinements to the technique may improve the procedure. In the second series of experiments (Chapter 3) two different versions of the bandwidth manipulation were assessed to determine whether one was more effective. In one version, exposure duration was adjusted for each subject and bandwidth level. In the other version, exposure duration was held constant bandwidth level was determined through a calibration procedure for each subject. Similar results were obtained in both cases.

A failure to replicate the results of previous studies should be further examined to determine whether the bandwidth procedure needs to be refined. For example, no asymmetry was demonstrated in response to the stimuli comprising vertical and lines tilted off vertical although strong asymmetries have previously been reported for related stimuli in visual search tasks (e.g. Treisman & Gormican, 1988; Poirier & Gurnsey, 1998) and in our own previous CPD experiment (Potechin & Gurnsey, 2001). Orientation bandwidth refers to a range of orientations from which each individual micropattern in the display can be sampled. In our oriented line stimuli, the vertical regions designated as having vertical lines were actually composed of a number of oriented lines with the possibility that no line was actually vertical. In effect, the discrimination may have appeared to be between two regions of off-vertical lines than to a vertical versus an off-vertical region. It is possible that an asymmetry would not be expected in this case.

Factors that may contribute to a difficulty obtaining a CPD across studies

Although it is not generally discussed, a particular difficulty in studies of the CPD had been to consistently elicit the CPD. Relatively minor factors such as the insertion of a grey screen before the stimulus presentation can strongly affect whether a CPD will be elicited or not. Meinecke and Donk (2000) demonstrated that a change in the stimulus as small as leaving only one of the micropattern spaces empty led to reduced performance in response to a texture which normally elicits a CPD. As it has been demonstrated that the CPD can be elicited using different paradigms and in response to different stimuli, it suggests that there are other factors to consider other than those that have been previously studied.

One factor that could have considerable effects on the CPD is practice effects. Similar effects have been demonstrated in other vision studies. Visual texture discrimination and target detection in a visual search task can be improved with practice (Fiorentini, 1989; Gurnsey & Browse, 1987), potentially to a ceiling level of performance (Gurnsey & Browse, 1989). As subjects often require considerable amounts of practice to obtain stable results when they are first exposed to CPD experiments, this may explain the inconsistency across studies. The effects of practice on the CPD should be studied directly to determine, what, if any, influence there is of practice or stimulus familiarity on the CPD.

Concluding remarks

These experiments make an important contribution to visual texture segmentation literature. A CPD obtained in the absence of a backward mask speaks against the temporal theory of the CPD as proposed by Keher (1989),

which asserts that a backward mask limits performance in the fovea and not the periphery due to differences in processing speed across the visual field. Further support for the spatial hypothesis comes from showing that the removal of high frequency information from the stimulus results in a reduction of the CPD. The spatial theory assumes that low spatial frequencies are not processed as effectively in the fovea. Increased foveal performance with high frequency attenuation shows that the low frequency mechanisms that exist at the fovea do effectively process the visual input. The spatial theory concentrates specifically on the influence of spatial factors on the emergence of the CPD. Taken together, these studies provide strong support for a spatial explanation of the CPD. However, it is important to note that an explanation for the CPD based on spatial factors does not preclude the existence of temporal factors in texture discrimination.

REFERENCES

- Anderson S.A., Mullen, K.T. & Hess, R.F. (1991). Human peripheral spatial resolution for achromatic and chromatic stimuli: Limits imposed by optical and retinal factors. *Journal of Physiology*, **442**, 47-64.
- Appelle, S. (1972). Perception and discrimination as a function of stimulus orientation: The "oblique effect" in man and animals. *Psychological Bulletin*, **4**, 266-278.
- Azzopardi, P., Jones, K. E., & Cowey, A. (1999). Uneven mapping of magnocellular and parvocellular projections from the lateral geniculate nucleus to the striate cortex in the macaque monkey. *Vision Research*, **39**, 2179-2189.
- Beck, J. (1966). Effect of orientation and of shape similarity on perceptual grouping. *Perception and Psychophysics*, **1**, 300-302.
- Beck, J. (1972). Similarity grouping and peripheral discriminability under uncertainty. *American Journal of Psychology*, **85**, 1-19.
- Beck, J. (1982). Textural segmentation. In J Beck (Ed.) *Organization and Representation in Perception*, Hillsdale, NJ: Erlbaum. pp 285-317.
- Beck, J., Prazdny, K., & Rosenfeld, A. (1983). A theory of textural segmentation. In J. Beck, B. Hope, & A. Rosenfeld (Eds.) *Human and Machine Vision*, New York: Academic Press. pp 1-37.
- Bergen, J.R. (1991). Theories of visual texture perception. In D. Regan, (Ed.) *Spatial Vision*, CRC Press. pp. 114-133.
- Bergen, J. R., and Adelson, E. H. (1988). Early vision and texture perception. *Nature*, **333**, 363-364.

- Bergen, J. R., & Julesz, B. (1983). Parallel versus serial processing in rapid pattern discrimination. *Nature*, **303**, 696-698.
- Bergen, J. R. & Landy, M. S. (1991). Computational modeling of visual texture segregation. In Landy, M. S. & Movshon, J. A. (Eds.), *Computational Models of Visual Processing* Cambridge, MA: MIT Press. pp. 253-271.
- Caelli, T., & Julesz, B.(1978). On perceptual analyzers underlying visual texture discrimination : Part I. *Biological Cybernetics*, **28**, 167-175.
- Caelli, T., Julesz, B., & Gilbert, E. (1978). On perceptual analyzers underlying visual texture discrimination : Part II. *Biological Cybernetics*, **29**, 201-214.
- Campbell F. W. & Green D. G. (1965) Optical and retinal factors affecting visual resolution. *Journal of Physiology*, **186**, 576-593.
- Campbell, F.W. & R.W. Gubisch. (1966). Optical quality of the human eye. *Journal of Physiology*, **186**, 558-578.
- Carrasco, M., Evert, D. L., Chang, I., & Katz, S.M. (1995). The eccentricity effect: Target eccentricity affects performance on conjunction searches. *Perception & Psychophysics*, **57**, 1241-1261.
- Carrasco, M., Loula, F, & Ho, X-F. (in press). How attention enhances spatial resolution: Evidence from selective adaptation to spatial frequency.
- Carrasco, M., McElree, B., Denisova, K., & Giordano, A.M. (2003). Speed of visual processing increases with eccentricity. *Nature Neuroscience*, **6**, 669-670.
- Carrasco, M., Penpeci-Talgar, C. & Eckstein, M. (2000). Spatial attention increases contrast sensitivity across the CSF: Support for signal enhancement. *Vision Research*, **40**, 1203-1215.

- Chubb, C., & Sperling, G. (1988). Drift-balanced random stimuli: a general basis for studying non-Fourier motion perception. *Journal of the Optical Society of America A*, **5**, 1986-2007.
- Connolly, M., & Van Essen, D. C. (1984). The representation of the visual field in parvocellular and magnocellular laminae of the lateral geniculate nucleus in the macaque monkey. *Journal of Comparative Neurology*, **226**, 544-564.
- Curcio, C.A. & Allen, K.A. (1990). Topography of ganglion cells in human retina. *Journal of comparative Neurology*, **300**, 5-25.
- Curcio, C.A., Sloan, K.R., Kalina, R.E. & Hendrickson, A.E. (1990). Human photoreceptor topography. *Journal of Comparative Neurology*, **292**, 497-523.
- Curcio, C.A., Sloan, K.R. Jr, Packer, O., Hendrickson, A.E. & Kalina, R.E. (1987). Distribution of cones in human and monkey retina: individual variability and radial asymmetry. *Science*, **236**, 579-582
- DeValois, R. L., & DeValois, K. (1988). *Spatial Vision*. New York: Oxford University Press.
- Duncan, J., & Humphreys, G. W. (1989). Visual search and stimulus similarity. *Psychological Review*, **96**, 433-458
- Fiorentini, A. (1989). Differences between fovea and parafovea in visual search processes. *Vision Research*, **29**, 1153-1164.
- Foster, D.H., & Ward, P.A. (1991). Asymmetries in oriented-line detection indicate two orthogonal filters in early vision. *Proceedings of the Royal Society of London, Series B*, **243**, 75-81.
- Foster, D.H., & Westland, S. (1998). Multiple groups of orientation-selective visual mechanisms underlying rapid orientated-line detection. *Proceedings of the Royal Society of London, Series B*, **265**, 1605-1613.

- Foster, D.H., & Westland, S. (1995). Orientation contrast vs. orientation in line-target detection. *Vision Research*, **35**, 733-738.
- Gibson, J. J. (1950). *The perception of the visual world*. New York: Houghton Mifflin
- Graham, N. (1989). *Visual pattern analyzers*. New York: Oxford University Press.
- Graham, N., Beck, J., & Sutter, A. (1992). Nonlinear processes in spatial-frequency channel models of perceived segregation: Effects of sign and amount of contrast. *Vision Research*, **32**, 719-743.
- Graham, N., & Sutter, A. (1998). Spatial summation in simple (Fourier) and complex (non-Fourier) texture channels. *Vision Research*, **38**, 231-257.
- Graham, N., Sutter, A., & Venkatesan, C. (1993). Spatial-frequency- and orientation- selectivity of simple and complex channels in region segmentation. *Vision Research*, **33**, 1893-1911.
- Grossberg, S. & Mignolla, E. (1985). Neural dynamics of perceptual grouping: textures, boundaries, and emergent segmentations. *Perception and Psychophysics*, **38**, 141-171.
- Grossberg, S. & Williamson, J. R. (1999). A self-organizing neural system for learning to recognize textured scenes. *Vision Research*, **39**, 1385-1406.
- Gurnsey, R. & Browse, R. A. (1987). Micropattern properties and presentation conditions influencing visual texture discrimination. *Perception and Psychophysics*, **41**, 239-252.
- Gurnsey, R., & Browse, R. A. (1988). Aspects of Visual Texture Discrimination. In Z. W. Pylyshyn (Ed.) *Computational Processes In Human Vision: An Interdisciplinary Perspective*. Ablex Publishing Corporation: Norwood, NJ.
- Gurnsey, R. & Browse, R. A. (1989). Asymmetries in visual texture discrimination. *Spatial Vision*, **4**, 31-44.

- Gurnsey, R., Di Lenardo, D., & Potechin, C. (2004). Backward masking and the central performance drop. *Vision Research*, **44**, 2587-2596.
- Gurnsey, R., & Laundry, D.S. (1992). Texture discrimination with and without abrupt texture gradients. *Canadian Journal of Psychology*, **46**, 306-332.
- Gurnsey, R., Pearson, P., & Day, D. (1996). Texture segmentation along the horizontal meridian: Nonmonotonic changes in performance with eccentricity. *Journal of Experimental Psychology: Human Perception and Performance*, **22**, 738-757.
- Gurnsey, R., & von Grünau, M. (1997). Illusory contour-motion arising from translating terminators. *Vision Research*, **37**, 1007-1024.
- Harmon, L. D., & Julesz, B. (1973). Masking in visual recognition: Effects of two-dimensional filtered noise. *Science*, **180**, 1194-1197.
- Harvey, Jr., L. O., & Gervais, M. J. (1981). *Journal of Experimental Psychology: Human Perception and Performance*, **22**, 741-753.
- Hubel, D. H., & Weisel, T. N. (1974). Uniformity of monkey striate cortex: A parallel relationship between field size, scatter, and magnification factor. *Journal of Comparative Neurology*, **158**, 295-306.
- Jennings, J. A., & Charman, W. N. (1981). Off-axis image quality in the human eye. *Vision Research*, **21**, 445-455.
- Julesz, B. (1962). Visual pattern discrimination. *IRE Trans. Information Theory*, **8**, 84-92.
- Julesz, B. (1981). Textons, the elements of texture perception, and their interactions. *Nature*, **290**, 91-97.
- Julesz, B. (1984). A brief outline of the texton theory of human vision. *Trends in Neurosciences*, **7**, 41-45.

- Julesz, B. & Bergen, J. R. (1983). Textons, the fundamental elements in preattentive vision and perception of textures. *Bell System Technical Journal*, **62**, 1619-1645.
- Julesz, B., Gilbert, E.N., Shepp, & L.A. Frisch, H.L. (1973). Inability of humans to discriminate between visual textures that agree in second-order statistics – revisited. *Perception*, **2**, 391-405.
- Julesz, B., Gilbert, E. N., & Victor, J. D. (1978). Visual discrimination of textures with identical third-order statistics. *Biological Cybernetics*, **31**, 137-140.
- Joffe, K. M., & Scialfa, C. T. (1995). Texture segmentation as a function of eccentricity, spatial frequency and target size. *Spatial Vision*, **9**, 325-342.
- Kehrer, L. (1987). Perceptual segregation and retinal position. *Spatial Vision*, **2**, 247-261.
- Kehrer, L. (1989). Central performance drop on perceptual segregation tasks. *Spatial Vision*, **4**, 45-62.
- Kehrer, L. (1994). A simulation of orientation contrast detection with Watson's gabor filter model. Poster presentation ECVP 1994, Eindhoven.
- Kehrer, L. (1997). The central performance drop in texture segmentation: a simulation based on a spatial filter model. *Biological Cybernetics*, **77**, 297-305.
- Kehrer, L., & Meineke, C. (2003). A space-variant filter model of texture segregation: Parameter adjustment guided by psychophysical data. *Biological Cybernetics*, **88**, 183-200.
- Kingdom, F. A. & Keeble, D. R. (1996). A linear system approach to the detection of both abrupt and smooth spatial variation in orientation-defined textures. *Vision Research*, **36**, 409-420.

- Kingdom, F. A. & Keeble, D. R. (1999). On the mechanisms for scale invariance in orientation-defined textures. *Vision Research*, **39**, 1477-1489.
- Kingdom, F. A. & Keeble, D. R. (2000). Luminance spatial frequency differences facilitate the segmentation of superimposed textures. *Vision Research*, **40**, 1077-1087.
- Kingdom, F. A. A., Prins, N. & Hayes, A. (2003). Mechanism independence for texture-modulation detection is consistent with a filter-rectify-filter mechanism. *Visual Neuroscience*, **20**, 65-76.
- Lamme, V. A. F. (1995). The neurophysiology of figure-ground segregation in primary visual cortex. *Journal of Neuroscience*, **15**, 1605-1615.
- Lamme V.A.F., Roelfsema P.R. (2000). The distinct modes of vision offered by feedforward and recurrent processing. *Trends in Neuroscience*, **23**, 571-579.
- Landy, M.S. & Bergen, J.R. (1991). Texture segregation and orientation gradient. *Vision Research*, **31**, 679-691.
- Landy, M. S. & Graham, N. (2004). Visual perception of texture. In Chalupa, L. M. & Werner, J. S. (Eds.), *The Visual Neurosciences* Cambridge, MA: MIT Press. pp. 1106-1118.
- Landy, M. S. & Oruç, I. (2002). Properties of second-order spatial frequency channels. *Vision Research*, **42**, 2311-2329.
- Livingstone, M., & Hubel, D. (1988). Segregation of form, color, movement, and depth: Anatomy, physiology, and perception. *Science*, **240**, 740-749.
- Liu, X. & Wang, D. (2002). A spectral histogram model for texture modeling and texture discrimination. *Vision Research*, **42**, 2617-2634.
- Malik, J., & Perona, P. (1990). Preattentive texture discrimination with early vision mechanisms. *Journal of the Optical Society of America A*, **7**, 923-932.

- Marcos, S., Tornow, R.-P., Elsner, A.E., and Navarro, R. (1997). Foveal cone spacing and cone photopigment density difference: objective measurements in the same subjects. *Vision Research*, **37**, 1909-1915.
- McCourt, M. E. & Foley, J. M. (1985). Spatial frequency interference on grating-induction. *Vision Research*, **25**, 1507-1515.
- McMahon, M. J., & McLeod, D. I. A. (2003). The origin of the oblique effect examined with pattern adaptation and masking. *Journal of Vision*, **3**, 230-239.
- Meinecke, C. (1989). Retinal eccentricity and the detection of targets. *Psychological Research*, **51**, 107-116.
- Meinecke, C., & Kehrner, L. (1994). Peripheral and foveal segmentation of angle textures. *Perception & Psychophysics*, **56**, 326-334.
- Meinecke, C. & Kehrner, L. (1994b). How irrelevant are 'irrelevant' texture elements? *Perception*, **23** (Supplement), 37.
- Meinecke, C., Kimchi, R., and Grandegger, C. (2002). A reversal in the direction of detection asymmetry: Effects of spatial density, spatial regularity, and retinal eccentricity. *Perception & Psychophysics*, **64**, 829-843.
- Merigan, W.H. and Katz, L.M. (1990) Spatial resolution across the macaque retina. *Vision Research*, **30**, 985-992.
- Morrone, M. C., Burr, David C., & Ross, J. A. (1983). Added noise restores recognizability of coarse quantized images. *Nature*, **305**, 226-228.
- Morikawa, K. (2000). Central performance drop in texture segmentation: the role of spatial and temporal factors. *Vision Research*, **40**, 3517-3526.
- Neisser, U. (1967). *Cognitive psychology*. New York : Appleton-Century-Crofts.
- Nothdurft, H. C. (1985). Sensitivity for structure gradient in texture discrimination task. *Vision Research*, **25**, 1957-1968.

- Pearson, P., & Gurnsey, R. (1992). Texture discrimination with foveal and peripheral presentation. *Investigative Ophthalmology and Visual Science*, **33**, S960.
- Poirier, F. J., & Gurnsey, R. (1998). The effects of eccentricity and spatial frequency on the orientation discrimination asymmetry. *Spatial Vision*, **11**, 349-66.
- Potechin, C., and Gurnsey, R (2001). Asymmetry and the central performance drop. *Investigative Ophthalmology & Visual Science*, **42**, S613.
- Potechin, C., and Gurnsey, R. (2003). Masking is not required to elicit the central performance drop. *Spatial Vision*, **16**, 393-406.
- Robson, J.G. (1980). Neural Images: The physiological basis of spatial vision. In C.S. Harris (Ed.). *Visual Coding and Adaptability*, Hillsdale NJ: Erlbaum.
- Robson, J.G., & Graham, N. (1981) Probability summation and regional variation in contrast sensitivity across the visual field. *Vision Research*, **21**, 409-418.
- Rovamo, J., & Virsu, V. (1979). An estimation and application of the human cortical magnification factor. *Experimental Brain Research*, **37**, 495-510.
- Rovamo, J., Virsu, V., & Näsänen, R. (1978). Cortical magnification factor predicts the photopic contrast sensitivity of peripheral vision. *Nature*, **271**, 54-56.
- Rubenstein, B. S., & Sagi, D. (1989). Spatial variability as a limiting factor in texture discrimination tasks: Implications for performance asymmetries. *Technical report for the The Weizmann Institute of Science*, 1-26.
- Rubenstein, B. S.; & Sagi, D. (1990). Spatial variability as a limiting factor in texture-discrimination tasks: Implications for performance asymmetries. *Journal-of-the-Optical-Society-of-America-A:-Optics-and-Image-Science*, **7**, 1632-1643.

- Rubenstein B.S., & Sagi D. (1996). Texture segmentation: the role of line terminations, size, and filter wavelength. *Perception & Psychophysics*, **58**, 489-509.
- Saarinen, J., Ravamo, J., and Virsu, V. (1987). Texture discrimination at different eccentricities. *Journal of the Optical Society of America A*, **4**, 1699-1703.
- Schmolesky M. T., Wang, Y., Hanes, D. P., Thompson, K. G., Leutgeb, S., Schall, J. D., & Leventhal, A. G. (1988). Signal Timing Across the Macaque Visual System. *Journal of Neurophysiology*, **79**, 3272-3278.
- Sebe, N. & Lew, M.S. (2001). Texture Features for Content-based Retrieval. In Michael S. Lew (Ed.), *Principles of Visual Information Retrieval*. London, UK: Springer-Verlag. pp. 51-86.
- Sezikeye, F.X., & Gurnsey, R. (2005). Texture discrimination asymmetries are size dependent. Presentation to the Canadian Society for Brain, Behaviour and Cognitive Science, July, Montreal.
- Song, Y., & Baker, C. L. (2006). Neural mechanisms mediating responses to abutting gratings: Luminance edges vs. illusory contours. *Visual Neuroscience*, **23**, 181-199.
- Thibos, L.N., Cheney, F.E. and Walsh, D.J. (1987) Retinal limits to the detection and resolution of gratings. *Journal of the Optical Society of America A*, **4**, 1524-1529.
- Treisman, A., & Gormican, S. (1988). Feature analysis in early vision: Evidence from search asymmetries. *Psychological Review*, **95**, 15-48.
- Treisman, A. & Souther, J. (1985). Search asymmetry: A diagnostic for preattentive processing of separable features. *Journal of Experimental Psychology: General*, **114**, 285-310.

- Van Tonder, G. J., & Ejima, Y. (2000). From image segmentation to anti-textons. *Perception*, **29**, 1231-1247.
- Virsu, V., & Rovamo, J. (1979). Visual resolution, contrast sensitivity, and the cortical magnification factor. *Experimental Brain Research*, **37**, 1-16.
- von Berg, J., Ziebell, O., & Stiehl, H. S. (2002). Texture segmentation performance related to cortical geometry. *Vision Research*, **42**, 917-1929.
- Wikler, K.C., Williams, R. W., & Rakic, P. (1990). Photoreceptor mosaic: number and distribution of rods and cones in the rhesus monkey retina. *Journal of Comparative Neurology*, **297**, 499-508.
- Williams, D. and Julesz, (1992). Perceptual asymmetry in texture perception. *Proceeding of the national Academy of Science*, **89**, 6531-6534.
- Wilson, H. R., Ferrera, V. P., & Yo, C. (1992). A psychophysically motivated model for two-dimensional motion perception. *Visual Neuroscience*, **9**, 79-97.
- Wilson, H. R., & Wilkinson, F. (1998). Detection of global structure in glass patterns: Implications for form vision. *Vision Research*, **38**, 2933-2947.
- Wolfe, J. M. (1992). 'Effortless texture segmentation and 'parallel' search are not the same thing. *Vision Research*, **32**, 757-763.
- Wolfe, J. M. (1998). Visual Search. In H. Pashler (Ed.), *Attention*, Hove, England UK: Psychology Press/Erlbaum (UK). pp. 13-73.
- Wolfson, S. S. & Landy, M.S (1998). Examining edge- and region-based texture analysis mechanisms. *Vision Research*, **38**, 439-446.
- Wright, M. J., & Johnston, A. (1983). Spatiotemporal contrast sensitivity and visual field locus. *Vision Research*, **23**, 983-989.
- Yeshurun, Y. & Carrasco, M. (1998). Attention improves or impairs visual performance by enhancing spatial resolution. *Nature*, **396**, 72-75.

- Yeshurun, Y. & Carrasco, M. (1999). Spatial attention improves performance in spatial resolution tasks. *Vision Research*, **39**, 293-306.
- Yeshurun, Y., & Carrasco, M. (2000). The locus of attentional effect in texture segmentation. *Nature Neuroscience*, **3**, 622-627.